DOCINADE

Doctorado en Ciencias Naturales para el Desarrollo

Énfasis en Gestión y Cultura Ambiental

Tesis de Doctorado

Generación de un modelo de monitoreo de la contaminación atmosférica por metales pesados en zonas de flujo vehicular, basado en las propiedades magnéticas de biomonitores y polvo urbano

M.Sc. Teresa Salazar Rojas

Dr. Guillermo Calvo Brenes
Director de Tesis

Dr. Fredy Rubén Cejudo Ruiz
Asesor de Tesis

Dr. Marco Vinicio Gutiérrez Soto
Asesor de Tesis

Cartago, Costa Rica, Marzo 2023

MIEMBROS DEL TRIBUNAL EXAMINADOR

TEC | Tecnológico de Costa Rica

Firmado digitalmente por TEODOLITO GUILLEN GIRON (FIRMA)
Fecha: 2023.03.27 14:44:53 -06'00'

Dr. Teodolito Guillén Girón

Dirección de Posgrados TEC

Firmado digitalmente por DAVID ALBERTO VALVERDE BARQUERO (FIRMA)
Fecha: 2023.03.27 13:41:39 -06'00'

Dr. David Valverde Barquero

Coordinador del General DOCINADE

GUILLERMO DE JESUS CALVO BRENES (FIRMA)

Digitally signed by GUILLERMO DE JESUS CALVO BRENES (FIRMA)
Date: 2023.03.24 15:55:50 -06'00'

Dr. Guillermo Calvo Brenes

Director de tesis

Fredy Ruben Cejudo Ruiz

Firmado digitalmente por Fredy Ruben Cejudo Ruiz
Nombre de reconocimiento (DN): cn=Fredy Ruben Cejudo Ruiz, o=Instituto de Geofísica UNAM, ou=UNAM, email=ruben@igeofisica.unam.mx, c=MX
Fecha: 2023.03.27 09:46:05 -06'00'

Dr. Fredy Rubén Cejudo Ruiz

Miembro del Comité Asesor de Tesis

MARCO VINICIO GUTIERREZ SOTO (FIRMA)

Digitally signed by MARCO VINICIO GUTIERREZ SOTO (FIRMA)
Date: 2023.03.27 10:06:13 -06'00'

Dr. Marco Vinicio Gutiérrez Soto

Miembro del Comité Asesor de tesis

Tabla de contenidos

Índice de Figuras

Índice de Cuadros

Declaración de autenticidad

Yo Teresa Salazar Rojas, estudiante del Doctorado en Ciencias Naturales para el Desarrollo, declaro que la Tesis Doctoral que presento para su exposición y defensa titulada "*Generación de un modelo de monitoreo de la contaminación atmosférica por metales pesados en zonas de flujo vehicular basado en las propiedades magnéticas de bioindicadores y polvo urbano*" y comité asesor de tesis son el Dr. Guillermo Calvo Brenes (director de tesis), Dr. Fredy Rubén Cejudo Ruiz (asesor) y el Dr. Marco Vinicio Gutiérrez Soto (asesor), es original y que todas las fuentes utilizadas para su realización han sido debidamente citadas en el mismo. Este material no lo he presentado, en forma parcial o total, como una tesis en esta u otra institución.

Cartago, Costa Rica a 24 de marzo de 2023.

TERESA SALAZAR ROJAS (FIRMA)

Firmado digitalmente por TERESA SALAZAR ROJAS (FIRMA)
Fecha: 2023.03.27 15:44:41 -06'00'

Firma Teresa Salazar Rojas

Agradecimientos

A Dios, por ser mi mayor guía en todos estos años y por darme la fortaleza para seguir adelante y lograr culminar esta etapa de mi vida.

A mi Tutor, Guillermo Calvo y Asesores Rubén Cejudo y Marco Gutierrez, por instruirme en todo este proceso y siempre brindarme su ayuda de la mejor forma.

A mis asesores de doctorado, a mis profesores y al programa DOCINADE, por todas sus enseñanzas que me permitieron crecer profesionalmente.

Al Tecnológico de Costa Rica y la Universidad Nacional Autónoma de México (Morelia), por brindar los recursos necesarios para la elaboración de este trabajo.

Dedicatoria

A mi familia, esposo, hijos y hermana por ser mi fuente de amor, apoyo y alegría.

A Benilda Rojas Vargas, mi madre, por darme más que la vida, y cuyas enseñanzas son pilar de mi existencia.

Resumen

La contaminación atmosférica urbana es uno de los problemas medioambientales más serios a los que se enfrenta la humanidad ante el rápido crecimiento económico y demográfico. Los efectos en la salud asociados a la contaminación atmosférica están relacionados con problemas respiratorios, principalmente correlacionados con la exposición temporal a material particulado (PM, siglas en inglés), especialmente las más finas (PM con diámetro ≤ 2.5 µm), que provocan lesiones cardiopulmonares y difusión sistémica. Entre los diferentes componentes del PM se encuentran los metales pesados (MPs), los cuales son especialmente peligrosos para los seres vivos ya que se bioacumulan, causando importantes efectos negativos sobre el bienestar humano y el medio ambiente. Esta tesis tuvo como objetivo establecer un modelo para predecir las concentraciones de MPs en hojas y polvo de carretera, a través de las mediciones de sus propiedades magnéticas. Para ello, se usó algoritmos de aprendizaje automático, la regresión lineal automática (MLR, siglas en inglés) y de soporte de vectorial automático (SVM, siglas en inglés) para establecer modelos de predicción de MPs basados en las propiedades magnéticas del PM depositado en hojas y polvo de la carretera. Se hizo un muestreo de polvo de carreteras y hojas de dos especies comunes de tipo perenne (Cupressus *lusitánica* y Casuarina *equisetifolia*) durante dos años en la Gran Área Metropolitana (GAM) de Costa Rica. Los resultados mostraron tanto en la etapa de entrenamiento como en la de prueba, que las concentraciones de Fe, Cu, Cr, V y Zn fueron bien estimadas por los modelos de predicción SVM, con valores R^2 ajustados > 0.7 y las concentraciones de Pb y Ni fueron estimados con menor precisión, con valores R^2 ajustados < 0.7. El modelo de SVM que estimó mejor la concentración de MPs a partir de propiedades magnéticas fue el que se obtuvo de las hojas de *C*. *equisetifolia*, en comparación con *C. lusitanica* y el polvo de la carretera, mostrando valores R^2 ajustados más altos y error medio absoluto (MAE) y el error medio cuadrático (RMSE), más bajos. Es posible establecer un modelo de SVM en la GAM de Costa Rica para determinar indirectamente la concentración de elementos en material particulado depositado en hojas mediante el uso de propiedades magnéticas, permitiendo disminuir los costos, tiempos y generación de desechos para el monitoreo de MPs en las áreas urbanas.

Palabras claves

Biomonitores; propiedades magnéticas; polvo urbano; metales pesados; soporte de vectores automático; regresión lineal automática; índice de carga de contaminación.

Abstract

Urban air pollution is one of the most serious environmental problems facing humanity in the context of rapid economic and demographic growth. The health effects associated with air pollution are related to respiratory problems, mainly correlated with temporary exposure to particulate matter (PM), especially the finest particles (PM with diameter ≤ 2.5 μm), which cause cardiopulmonary lesions and systemic diffusion. Among the different components of PM are heavy metals (PMs), which are particularly hazardous to living beings as they bioaccumulate, causing significant negative effects on human well-being and the environment. This thesis aims to establish a model to predict PM concentrations in leaves and road dust through measurements of their magnetic properties. For this purpose, machine learning, automatic linear regression (MLR) and automatic support vector (SVM) algorithms were used to establish prediction models of PMs based on the magnetic properties of PM deposited in leaves and road dust. Road dust and leaves of two common evergreen species (*Cupressus lusitanica* and *Casuarina equisetifolia*) were sampled for two years in the Greater Metropolitan Area (GAM) of Costa Rica. The results showed in both the training and test stages that the concentrations of Fe, Cu, Cr, V and Zn were well estimated by the SVM prediction models, with adjusted R^2 values > 0.7 and the concentrations of Pb and Ni were estimated less accurately, with adjusted R^2 values < 0.7. The SVM model that best estimated the concentration of PMs from magnetic properties was the one obtained from *C. equisetifolia* leaves, compared to that from *C. lusitanica* and road dust, showing higher adjusted R^2 values and lower mean absolute error (MAE) and root mean square error (RMSE). It is possible to establish an SVM model in the GAM of Costa Rica to indirectly determine the concentration of elements in particulate matter deposited on leaves by using magnetic properties, allowing to reduce costs, time and waste generation for HMs monitoring in urban areas.

Keywords

Biomonitor; magnetic property; urban dust; heavy metals; support vector machine; machine lineal regression; pollution load index.

1. Introducción

La contaminación atmosférica urbana es uno de los problemas medioambientales más serios a los que se enfrenta la humanidad debido al rápido crecimiento económico (industrial y tecnológico) y demográfico. Según estimaciones de la OMS (Organización Mundial de la Salud) en el 2019, el 99% de la población mundial vivía en lugares donde no se cumplían los niveles de las directrices de calidad del aire (World Health Organization, 2021). Es por ello que dos de los objetivos de Desarrollo Sostenible (3 y 11) de la Organización de Naciones Unidas tratan directamente sobre esta problemática. El objetivo 3 "Salud y Bienestar para todos" en su indicador "3.9.1 Tasa de mortalidad atribuida a la contaminación de los hogares y del aire ambiente" y el objetivo 11 "Ciudades y Comunidades Sostenibles" con su indicador "11.6.2 Niveles medios anuales de partículas finas en suspensión en las ciudades" (Naciones Unidas, n.d.). Los efectos en la salud asociados a la contaminación atmosférica están relacionados con problemas respiratorios, principalmente correlacionados con la exposición temporal a PM, especialmente la fracción más finas (PM con diámetro ≤ 2.5 μm), que provocan lesiones cardiopulmonares y difusión sistémica (Losacco & Perillo, 2018, Polezer et al., 2018, Yap et al., 2019). Entre los diferentes tipos de fuentes antropogénicas de PM, se encuentran el uso de combustibles fósiles en la industria y en el transporte, este último es de mayor relevancia, debido al aumento de unidades vehiculares en circulación en el mundo. El crecimiento de la producción del 2000 al 2018 fue de: 34% en automóviles y de 128% en camiones (Davis & Robert, 2021). En Costa Rica el crecimiento anual del parque vehicular, ha sido de un promedio de 6% desde 1980 hasta 2019, con un incremento de casi diez veces, pasando de 180,986 unidades en 1980 a 1,752,813 vehículos en 2019. Siendo además el parque vehicular principalmente de motores de combustión, en 2019 la distribución del tipo de combustible fue; 82% vehículos de gasolina, 17.3% diésel y el 0.7% restante a vehículos híbridos eléctricos o de gas (Nation State Program, 2020).

Las emisiones de los vehículos generan gases de efecto invernadero, material particulado (PM_{10}, $PM_{2,5}$), con contenido de MPs (Cr, Cu, Ni, Pb, V, Fe y Zn), por la quema de combustible y el desgaste del motor y piezas vehiculares (Winkler et al., 2020). Los MPs son especialmente relevantes porque estos no pueden ser degradados o destruidos naturalmente; aunque, pueden ser diluidos por agentes físico-químicos o atrapados dentro del PM y por lo tanto ser

transportados y distribuidos en los diferentes medios (suelo, agua y aire) en los ecosistemas, uniéndose a las cadenas tróficas donde pueden ser bioacumulados (Leng et al., 2018). De ahí su definición según de la Agencia de Protección Ambiental (EPA, por sus siglas en inglés), un MP es un “residuo peligroso común; que puede dañar a los organismos a bajas concentraciones y tiende a acumularse en la cadena alimentaria" (US-EPA, 2022).

La calidad del aire se analiza normalmente mediante el uso de redes de estaciones de monitoreo que miden los gases contaminantes, las partículas en suspensión y metales pesados (comúnmente medidos: Pb, Cr, Cu, V, Zn, Fe, Ni y Cd). Estas estaciones funcionan las 24 horas del día durante todo el año y usan filtros generalmente de cuarzo, fibra de vidrio o teflón. El monitoreo también puede hacerse mediante monitoreo de bandas espectrales que emiten los satélites meteorológicos. El funcionamiento de las estaciones puede ser automatizada, semi automatizada o manual. En esta última, la estación de monitoreo usa un medio de recolección de contaminantes (filtros pasivos), que luego serán analizados químicamente en un laboratorio, este método resulta ser lento y caro (Wilson et al., 2005). Esto hace que la implementación de estaciones de monitoreo en zonas urbanas sea reducida debido a los altos costos de inversión y mantenimiento (Leng et al., 2018).

Una de las evaluaciones más reconocidas es el índice de desempeño ambiental (EPI en inglés), desarrollado por las universidades de Yale y Columbia. En EPI la posición de Costa Rica para el 2022 fue para calidad del aire, el puesto 43 a nivel mundial y en el 8 a nivel de Latinoamérica y con respecto al indicador de metales pesados fue 77 a nivel mundial y 14 a nivel de Latinoamérica, lo cual es indicativo de que existe espacio para mejora en ambos temas (Programa Estado de la Nación, 2022). En el país, el monitoreo de la contaminación del aire se realiza a través de una red de monitoreo de la calidad del aire (REMCA) en algunos sitios GAM (11 equipos de medición, 8 estaciones manuales) (Poveda et al., 2020). Además, la embajada de los Estados Unidos en Costa Rica, cuenta con una estación de monitoreo diario de $PM_{2.5}$ en sus instalaciones en Pavas, que forma parte del Índice de Calidad del Aire en Tiempo Real (WAQI en inglés) (World Air Quality Index Team, 2020). Es así como según los informes de REMCA los problemas de contaminación del aire en el país están asociados principalmente a la densidad industrial, comercial y de tráfico (Briseño-Castillo et al., 2015). En el informe de calidad del aire del GAM 2017-2018 se reportaron concentraciones anuales de $PM_{2.5}$ superiores al valor permitido

en la legislación nacional (15 µg/m^3) en 8 de los sitios de monitoreo manual (Poveda et al., 2020), y superiores al valor límite (5 µg/m^3) establecido por la OMS (World Health Organization, 2021). La Embajada de USA, ha reportado en el WAQI, valores $PM_{2.5}$, considerados de calidad del aire moderado para algunas horas del día para 2020-2022 (World Air Quality Index Team, 2022). También se reportan incumplimiento del PM_{10} establecido por la OMS (15 µg/m^3), para la ciudad de San José para los años 2017-2021 (Programa Estado de la Nación, 2022).

Adicionalmente a la contaminación del aire que se presenta en algunos sitios del país, no se cuenta con suficientes estaciones de monitores, ya que las mismas implican costos importantes en instalación, mantenimiento, operación y cuidado para evitar el vandalismo, lo cual limita la expansión de la red de monitoreo. Además, los estudios de diagnóstico y control para determinar el contenido de MPs en el medio ambiente no se llevan a cabo con la periodicidad y el alcance requeridos, debido al elevado costo, tiempo e infraestructura necesarios para los análisis químicos (Poveda et al., 2020).

Recientemente, se ha estudiado el desarrollo de modelos de predicción de la contaminación atmosférica que usan algoritmos de aprendizaje automático para mejorar la eficacia de los programas de vigilancia de la contaminación atmosférica (Li et al., 2017; Leng et al., 2018; Li et al., 2020; Dai et al., 2020). Para su construcción, puede utilizarse el aprendizaje automático de tipo no supervisado, en el que los algoritmos generan respuestas a partir de datos desconocidos y no etiquetados con el fin de descubrir patrones en nuevos conjuntos de datos. Los algoritmos de agrupación, como *K-means*, suelen utilizarse en el aprendizaje automático no supervisado. Este tipo de aprendizaje es más complejo en su programación. El otro tipo de aprendizaje, el supervisado, el usuario entrena al programa para que genere una respuesta basada en un conjunto de datos conocidos y etiquetados. Ejemplo de ello son los algoritmos de clasificación y regresión, incluidos los bosques aleatorios, los árboles de decisión y el de soporte de vectores automático (Dai et al., 2020), este último utilizado en este estudio.

Adicionalmente, se están desarrollando metodologías alternas a las tradicionales de colecta y medición de contaminantes atmosféricos, que además pueden ser utilizados como fuente de datos de entrada para la creación de estos modelos predictivos de la contaminación del aire. Estas son el uso de biomonitores y las propiedades magnéticas de muestras ambientales. La primera es un método alterno, al uso de filtros, para la captación de contaminantes atmosféricos,

mediante el uso de las hojas de biomonitores. Esta tiene varias ventajas, como su menor costo, simples de muestrear y producción de datos fiables relacionados con el contenido de contaminantes atmosféricos e información sobre sus efectos en los sistemas vivos (Leng et al., 2018). Referente al uso de plantas se debe de considerar que el grado de retención y encapsulación de partículas, va a variar dependiendo del tipo de la misma, lo que señala la importancia de las características de la hoja (rugosidad, suavidad, vellosidad, longitud y rigidez del pecíolo, orientación, etc.), composición química de la cutícula (cantidad de constituyentes de cera individuales responsables de la hidrofobicidad de la cutícula) y la estructura de la cutícula (espesor, morfología, alteración de la estructura con la edad, presencia de cristales de cera epicuticular) (Bussotti et al., 2014). También es difícil distinguir entre la cantidad de MPs que se absorben del suelo y los que se captan del aire; sin embargo, hay evidencias de que en el caso de las plantas cercanas a las carreteras, la ingesta foliar procede de las partículas transportadas por el aire y los MPs que son el resultado de la quema de combustible y al desgaste del motor y otras piezas de los vehículos (Oliva & Espinosa, 2007; Sharma et al., 2020; Winkler et al., 2020).

La segunda metodología es un método indirecto de monitoreo temporal de la contaminación del aire mediante propiedades magnéticas de biomonitores, suelo y polvo de carretera que permiten realizar diagnósticos con bastante precisión, sin destrucción de la muestra, con poca inversión de tiempo y menores costos, lo cual ha sido demostrado por estudios realizados en diferentes países, entre ellos; Italia (Winkler et al., 2003), España (Davila et al., 2006), México (Aguilar et al., 2012), Inglaterra (Hofman & Samson, 2014), India (Rai & Panda, 2015), Japón (Kawasaki et al., 2017), Irán (Kardel et al., 2018), USA (Gillooly et al., 2019), China (Wang et al., 2019), Argentina (Chaparro et al., 2020). El origen del magnetismo de los materiales se debe a la composición del átomo, específicamente a tres particularidades del electrón; su momento angular intrínseco (llamado spin), su momento angular orbital y su distribución dentro de cada elemento. El momento magnético total de un átomo viene dado por la suma vectorial de los momentos electrónicos. Si los momentos magnéticos orbitales y de espín de un átomo están orientados de forma que se anulan mutuamente, el átomo tiene un momento magnético nulo. Es decir, tiene un comportamiento diamagnético. Si, por el contrario, la cancelación es sólo parcial, el átomo tiene un momento magnético permanente. Entonces tiene un comportamiento paramagnético. El ferromagnetismo es un comportamiento, en el cual los momentos angulares e intrínsecos de los electrones presentan una máxima alineación que genera un fuerte momento magnético de los

materiales, el cual es mucho mayor que el comportamiento diamagnético y el paramagnético. Está asociado a los elementos hierro (de ahí su nombre), níquel y cobalto pero también se da en muchos minerales naturales, como ciertos óxidos de hierro (Evans & Heller, 2003). Las muestras ambientales usadas en magnetismo ambiental (suelo, sedimento y material botánico) pueden contener una mezcla de diversos materiales magnéticos (diamagnéticos, paramagnéticos, ferroferrimagnéticos y antiferromagnéticos), conteniendo mayor cantidad de minerales ferrimagnéticos entre mayor será su origen antrópico (Bautista & Gogichaishvili, 2018).

El uso de biomonitores y las propiedades magnéticas es posibles ya que las partículas que se depositan sobre la plantas, son atrapadas y encapsuladas en la cutícula, funcionando como filtros pasivos. En ambientes urbanos, las plantas que se encuentran cerca de la fuentes emisoras contienen una concentración de PM con contenido de materiales ferrimagnéticos (óxidos e hidróxidos de hierro). El material particulado que proviene de quema de combustibles fósiles, procesos metalúrgicos, emisiones de los vehículos, abrasión y corrosión de piezas metálicas contienen minerales magnéticos que contienen MP. Los minerales magnéticos (maghemita, la magnetita y/o la titanomagnetita) adsorben y absorben iones de MP, es por esta razón que un monitoreo de MPs en el aire puede hacerse de forma indirecta mediante el uso de propiedades magnéticas. El uso de un enfoque magnético como una herramienta de medición es más simple y más rentable que los métodos químicos tradicionales (Cejudo et al., 2015; Li et al., 2017; Hofman et al., 2017).

Los parámetros magnéticos generalmente empleados con un enfoque ambiental son: la susceptibilidad magnética (κ) y la magnetización remanente isotérmica de saturación (MRIS), debido a que estas propiedades muestran una relación proporcional con la concentración de ciertos MPs (Aguilar et al., 2011). La susceptibilidad magnética (κ) mide la capacidad que tiene un mineral para magnetizarse en presencia de un campo magnético, proporciona información sobre los minerales que se encuentran en el polvo, los sedimentos, los suelos y las rocas, especialmente los minerales magnéticos que contienen hierro (Dearing, 1999). La MRIS permite identificar la presencia de minerales de baja y alta coercitividad magnética por medio de su interacción con un campo magnético. Los minerales de baja coercitividad (ferrimagnéticos) interactúan rápidamente con campos de 200 a 300 mT. Mientras que, los minerales de alta

coercitividad (antiferromagnéticos) interaccionan con campos magnéticos de 1 a 2 Teslas (Dearing, 1999).

Considerando los niveles de contaminación del aire en algunos sectores del país y partiendo de la necesidad de alternativas para ampliar, en escala espacial y temporal, el monitoreo de la contaminación por MPs, se propuso la creación de modelos predictivos estadísticos, basados en métodos alternativos de apoyo a los tradicionales, efectivos, de menor costo en recursos y tiempo. Para ello se eligió como sitio de estudio la GAM, en esta se seleccionaron los sitios de muestreo partiendo de las rutas vehiculares primarias y utilizando como criterio de selección la densidad vehicular. En los sitios se tomaron muestras de biomonitores y polvo de carretera en dos periodos (2020 y 2021) en época seca (febrero-marzo). Las muestras se analizaron química y magnéticamente para posteriormente identificar las correlaciones estadísticas entre el contenido de metales pesados (Fe, Cu, Cr, Pb, Ni, V, Cd y Zn) y las propiedades magnéticas (χlf y $\chi df\%$), con el fin de crear modelos de predicción. Los modelos fueron creados utilizando enfoques de aprendizaje automático, MLR y SVM. Los mismos fueron validados por medio de 3 métodos; validación cruzada (Data Split 80/ 20 en inglés), prueba de los modelos con datos de sitios de muestreo nuevos y la creación de una matriz de confusión. Adicionalmente, con los datos de los resultados químicos en biomonitores y polvo de carretera se obtuvo el índice de contaminación, Factor de Enriquecimiento (FE) (Okedeyi et al., 2014; Cai et al., 2015). También se realizó una evaluación de la contaminación para los sitios de estudio aplicando los índices; el Factor de Contaminación (FC) (Maurya & Kumari, 2021; Bisht et al., 2022) y el índice de carga de contaminación (PLI siglas en inglés) (Ihl et al., 2015; Olusegun et al., 2021). Estos últimos utilizados para la construcción de matriz de confusión.

Esta investigación es la primera en el país que relaciona las propiedades magnéticas con el contenido de metales pesados en diferentes muestras ambientales, además de la utilización de herramientas de modelaje automático, como el MLR y SVM, para identificar contenido de metales pesados, dando paso a un método de monitoreo de bajo costo en recursos y tiempo, eficiente que podría tener implicaciones importantes como método de cribado (en inglés, screening) para el reconocimiento de posibles cargas de contaminación por metales pesados, que apoyaría las metodologías de monitoreo tradicionales.

2. Objetivos

2.1. Objetivo general

Generar un modelo de monitoreo de la contaminación atmosférica por metales pesados en zonas de flujo vehicular basado en las propiedades magnéticas de bioindicadores y polvo urbano.

2.2. Objetivos específicos

1. Determinar parámetros magnéticos y contenido de metales pesados en diferentes bioindicadores y polvo urbano en distintas zonas de la Gran Área Metropolitana (GAM).

2. Analizar mediante métodos estadísticos las correlaciones entre varios contaminantes atmosféricos y las propiedades magnéticas de bioindicadores y polvo urbano.

3. Formular un modelo estadístico que permita cuantificar el contenido de metales pesados a través de las mediciones de las propiedades magnéticas en bioindicadores y polvo urbano.

3. Síntesis

Se escribieron cuatro artículos relacionados con los diferentes objetivos específicos de este trabajo, y que sumados responden al cumplimiento del objetivo general de este trabajo: Generar un modelo de monitoreo de la contaminación atmosférica por MPs en zonas de flujo vehicular basado en las propiedades magnéticas de bioindicadores y polvo urbano como método alternativo de bajo costo.

El primer artículo, titulado "*Magnetic and chemical testing in plants, road dust and soil, as indicators of atmospheric pollution*", corresponde a los resultados de un estudio preliminar relacionado con el Objetivo específico 1: Determinar parámetros magnéticos y contenido de MPs en diferentes bioindicadores y polvo urbano en distintas zonas de la GAM. En este artículo se desarrolló la metodología de selección de los sitios de estudios y de los bioindicadores, así como el tipo de muestreo y obtención de la concentración de MPs. Se analizaron 3 diferentes tipos de plantas como posibles biomonitores de la contaminación del aire por metales pesados; el ciprés (*Cupressus lusitanica),* el limón ácido (género *Citrus*) y el laurel de la India (*Ficus benjamina L*.), el polvo de carretera y suelo (superficial y profundo). Los resultados indicaron que el material particulado retenido en *Cupressus lusitanica* y el polvo de carretera exhibieron las características magnéticas y de concentración de MP necesarias para la generación del modelo predictivo. Además, se identificó la necesidad de realizar una nueva selección de sitios de muestro basados en la diferencia de la densidad vehicular, con el fin de identificar diferentes niveles de concentración de MPs para que los modelos a generar fueran capaces de trabajar bajo esta variable. El resultado más importante de este trabajo fue la comprobación de la correlación lineal entre las propiedades de susceptibilidad magnética másica (χlf) y la magnetización remanente isotérmica de saturación (MRIS), permitiendo identificar el uso de una sola propiedad magnética como variable preferencial para la construcción del modelo predictivo, lo cual disminuyo los costos analíticos.

El segundo artículo, titulado "*Assessing Magnetic Properties and Heavy Metal Content as a Screening Method for Air Pollution Monitoring*" cubre aspectos de los Objetivos específicos 1 y 2: Con respecto al Objetivo específico 1, el artículo muestra los resultados químicos y de propiedades magnéticas de las muestras de estudio, las cuales se utilizaron de entrada (*input*) en la construcción de los modelos predictivos. Con respecto al Objetivo Específico 2, "Analizar mediante métodos estadísticos las correlaciones entre varios contaminantes atmosféricos y las

propiedades magnéticas de bioindicadores y polvo urbano", el artículo incluye los productos de los análisis estadísticos; coeficientes de correlación de Pearson. Encontrándose correlaciones significativas entre χlf y todos los metales estudiados en ambos biomonitores y con el hierro para el polvo de carretera. En este artículo, se hizo un análisis con respecto a los factores de enriquecimiento (FE), para los biomonitores y para el polvo de carretera, en estos análisis se encontró contenido cadmio por debajo de los límites de detección por lo que no se consideró en las evaluaciones de FE ni en los modelos. También, en este trabajo se comprueba la existencia de material particulado depositado en los biomonitores conclusión que se obtuvo un análisis de imágenes de microscopia electrónica de barrido (SEM).

El tercer artículo lleva por título "*Comparison Between Machine Linear Regression (MLR) and Support Vector Regression (SVR) as Model Generators for Heavy Metal Assessment Captured in Biomonitors and Road Dust*". El mismo está relacionado con el Objetivo específico 3: Formular un modelo estadístico que permita cuantificar el contenido de MPs a través de las mediciones de las propiedades magnéticas en bioindicadores y polvo urbano. El artículo comprende la creación y selección de los modelos de predicción de la concentración de MPs a partir de las propiedades magnéticas. Así mismo de la discriminación del mejor monitor entre los biomonitores y el polvo urbano estudiados. Para la creación de los modelos se utilizó el abordaje de aprendizaje automático (machine learning en inglés,) ya que el mismo permite la construcción y selección del modelo más eficiente posible a partir de los datos del estudio. Utilizando para ello los enfoques de la regresión lineal automática (MLR en inglés) y el soporte de vectorial automático (SVM en inglés) los cuales usaron las variable de simple (χlf) y múltiple (χlf y χdf%) dependiendo de las propiedades magnéticas utilizadas como entrada en los modelos. Considerando el índice de mejora (IR en inglés) para la selección del mejor modelo para cada monitor y metal estudiado. En este artículo se presentan los resultados de validación de los modelos por medio de: Validación cruzada (Data Split en inglés) y el uso de estimados con datos obtenidos en nuevos sitios. Considerando como criterio para evaluar el rendimiento de los modelos el R-cuadrado ajustado (R^2) y para evaluar la eficacia predictiva de los modelos el error medio absoluto (MAE) y el error medio cuadrático (RMSE).

De acuerdo con los resultados obtenidos, la utilización de propiedades magnéticas de las hojas de biomonitores sumadas al modelaje estadístico, permiten hacer predicciones acertadas (R^2

ajustado > 0,7) para varios de los MPs estudiados y para otros se pueden obtener estimaciones aproximadas (R^2 ajustado < 0,7), lo que permite utilizarlos como método de cribado.

El cuarto artículo titulado "*Assessing Heavy Metals Pollution Load Index (PLI) in Plants and Road Dust from Vehicular Emission*", presentó valoraciones de carga de contaminación considerando los índices de FC y PLI, empleando los resultados químicos de los MPs. Para esto se realizó una prueba de multi rango para los resultados de los análisis químicos resultando en una propuesta de valores límites de contaminación para los biomonitores estudiados y el polvo de carretera. Dichos límites fueron utilizados para el cálculo del PLI para los años 2020 y 2021, revelándose contaminación importantes por MPs en algunos de los sitios de muestreo y diferencias entre los años de muestreo. Posteriormente se realizó una matriz de confusión utilizando los valores de PLI químicos como referencia y los PLI estimados por los modelos creados, obteniéndose datos adicionales de validación (exactitud, sensibilidad y especificidad) para los modelos creados considerando este índice de contaminación.

4. ARTÍCULOS

4.1 Magnetic and chemical testing in plants, road dust and soil, as indicators of atmospheric pollution

Salazar-Rojas, T; Cejudo-Ruiz, F. R.; Calvo-Brenes; G., (2022, en revisión) Magnetic and chemical testing in plants, road dust and soil, as indicators of atmospheric pollution. Enviado a revista *Water, Air, & Soil Pollution*.

Magnetic and chemical testing in plants, road dust and soil, as indicators of atmospheric pollution

Teresa Salazar-Rojas [1]*

Fredy Ruben Cejudo-Ruiz[2]

Guillermo Calvo-Brenes [3]

Abstract

Airborne particulate pollution, which contains heavy metals (HMs) among other contaminants, is associated with many health effects related to respiratory problems, such as cardiopulmonary lesions and systemic diffusion. This study aimed to evaluate the levels of HMs contamination using different biomonitors and indicators, as well as to evaluate the relationship between HMs content and magnetic properties in leaves of different types of biomonitors. For analysis, 180 samples were taken from biomonitors; *Cupressus lusitanica* (Cupressaceae), *Citrus* (Rutaceae), and *Ficus benjamina* (Moraceae), and road dust, surface and, deep soil. Seven HMs were measured: Cu, Pb, Ni, Cr, Fe, V, and Zn in all samples. Specific susceptibility (χlf), and isothermal remanent magnetization curves (IRM) were

[1] * Doctorado en Ciencias Naturales para el Desarrollo (DOCINADE), Escuela de Química, Tecnológico de Costa Rica; Universidad Nacional, Universidad Estatal a Distancia, Costa Rica; tsalazar@itcr.ac.cr; Código ORCID 0000000223663638.

[2] Instituto de Geofísica, Universidad Nacional Autónoma de México; Michoacán, México; ruben@geofisica.unam.mx, Código ORCID 0000-0003-1003-5664

[3] . Escuela de Química, Tecnológico de Costa Rica; Cartago, Costa Rica; gcalvo@itcr.ac.cr, Código ORCID 00000002-7021-3509.

Corresponding author: tsalazar@itcr.ac.cr. Teresa Salazar Rojas, Escuela de Química, Tecnológico de Costa Rica, Cartago, Apartado postal: 159-7050, Costa Rica.

assessed in biomonitors samples. The results revealed that the major biomonitor was *C. lusitanica*, which also showed the highest χlf (20.54 x10^8 m^3/kg) and IRM (2.66 mAm^2/kg). Additionally, given the low coercivity of the magnetic material found in the χlf and SIRM values, those magnetic properties can be used interchangeably to determine the magnetic minerals in the biomonitors studied. We conclude that the use of bioindicators and indicators presents a potential to be used as an alternative method for contaminant monitoring and the use of magnetic properties is feasible to measure air pollution.

Keywords: heavy metals, biomonitors, road dust, air pollution, magnetic properties, soil.

1. Introduction

Health effects associated with air pollution are related to respiratory problems, mainly correlated with time exposure of people to particulate matter (PM), especially the finer ones ($PM_{2,5}$), which cause cardiopulmonary injuries and systemic diffusion (Losacco & Perillo, 2018; Polezer et al., 2018; Lee et al., 2019). Among the different types of anthropogenic PM sources (PM_{10} and $PM_{2.5}$), are fossil fuels and their use in transportation is gaining more attention due to the excessive increase in the number of vehicles worldwide. The production growth from 2000 to 2018 was 34% for cars and 128% for trucks (Davis & Robert, 2021), causing a decrease in people health, mainly in cardiorespiratory diseases and diversification of environmental pollutants. Vehicle emissions generate greenhouse gases, PM_{10}, $PM_{2.5}$, as well as HMs (Cr, Cu, Ni, Pb, V, Fe, and Zn), due to combustion fuel and vehicles engine wear (Adachi & Tainosho, 2004; Ojekunle et al., 2015). HMs are especially relevant because they cannot be degraded or destroyed; although, they can be diluted by physical-chemical agents and therefore be leached, which then can form soluble complexes and then be transported and distributed in ecosystems by joining trophic chains where they can be bioaccumulated (Reyes et al., 2016). Among the different HMs, iron is a vastly common element in the environment; however, its presence is relevant because its coexistence with Ni, Cu, Zn, Cr, Cd and Pb is typically associated with traffic (Adachi & Tainosho, 2004).

Air pollution monitoring in Costa Rica is carried out through an air quality monitoring network in some sites of the Great Metropolitan Area (Briseño-Castillo et al., 2015). In addition, the United States embassy in San José, Costa Rica performs daily monitoring of $PM_{2.5}$ which is part of the Real-Time Air Quality Index (AQI) (World Air Quality Index Team, 2020). As a result

of this monitoring, it was found that Costa Rican air pollution problems are mainly associated with industrial, commercial, and traffic density (Briseño Castillo et al., 2015). For instance, since 2013 monitoring sites have reported concentrations of $PM_{2.5}$ (annual average of 15 $\mu g/m^{3)}$, which exceed the WHO limit (10 $\mu g/m^3$) (Briseño-Castillo et al., 2015; Poveda et al., 2020). Besides, the country has had significant annual growth in the vehicle fleet, an average of 6% each year from 1980 to 2019, increasing almost tenfold, from 180,986 units in 1980 to 1,752,813 in 2019. The vehicle fleet is mostly based on combustion engines, in 2019 the fuel type distribution was; 82% gasoline vehicles, 17.3% diesel, and the remaining 0.7% to hybrid electric or gas vehicles (Nation State Program, 2020).

Monitoring stations are expensive in installation and maintenance besides exposed to vandalism. An alternative method for air pollutants capture is the use of biomonitors, which have several advantages, like their lower cost as well as providing reliable data related to air pollutants content and information about its effects on living systems (Tomašević et al., 2011). This is possible because suspended particles (PM) deposit in the plants near roads and particles smaller than 10 µm in diameter (PM_{10}) can be trapped and encapsulated in the cuticle of the plant leaves (Bussotti et al., 2014).

Additionally, diagnostic and control studies to determine the content of HMs in the environment are not carried out with the required periodicity and extent, due to the high cost, time, and infrastructure required for chemical analysis. Therefore, techniques such as environmental magnetism have been studied, which allow relating the concentration of HMs in environmental samples with good precision, economical and easy to perform (Cejudo et al., 2015). This relationship has been the subject of many studies; *Tilia platyphyllos* (Malvaceae) (Mitchell & Maher, 2009); *Ficus benjamina* (Moraceae) (Aguilar et al., 2012); (Castañeda-Miranda et al., 2020); in urban soil, urban dust and leaves of *Sambucus nigra* (Viburnaceae) (Aguilar et al., 2013); in trees of *Platanus hispanica* (Platanaceae) (Aguilar et al., 2013), *Chamaecyparis lawsoniana* (Cupressaceae), *Ligustrum japonicum* (Oleaceae) and *Pinus brutia* subsp. eldarica (Pinaceae) (Kardel et al., 2018b; Khamesi et al., 2020). The results are significantly correlated in most of those matrices with magnetic properties and particulate matter contamination, making this method appealing for being less time consuming, nondestructive and lower cost. Therefore, the novelty of this work is the evaluation of new techniques on indicators such as soil and road dust and the inclusion of unreported species commonly found

in tropical climates. In addition to the evaluation of magnetic properties in bioindicators in different seasonal variations.

Considering the high levels of air pollution reported in some areas of the country, plus the necessity to find alternative and effective methods of a lower cost that may allow expanding the country's air quality monitoring program. The aims of this study were to evaluate the levels of HMs contamination using different biomonitors and indicators, as well as to evaluate the relationship between HMs content and magnetic properties in leaves of different types of biomonitors.

2. Material and methods

2.1 Sampling site

The study was carried out within the Great Metropolitan Area (GMA) of Costa Rica, which is located in the central region of the country, Fig. 1. The GMA has altitudinal variations from 500 to 3400 m above sea level (Ministry of Housing and Human Settlements, 2013). Even though it comprises only 3.8% of the national territory, 70% of the vehicle fleet, 60% of the population, and 85% of the industry are concentrated in this region (Briseño-Castillo et al., 2015). Geographically, the country is located within the planetary strip between the parallels Tropic of Cancer and Tropic of Capricorn, defined as Tropical Zone. This region confers tropical characteristics to its ecological environment: forests, hydrographic network, soils and climate (Solano et al., 2020).

Fig. 1. Study domain in the GMA of Costa Rica

The sites were selected due to their vehicle density obtained from the Traffic Information Yearbook 2019 (Ministry of Public Construction and Transportation, 2020): one low density (1), three medium density (2, 3, and 4), and one high density (5) (Table 1 and Fig. 1). Other criteria was their proximity to registered air quality monitoring sites, some with higher air pollution values of PM_{10} than the WHO recommended limit of an annual average of 20 $\mu g/m^3$ and the maximum value recorded in 24 hours of 50 $\mu g/m^3$ (Briseño-Castillo et al., 2015).

Table 1. Sample sites with the average daily number of vehicles and PM values registered.

#	Site Name	Daily average of vehicles[4]	PM_{10} Annual Average ($\mu g/m^3$)[2]	PM_{10} Maximum recorded in 24 hours ($\mu g/m^3$)[2]
1	Coronado, San José	2180	N.A	N.A.
2	Ribera of Belén, Heredia	11579	30	54
3	Alajuela, Alajuela	14373	30	78
4	Hatillo 4, San José	14868	26	47
5	Ochomogo, Cartago	25990	N.A	N.A

[1] (Ministry of Public Construction and Transportation, 2020). [2] (Briseño-Castillo et al., 2015). N.A. Not available.

The land use in all selected sites was residential with some commercial spots, except for Ochomogo which also presents some industries. All the samples were taken near the road, where more traffic pollutants are accumulated (Kawasaki et al., 2017).

2.2 Sampling and Sample preparation

2.2.1 Plants

The species were selected, after carrying out a census in July 2017, considering criteria of abundance, accessibility, longevity, and proximity to the road. A range of 1 to 3 trees of each species was sampled at each sampling site. The selected biomonitors are perennials, with a foliage duration of 2 years or more: *Cupressus lusitanica* (Cupressaceae) (Zamudio & Carranza, 1994), *Citrus* (Rutaceae) (Zhang et al., 2009), and *Ficus benjamina* (Moraceae) (Castañeda-Miranda et al., 2020). The first biomonitor will be referred to as Cypress, the second as Citric, and the third one as Ficus.

For analisys, 90 plant leaves samples were collected bimonthly from August 2017 to June 2018. Around 20 mature leaves per biomonitor were taken with hand shears in the lateral canopy facing the roadside at a height of 1.5 to 2.0 m, considering the normal human breathing height. Samples were stored in Petri dishes and transferred into an appropriate container.

Samples were dried at (55 ±1) ºC to constant weight and then ground for subsequent analysis at the laboratory following Aguilar et al., (2012).

2.2.2 Soil and Road dust

Sixty soil samples were collected bimonthly at the same sampling sites of the plants from August 2018 to June 2019. Approximately 1 kg of two composite samples was taken for each of the sites, considering the upper layer (surface soil, 5 cm) and another at one meter deep, using a hand drill digger (deep soil) to see possible heavy metal accumulation according to the method used by Huang et al., (2017).

Thirty road dust samples were collected on the road at the same sampling sites of the plants and for the same period, from August 2017 to August 2018. One square meter of the road surface was swept at the edge of the road, to ensure traffic dust as a main source of HMs according to Sanleandro et al., (2018).

2.3 Chemical Methods

Unwashed leaf powder samples were used for the analysis, as some wash/unwashed experiments show that this is the optimal method for the HMs of interest and the objective of this study (Gillooly et al., 2019); (Khamesi et al., 2020). Duplicates of the samples were analyzed for metal content: Cu, Cr, Cu, Ni, Pb, V, Zn, and Fe. All plants and soil samples were analyzed for HMs content by the Method 3050b Acid Digestion of Sediments, Sludges, and Soils (U.S. EPA, 1996) and measurements were carried out in an Atomic Absorption Spectrophotometer (Perkin Elmer, model AAnalyst 800), supported by a graphite furnace, and a hydride generator (Perkin Elmer, model FIAS 100), for the determination of concentrations at trace level. IV-Stock-10 from Inorganic Ventures was used as a reference standard.

2.4 Magnetic Measurements

2.4.1 Magnetic Susceptibility

The magnetic susceptibility of the samples was determined following the recommendations of (Dearing, 1999). Dry samples were crushed with a mortar and packed tightly in a 10 cm^3 plastic container. A Bartington MS2B single sample dual frequency sensor and a Bartington MS3

Magnetic Susceptibility Meter were used to measure the susceptibility at low frequency (κ_{LF} at 0,46 kHz) and high frequency (κ_{HF} at 46,0 kHz). Results were also used to determine:

The value of specific susceptibility:

$$\chi lf = \frac{\kappa lf}{\rho} \quad (1)$$

Where ρ is the density of the material in kg m^{-3}.

The percentage of frequency-dependent magnetic susceptibility:

$$\chi df\% = \left[\left(\frac{\kappa lf - \kappa hf}{\kappa lf}\right)\right] x\ 100 \quad (2)$$

Through these magnetic parameters, the concentration of magnetic material and the presence of ultrafine particles (≤ 30 nm) of ferrimagnetic (SP) characteristics in the leaves of biomonitors were identified.

2.4.2 Isothermal Remanent Magnetization

Isothermal remanent magnetization curves (IRM) of the dried encapsulated material were performed to detect the presence and concentration of the magnetic material in the leaves of the biomonitors. Several pulses of a magnetic field were applied in a range from 0 to 1000 mT with an IM-10 ASC pulse magnetizer. Between each applied pulse, the remanent magnetization was measured with a JR6 spinning magnetometer (AGICO). Subsequently, the applied field vs. the remanent magnetization was plotted to obtain the IRM curve.

The saturation isothermal remanent magnetization (SIRM) was used to identify and quantify the magnetic mineralogy of low magnetic coercivity present in the biomonitor leaves. The edits were made on the encapsulated sample, to which a directional magnetic field (+Z) of 1000 mT was applied using an ASC Scientific IM-10 pulse magnetizer, then the remanent magnetization was measured with a JR6 AGICO spinning magnetometer. Immediately after, a magnetic field in the opposite direction (-Z) of 300 mT was applied to the sample, and the remanent magnetization (MR_{-300}) was measured. With the data obtained, the S_{-300} ratio:

$$S_{-300} = \frac{IRM_{-300}}{SIRM} \quad (3)$$

This allows identifying the presence of magnetic minerals of low coercivity ($S_{-300} \geq 0.7$) or high coercivity (S_{-300} is < 0.7) in the material (Evans & Heller, 2003).

2.5 Statistical Analysis

The Statistical Program for Social Science Software (SPSS software, version 25) was used to graph the results. One-way analyses of variance (ANOVA) with the post-hoc Scheffe test, were performed to test the differences among samples/sites and Pearson's correlation analysis was carried to evaluate the relationship between HMs content in road dust and magnetic properties.

The magnetic properties correlations and the linear regression models for magnetic susceptibility values versus isothermal remanent magnetization for each biomonitor were evaluated using the Statgraphic Centurion XVI Software (Software, version 16.1.03).

The HMs content in indicators was evaluated according to national (Costa Rican Ministry of Health, 2013) as well as international regulations (Denneman and Robberse, 1990; World Health Organization, 1996; U.S. EPA, 2004) and related studies found in the literature. Since data on HMs in road dust are not available, soil standards were applied instead.

3 Results and Discussion

3.1 Plants HMs Content

Chemical analyses of heavy metal content were performed on each plant at each of the sampling sites (Fig. 2). Fig. 2a shows that the value of Cu in all sites and plants was at least twice higher than the allowed limit of 10 mg/kg (World Health Organization, 1996). Additionally, another author considers a normal Cu content in plants from 2 to 20 mg/kg, higher concentrations would be considered as HMs toxic condition for the plant (Caselles, 1998).

Pb, which is especially toxic to humans, animals, and plants, showed, Fig 2b, lower values than the limit (2 mg/kg) in almost all sites and plants, except for Cypress at the Ochomogo site (average of 15.15 ± 11.18 mg/kg), which is the highest vehicle density of all sites (Table 1) and present some industry. Besides the Pb average value in Ochomogo Cypress was many times higher than 1.80 mg/kg a value reported in pine needles by Khamesi et al. (2020) at Isfahan, Iran for heavy traffic road, so the high Pb value obtained could be due to another source than traffic.

Cr and Ni values, Fig. 2c, 2d, in all of the plants and sites studied were lower than the international maximum acceptable level, 30 mg/kg and 10 mg/kg respectively (World Health Organization, 1996). Nevertheless, Cypress in Ochomogo presented the highest Cr values (average 3.48 ± 1.88 mg/kg) of all biomonitors and sites.

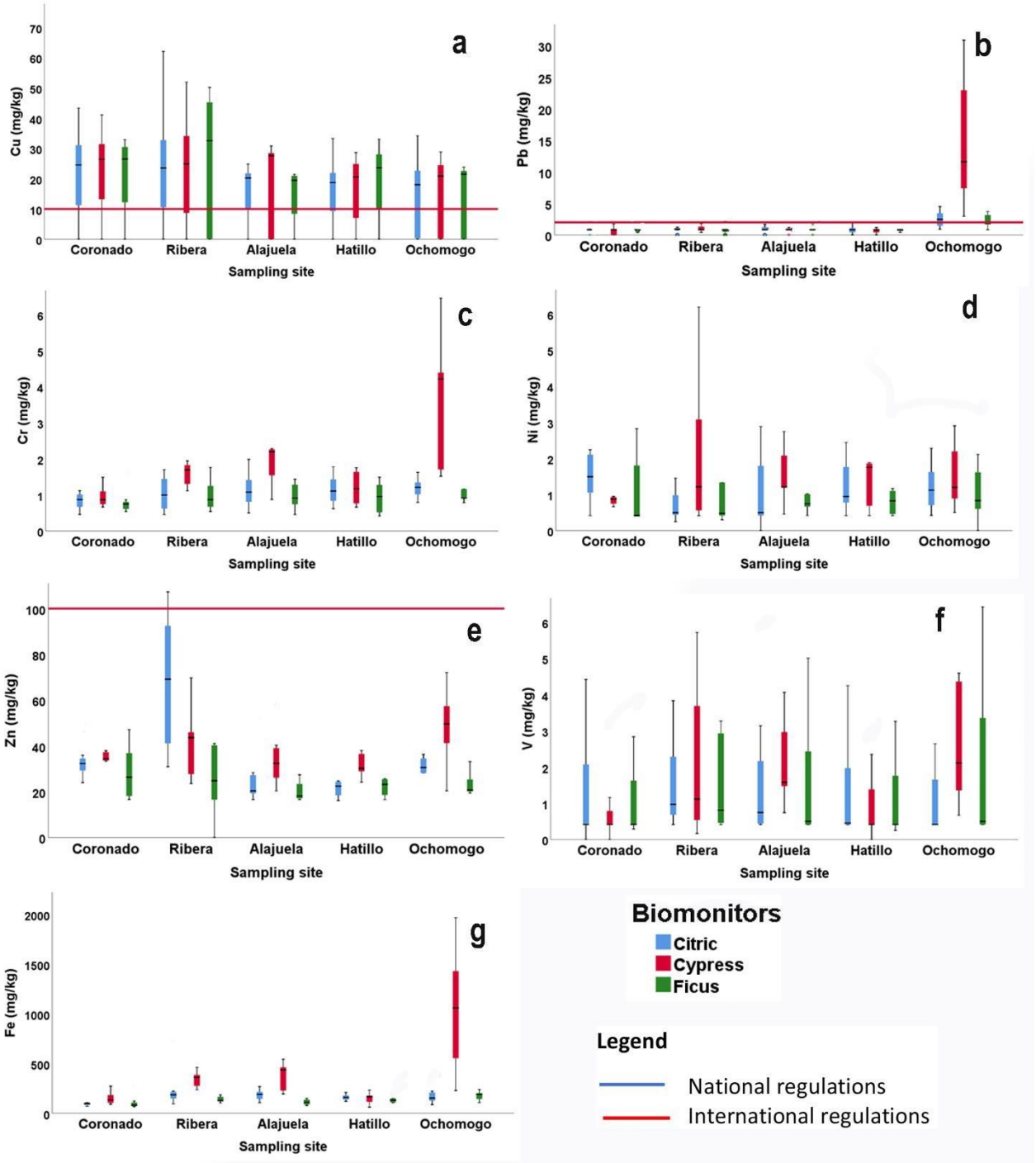

Fig. 2. Heavy metals concentration in plants leaves at sampling sites. a. Cu, b. Pb, c. Cr, d. Ni, e. Zn, f. V and g. Fe.

In the case of zinc (Fig. 2e), the values were below the WHO (1996) limit (100 mg/kg) and within the expected normal range (10 to 100 mg/kg) reported in plants by Simon-Hettich et al. (2001). Only the Ribera site overpassed the limits in Citric leaves (highest value 107.31 mg/kg). Most of the data showed acceptable values around 46 mg/kg, found by Caselles (1998) in *Citrus limon* (L.) leaves in Murcia-Alicante, Spain at different distances from a highway.

About Vanadium values (Fig. 2f), there is no legislation known in plants, however, the content obtained was higher at least in one biomonitor, in all sites, than the reference range from 0.5 to 2.0 mg/kg, which is considered as acceptable in plants where there is no atmospheric V contamination reported according to Morrell et al. (1986) and Alcalá et al. (2009).

The acceptable Fe range for plants is from 2 to 250 mg/kg (Akguc et al., 2010), as shown in Fig. 2g most of the plants presented values within that range, except for Cypress in Alajuela (365.50 ± 142.85 mg/kg), Ochomogo (1032.02 ± 625.26 mg/kg) and Ribera (340.80 ± 80.58 mg/kg). Moreover, some authors as Levy, D.B., Redente, E.F., and Uphoff (1999) specified that Fe concentrations higher than 500 mg/kg in plants are considered toxic. Based on that, only Cypress in Ochomogo has the Fe average value above that limit, which could be explained by its highest vehicle density Table 1, and the influence of some nearby industries.

Overall concerning bioindicators, it appears to be Cu and V pollution in plants nearby roads in all sampled sites and Ochomogo for Pb and Fe as well. The Cu and Pb results are in agreement with the highest values HMs found in PM in the GMA (Costa Rica), by Briseño-Castillo et al, (2015): Pb (14.51 ng/m^3) and Cu (222.19 ng/m^3). The concentration of these elements was found to be enriched by sources that were not of crustal origin such as combustion of fossil hydrocarbons, vehicular traffic, emissions from metal-mechanical industries, etc (Briseño-Castillo et al, 2015).

For most of the HMs, there was no statistical difference among biomonitors (Scheffe's test $\alpha = 0.05$). However, some individual values were higher than the rest of the data: Cr, Pb, Zn, and Fe for Cypress in Ochomogo; Cr for Cypress in Alajuela and Zn for Cypress in Alajuela, Coronado, and Hatillo. In general terms, Fig 2 shows a trend of slightly higher HMs values for Cypress, compared to Citrus and Ficus, which coincides with the results found by Wang et al., (2006) and Kardel et al., (2018a), who concluded that a larger microroughness leaf surface, such as Cypress leaves, will accumulate a larger amount of dust particles.

3.2 Road Dust and Soil

The values of Cu in soil (Fig. 3a), in all sites, were above the national (20 mg/kg) (Costa Rican Ministry of Health, 2013) and international (36 mg/kg) (Denneman and Robberse, 1990) limit regulations. Moreover, many of them exceeded the highest limit for soil found in literature reviews (10 mg/kg) (Romero et al., 1986; Muller et al., 1994).

The concentration of Pb (Fig. 3b) was below the Costa Rican limit (72 mg/kg) (Costa Rican Ministry of Health, 2013) as well as the international limit (85 mg/kg) (Denneman and Robberse, 1990), except for the road dust average values in Alajuela (91.55 ± 30.02 mg/kg) and Ochomogo (100.44 ± 53.81 mg/kg) that were considerably higher.

Referring to Cr (Fig. 3c), most of the sampling sites were below the international maximum Cr value of 100 mg /kg) (Denneman and Robberse, 1990), except deep soil in Ochomogo (maximum value of 128.33 mg /kg). However, Costa Rican regulations set the limit value at 2 mg/kg, if that is considered, all the reported data would be above that acceptable value.

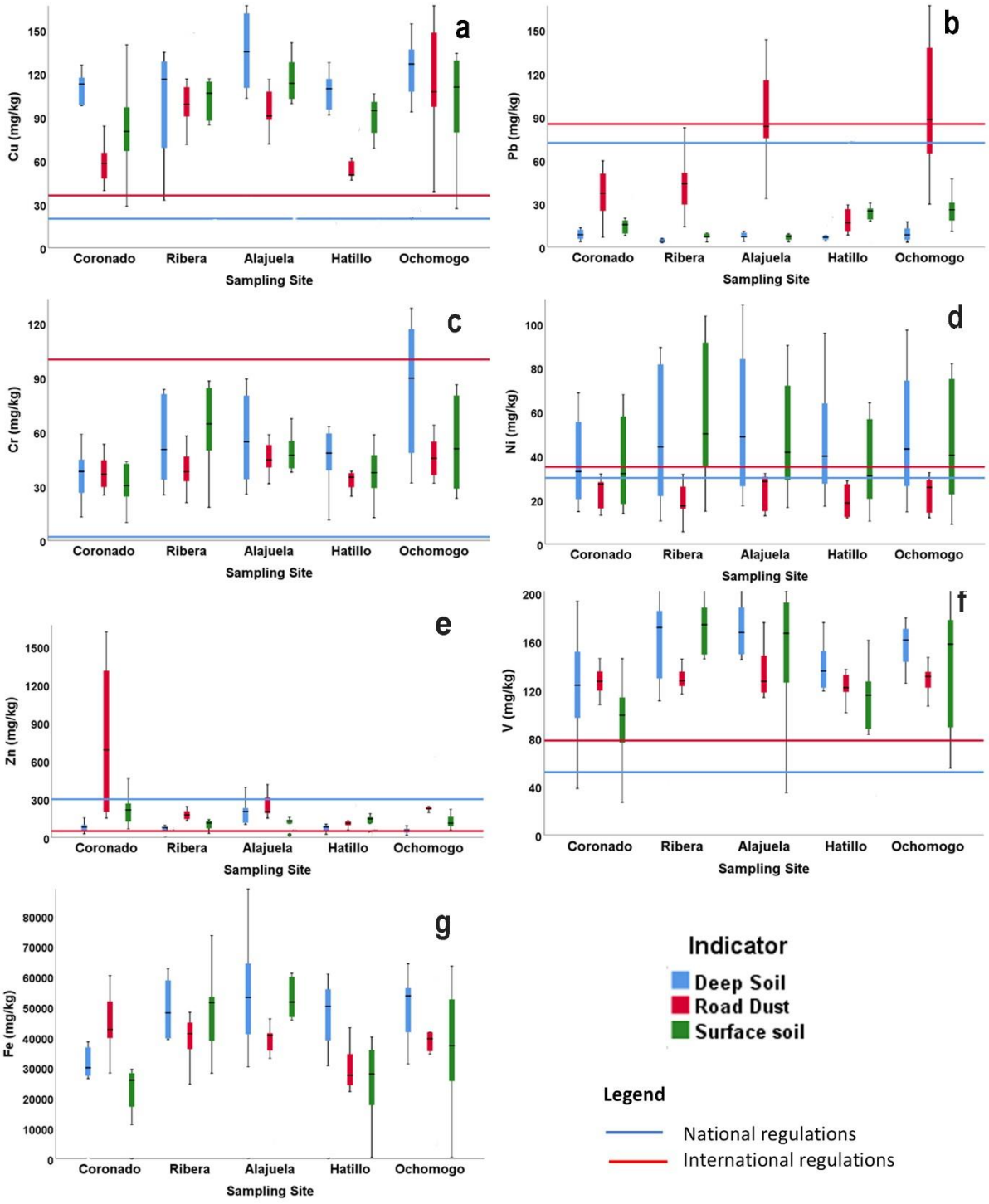

Fig. 3. Heavy metals concentration in road dust, deep and surface soil at sampling sites. a. Cu, b. Pb, c. Cr, d. Ni, e. Zn, f. V and g. Fe.

In Fig. 3d, all road dust samples were below the limit values for Ni, in contrast, most of the data for deep soil and surface soil were above both values limits, national (30 mg/kg) and international (35 mg/kg) (Denneman and Robberse, 1990).

About Costa Rican legislation for Zn (300 mg/kg) (Costa Rican Ministry of Health, 2013) most of the data obtained were below the level, except for road dust in Coronado (average value 774.55 ± 36.02 mg/kg) (Fig. 3e). However, considering the international limit of 50 mg/kg, almost all the data sites were higher than this level (Denneman and Robberse, 1990).

The V value (Fig. 3f), in all sites, was above national and international limits of 62 mg/kg (Costa Rican Ministry of Health, 2013) and 78 mg/kg (Denneman and Robberse, 1990), respectively. Some of the V values were even higher than the average value in the earth's crust of 150 mg/kg reported by Nielsen (1987). Regarding the Fe values obtained in surface soil, deep soil, and road dust, all of them were superior to those obtained by Peris, (2006) of 16.915 mg/kg in agricultural soils of Castellon, Spain. Nevertheless, the typical Fe concentration in soil varied in a range from 20000-550000 mg/kg (EPA, 2005), thus mostly deep soil samples presented data above this range.

In general, there seems to be Cu and V contamination at all sites, with similar results to biomonitors as well. Regarding other HMs, there is room for different interpretations depending on national and international legislation. However, the results show more HMs exceeding the limit concentrations in these indicators than in the biomonitors. It denotes higher HMs contamination in street dust, surface soil, and soils than in plants. A circumstance that should be considered by health authorities to protect people living near roads. Scheffe's test ($\alpha = 0.05$) showed no significant difference among most of the sampling sites and the different indicators for Cu, Ni, Zn, V, and Fe. However, some individual values were higher than the rest of the data: Pb for road dust in Alajuela and Ochomogo. Nevertheless, Fig 3 shows a trend, in most of the HMs where there is a higher content from road dust, to surface soil and to deep soil, which could be explained by the lixiviation.

Pondering the HMs content, in indicators and bioindicators, it showed the following order from highest to lowest content, Table 2. Since Fe showed the highest concentration on each indicator, it is first on the list (Table 2). In plants, its concentration was from 100 to 450 mg/kg, except Cypress in Ochomogo site with higher concentrations from 500 to1400 mg/kg, approximately. In soils and dust, concentration varies from 20000 to 65000 mg/kg, being the upmost at Ochomogo and those values could be explained due to the highest vehicle density

of the road nearby (25990 vehicle-day, see Table 1). Zn was next in order in plants, road dust, and surface soil; meanwhile, in deep soil, it appeared fourth on the list. Zn in plants ranged from 15 to 80 mg/kg; in road dust, its concentration was from 100 to 300 mg/kg and in soils was from 50 to 300 mg/kg. The Zn values found could be explained by the burning of fossil fuels (Weissmannová & Pavlovský, 2017) and the tire tread which contains ZnO particles (Adachi & Tainosho, 2004). The rest of the metals showed variable positions depending on the biomonitor and indicator.

Table 2. HM content order according to each indicator

Indicator	Metal content (mg/kg)
Plants	Fe>Zn>Cu>V>Pb, Cr, Ni
Road dust	Fe>Zn>V>Pb, Cu>Cr>Ni
Surface soil	Fe>Zn>V>Cu>Cr, Ni>Pb
Deep soil	Fe>V, Cu>Zn>Cr, Ni>Pb

3.3 Magnetic Measurements

3.3.1 Citric

The biomonitor Citrus (Fig. 4a), showed χlf values between 0.0094 to 0.0484 $x10^{-6}$ m^3 /kg for 2017 and 2018; SIRM values between 0.16 to 0.50 mAm^2/kg (Fig. 4b); χdf% some values >14 indicating a strong presence of superparamagnetic particles (<0.30 µm) (Fig. 4c) (Dearing, 1999) and Fig. 4d, S_{-300} values > 0.7 indicated the presence of low coercivity magnetic minerals (Evans & Heller, 2003).

In June 2018, Fig. 4a and 4b, the sites showed the highest χlf and SIRM values, while, in October 2017 the lowest values were reported. The Alajuela and Rivera sites presented the highest concentration of magnetic minerals in June 2018. In October 2017, the Hatillo site showed higher values of magnetic material compared to the other sites. A variability of magnetic material between monitoring sites is observed, a phenomenon that can be attributed to anthropogenic activity at each site.

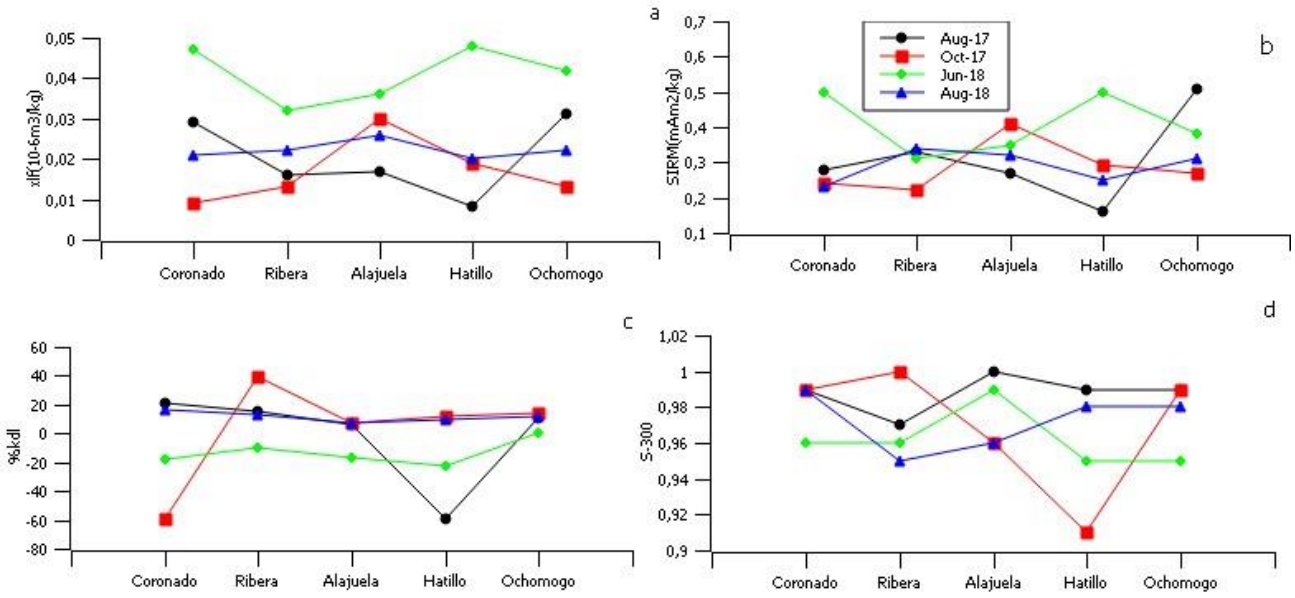

Fig. 4. a. Magnetic susceptibility value, b. saturation isothermal remanent magnetization, c. percentage of frequency dependent magnetic susceptibility, and d. S_{-300} ratio reported in the different sampling sites and sampling time for Citric.

3.3.2 Ficus

The biomonitor Ficus (Fig. 5a), χlf values between 0.010 to 0.0605 x10-6 m3/kg for 2017 and 2018; SIRM values between 0.16 to 0.44 mAm2/kg (Fig. 5b); χdf% some values >14 indicating a strong presence of superparamagnetic particles (<0.30 µm) (Fig. 5c), mainly in October. Fig. 5d, S-300 values, were > 0.7, indicating the presence of low coercivity magnetic minerals. The Rivera site in October 2017 reported an S300 value < 0.7 indicating the presence of high coercivity magnetic material, a material usually found in natural environments such as soil.

In Fig. 5, variability of magnetic material was observed between monitoring sites for the biomonitor Ficus. The Rivera site showed the highest concentration of magnetic material in October 2017 and June 2018. The Alajuela site recorded the lowest concentrations of magnetic material. In October 2018, the lowest concentration of magnetic material was recorded at that site.

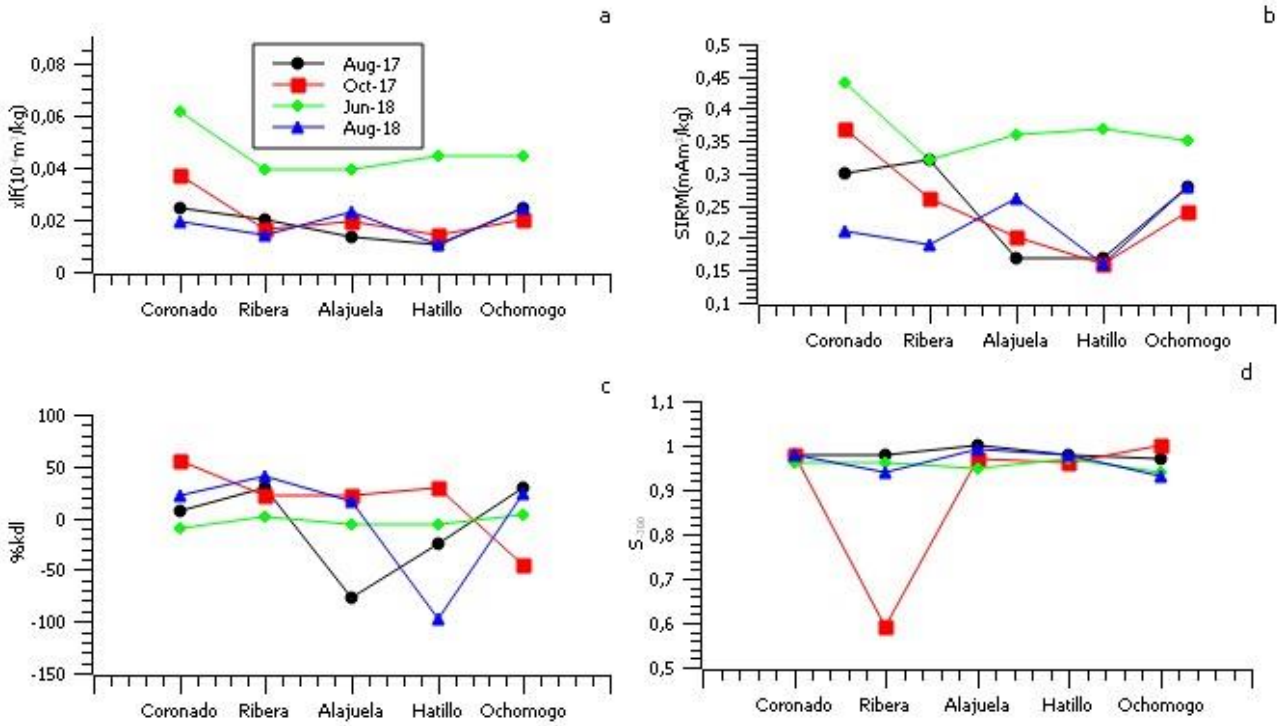

Fig. 5. a. Magnetic susceptibility value, b. saturation isothermal remanent magnetization, c. percentage of frequency dependent magnetic susceptibility, and d. S_{-300} ratio reported in the different sampling sites and sampling time for Ficus.

3.3.3 Cypress

Cypress showed (Fig. 6a), χlf values between 0.0157 to 0.02054 $x10^{-6}$ m^3/kg for 2017 and 2018; SIRM values between 0.35 to 2.66 mAm^2/kg (Fig. 6b). The highest concentration of magnetic material is recorded in June 2018, whereas the lowest concentration of magnetic material occurred in October 2017. However, in Fig. 6c, χdf% some values > 14 which indicated a strong presence of superparamagnetic particles (<0.30 µm), were presented in October 2017. In all months sampled (Fig. 6d), S_{-300} values > 0.7 were recorded, indicating the presence of low coercivity magnetic minerals.

In Fig. 6, a variability of magnetic material was observed among the monitoring sites for the Cypress. The Alajuela and Ochomogo sites presented the highest concentration of magnetic material for all sampling months. The recording of both magnetic parameters in the Cypress was similar. The amount of accumulated material in the Cypress was higher than in the other biomonitors.

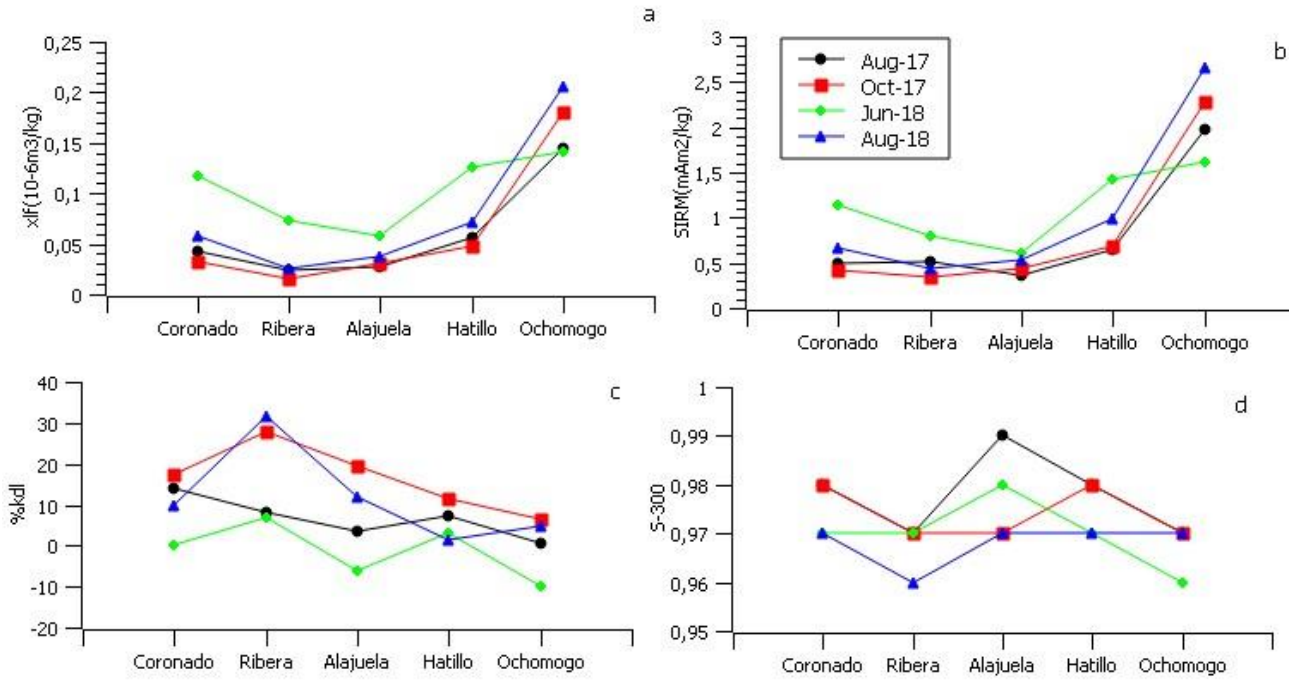

Fig. 6. a. Magnetic susceptibility value, b. saturation isothermal remanent magnetization, c. percentage of frequency dependent magnetic susceptibility, and d. S_{-300} ratio reported in the different sampling sites and sampling time for Cypress.

For utmost, all the sites and biomonitors showed the highest value in χlf and IRM in June, which can be explained, by June being the driest of the months measured in the study.

The IRM curves of the biomonitor samples exhibited saturation around 300 mT, and maintain a constant value between 700 to 1000 mT, so the presence of low coercivity magnetic material is scarce (Figure 8). All samples presented $S_{-300} > 0.7$, which corresponds to the presence of low coercivity magnetic material in all samples (Fig. 7). Similar to S_{-300} values, lower than 1.0, were found in *Ficus benjamina* by Aguilar et al., (2012) in Michoacán, México.

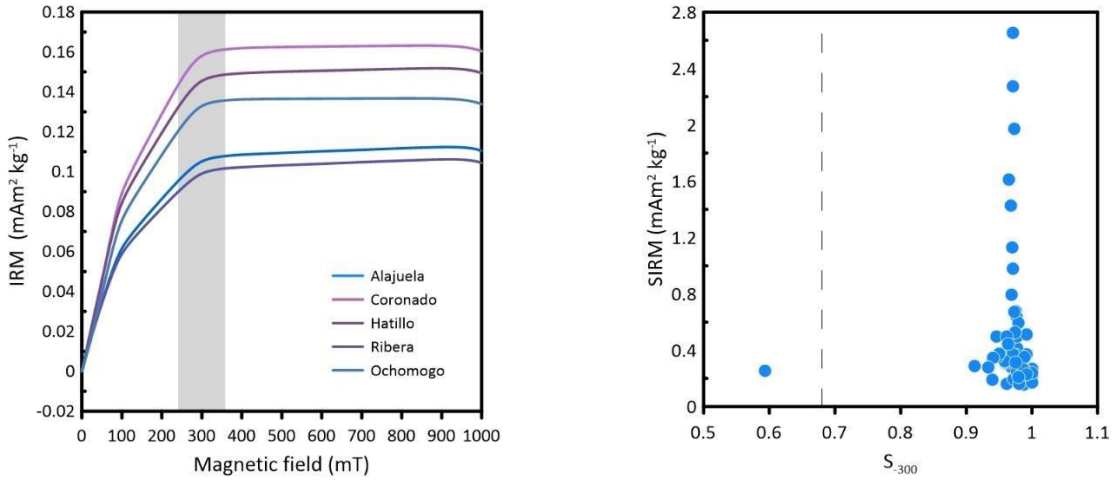

Fig. 7. IRM curve for citric and S_{-300} ratio of biomonitor samples.

Taking into account that plants are formed by organic matter, which should present a diamagnetic response (weak negative susceptibility) (Dearing, 1999), the results of Figures 4, 5, and 6, show the presence of magnetic material in plants, probably of anthropogenic origin, deposited by the air as PM. This coincides with HMs values obtained in the chemical analysis in plants, Fig. 2, and Table 3 that revealed a significative positive Pearson's correlation between the magnetic parameter χlf ($10^{-6}m^3/kg$), SIRM(mAm^2/kg), and 6 of the 7 HMs studied.

Table 3. Pearson's correlation for magnetic properties and HMs. Correlations with p <0,05 are shown in italic.

		Fe (mg/kg)	Cu (mg/kg)	Pb (mg/kg)	Cr (mg/kg)	Ni (mg/kg)	V (mg/kg)	Zn (mg/kg)
χlf ($10^{-6}m^3/kg$)	Pearson's correlation	*0.594*	0.031	*0.456*	*0.481*	-0.093	*0.226*	0.151
	Sig. (bilateral)	0.000	0.772	0.000	0.000	0.388	0.033	0.157
SIRM(mAm^2/kg)	Pearson's correlation	*0.688*	-0.106	*0.701*	*0.631*	0.146	0.173	0.127
	Sig. (bilateral)	0.000	0.425	0.000	0.000	0.271	0.191	0.339

Additionally, given the low coercivity of the magnetic material found in the χlf and SIRM values, a linear regression model for magnetic susceptibility values versus isothermal remanent magnetization for each biomonitor studied was evaluated to find out if those magnetic properties could be used interchangeably to determine the magnetic minerals.

A strong linear relationship was observed, Fig. 8 and Table 7, between the values of χlf and SIRM, with a linear correlation coefficient of 0.87 and an R^2 value of 77% for the biomonitor Citric, the Durbin-Watson (DW) statistical analysis showed that there is no indication of serial autocorrelation in the residuals with a confidence level of 95.0%. This means that the increase of low coercivity magnetic minerals in plants can be described by both parameters in terms of a linear relationship.

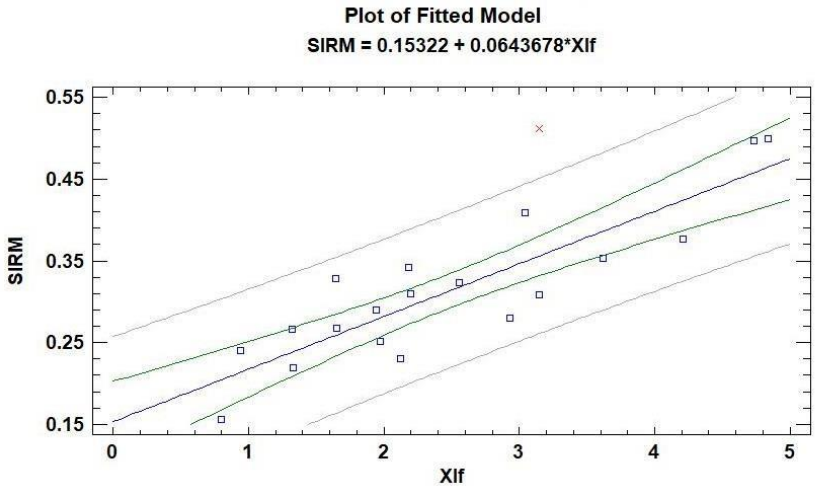

Fig. 8. Linear regression model for magnetic parameters of the Citric biomonitor.

A strong linear relationship was noted, Fig. 9 and Table 7, between the χlf and SIRM values, with a linear correlation coefficient of 0.98 and an R^2 value of 96% for the Cypress, the Durbin-Watson (DW) statistical analysis showed that there is no indication of serial autocorrelation in the residuals with a confidence level of 95.0%).

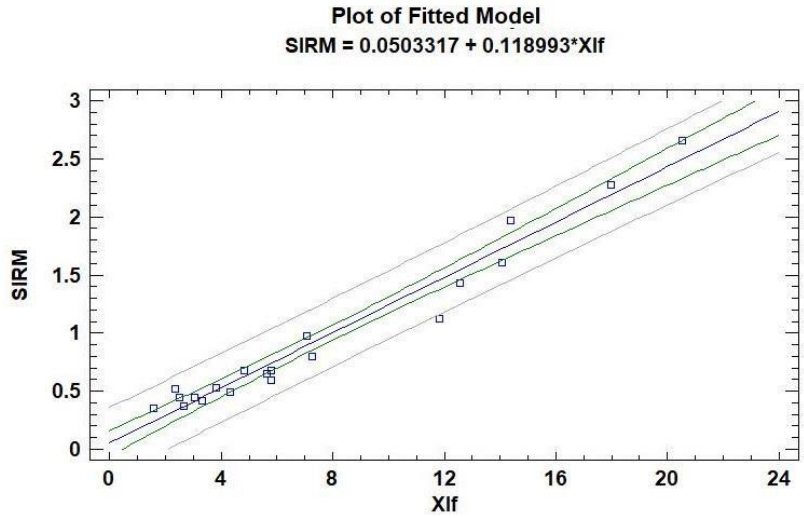

Fig. 9. Linear regression model for magnetic parameters of the Cypress biomonitor.

A strong linear relationship was observed in Fig. 10 and Table 4, between the χlf and SIRM values, with a linear correlation coefficient of 0.92 and an R^2 value of 85% for the Cypress. The Durbin-Watson (DW) statistical analysis showed that there is no indication of serial autocorrelation in the residuals with a confidence level of 95.0%.

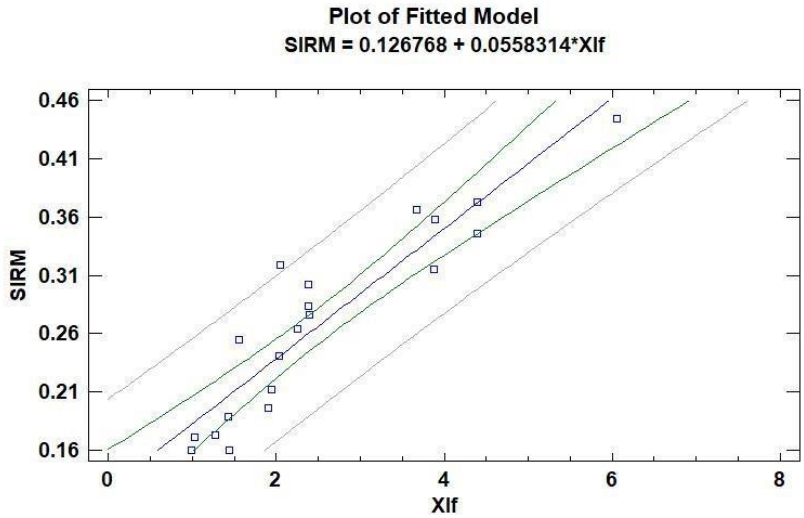

Fig. 10. Linear regression model for magnetic parameters of the Ficus bioindicator.

Table 4. Linear regression models for magnetic parameters and biomonitors

Bioindicator	Model	CC	R^2	Durbin-Watson
Citric	SIRM = 0.15322 + 0.0643678* χlf	0.88	76.98	2.541
Cypress	SIRM = 0.0503317 + 0.118993* χlf	0.98	96.22	1.904
Ficus	SIRM = 0.126768 + 0.0558314* χlf	0.92	84.88	1.615

The linear regression models (LRM) between χlf and SIRM of the biomonitors indicated that the concentration of magnetic material is proportional. The MRL model of Cypress showed a higher rate of change between χlf and SIRM, due to a higher concentration of material in its foliage (Figure 11). The results show that χlf and SIRM can be used interchangeably to determine the magnetic mineral in all the biomonitors, given the relationship between the parameters, the magnetic material found in the biomonitors has ferrimagnetic characteristics of low coercivity.

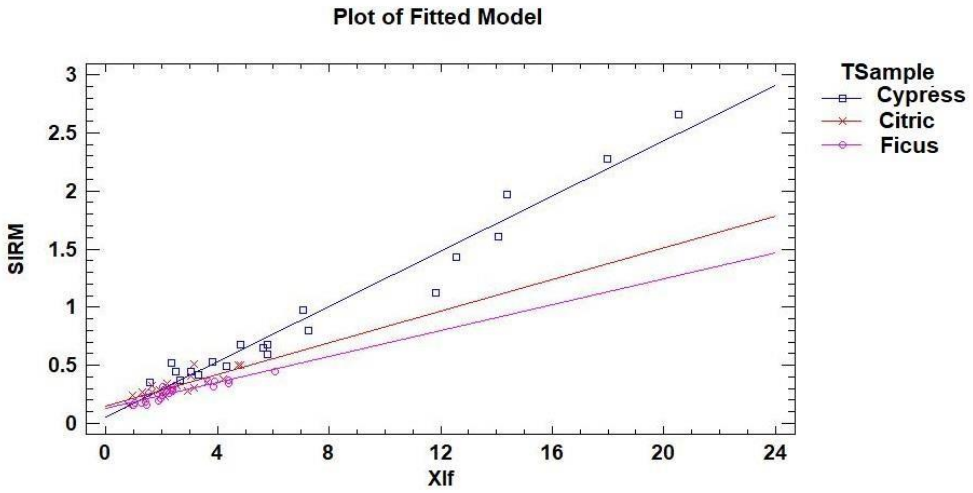

Fig. 11. Linear regression models between χlf and MRIS for the different biomonitors.

These correlation results show that χlf and SIRM can be used interchangeably to determine the magnetic mineral in the biomonitors, given the relationship between the parameters and the magnetic material found in the biomonitors has ferrimagnetic characteristics of low coercivity.

4 Conclusions

In general, the use of bioindicators and indicators in this research allowed us to determine compliance with different regulations, indicating their potential to be used as an alternative method for contaminant collection. *C. lusitanica* stood out in many of the measurements, probably based on its characteristics of a large microroughness leaf surface, that is not present in the other plants' leaves studied.

The difference in HMs content in indicators (road dust, surface soil to deep soil) is at least ten times higher than in plants; moreover, the trend within indicators, seems to indicate that the HMs content in the PM first accumulates on plant leaves, then leaches into road dust and surface soil, ending up in deep soil, the latter showing a higher non-compliance with national and international studies and higher values than other studies. Ochomogo site, with the highest vehicle density and nearby industries, showed the highest HMs values for many of the biomonitors and indicators, specific susceptibility, and isothermal remanent magnetization indicating that traffic density and industry have an important relation with pollution in nearby road plants and soils. The magnetic properties studied in different biomonitors leaves presented a positive correlation with many of HMs content, making this method feasible to measure air pollution. Moreover, susceptibility and isothermal remanent magnetization can be used interchangeably to determine the magnetic mineral in the biomonitors study, given the relationship between the parameters, and the magnetic material found in the biomonitors that have ferrimagnetic characteristics of low coercivity.

Declarations

Acknowledgements

The authors thank the Technological Institute of Costa Rica (ITCR) and the National Autonomous University of Mexico (UNAM), for their financial and administrative support. In addition, the Center for Research in Environmental Protection (CIPA), Center for Research and Chemical and Microbiological

Services (CEQIATEC) (Costa Rica) and Institute of Geophysics (Morelia) for their support to the project. Likewise, to the Costa Rican Petroleum Refinery (RECOPE) for their collaboration in taking samples at the Ochomogo site.

Compliance with ethical standards Bioindicators were collected in accordance with the ethical standards of the Technological Institute of Costa Rica.

Consent to participate Consent for publication

Conflict of interest the authors declare that they have no conflict of interest.

Availability of data and material Will be considered upon request.

Code availability Not applicable**.**

5 References

Adachi, K., & Tainosho, Y. (2004). Characterization of heavy metal particles embedded in tire dust. *Environment International*, *30*(8), 1009–1017. https://doi.org/10.1016/j.envint.2004.04.004.

Aguilar, B., Cejudo, R., Martínez, J., Bautista, F., Goguitchaichvili, A., Carvallo, C., & Morales, J. (2012). Ficus benjamina leaves as indicator of atmospheric pollution: A reconaissance study. *Studia Geophysica et Geodaetica*, *56*(3), 879–887. https://doi.org/10.1007/s11200-011-0265-1.

Aguilar, B., Mejía, V., Goguitchaichvili, A., Escobar, J., Bayona, G., Bautista, F., Morales, J., & Ihl, T. (2013). Reconnaissance environmental magnetic study of urban soils, dust and leaves from Bogotá, Colombia. *Studia Geophysica et Geodaetica*, *57*(4), 741–754. https://doi.org/10.1007/s11200-0120682-9.

Akguc, N., Ozyigit, I. I., Yasar, U., Leblebici, Z., & Yarci, C. (2010). Use of pyracantha coccinea Roem as a possible biomonitor for the selected heavy metals. *International Journal of Environmental Science and Technology*, *7*(3), 427–434. https://doi.org/10.1007/BF03326152.

Alcalá, J., Sosa, M., Moreno, M., Rodríguez, J., Quintana, C., Terrazas, C., & Rivero, O. (2009). Metales pesados en suelo urbano como un indicador de la calidad ambiental: ciudad de Chihuahua, México. *Multequina*, 39–54.

Briseño-Castillo, J., Herrera-Murillo, J., Solórzano-Arias, D., Beita-Guerrero, V. H., & Rojas-Marin, J. F. (2015). *VI Informe de Calidad del Aire Área Metropolitana de Costa Rica*. MINAE.

Bussotti, F., Pollastrini, M., Killi, D., Ferrini, F., & Fini, A. (2014). Ecophysiology of urban trees in a perspective of climate change. *Agrochimica*, *58*(3), 247–268. https://doi.org/10.12871/0021857201431.

Caselles, J. (1998). Levels of lead and other metals in citrus alongside a motor road. *Water, Air, and Soil Pollution*, *105*(3–4), 593–602. https://doi.org/10.1023/A:1004937224850

Castañeda-Miranda, A. G., Chaparro, M., Pacheco-Castro, A., Chaparro, M., & Böhnel, H. (2020). Magnetic biomonitoring of atmospheric dust using tree leaves of Ficus benjamina in Querétaro (México). *Environmental Monitoring and Assessment*, *192*(6). https://doi.org/10.1007/s10661-0208238-x.

Cejudo, R., Bautista, F., Quintana, P., Delgado, M. del C., Aguilar, D., Goguitchaichvili, A., & Morales, J. J. (2015). Correlación entre elementos potencialmente tóxicos y propiedades magnéticas en suelos de la Ciudad de México para la identificación de sitios contaminados: definición de umbrales magnéticos. *Revista Mexicana de Ciencias Geológicas*, *32*(1).

Costa Rican Ministry of Health. (2013). Reglamento sobre valores guía en los suelos para la descontaminación de sitios afectados por emergencias ambientales y derrames N° 37757-S. Sistema Costarricense de Información Juridíca. http://www.pgrweb.go.cr/scij/Busqueda/Normativa/Normas/nrm_texto_completo.aspx?param1=NRTC&nValor1=1&nValor2=75223&nValor3=93682&param2=1&strTipM=TC&lResultado=2&strSi m=simp.

Davis, S. C., & Robert, G. B. (2021). Transportation Energy Data Book (39th ed.). Oak Ridge National Laboratory. https://tedb.ornl.gov/wp-content/uploads/2021/02/TEDB_Ed_39.pdf.

Dearing, J. A. (1999). Using the Bartington MS2 System. Environmental Magnetic Susceptibility, 52.

Denneman and Robberse. (1990). Ministry of Housing. Netherlands Goverment.

Evans, M. E., & Heller, F. (2003). Environmental Magnetism: Principles and Applications of Enviromagnetics. Acadeic Press.

Gillooly, S. E., Michanowicz, D. R., Jackson, M., Cambal, L. K., Shmool, J. L. C., Tunno, B. J., Tripathy, S., Bain, D. J., & Clougherty, J. E. (2019). Evaluating deciduous tree leaves as biomonitors for ambient particulate matter pollution in Pittsburgh, PA, USA. *Environmental Monitoring and Assessment*, *191*(12). https://doi.org/10.1007/s10661-019-7857-6.

Huang, S. H., Yang, Y., Yuan, C. Y., Li, Q., Ouyang, K., Wang, B., & Wang, Z. X. (2017). Pollution evaluation of heavy metals in soil near smelting area by index of geoaccumulation (Igeo). *IOP Conference Series: Earth and Environmental Science*, *52,012095*. https://doi.org/10.1088/17426596/52/1/012095.

Kardel, F., Wuyts, K., De Wael, K., & Samson, R. (2018). Biomonitoring of atmospheric particulate pollution via chemical composition and magnetic properties of roadside tree leaves. *Environmental Science and Pollution Research*, *25*(26), 25994–26004. https://doi.org/10.1007/s11356-018-2592-z.

Kawasaki, K., Horikawa, K., & Sakai, H. (2017). Magnetic biomonitoring of roadside pollution in the restricted. *Environmental Science and Pollution Research*, 10313–10325. https://doi.org/10.1007/s11356-017-8702-5.

Khamesi, A., Khademi, H., & Zeraatpisheh, M. (2020). Biomagnetic monitoring of atmospheric heavy metal pollution using pine needles: the case study of Isfahan, Iran. *Environmental Science and Pollution Research*, *27*(25), 31555–31566. https://doi.org/10.1007/s11356-020-09247-5.

Lee, D., Robertson, C., Ramsay, C., Gillespie, C., & Napier, G. (2019). Estimating the health impact of air pollution in Scotland, and the resulting benefits of reducing concentrations

in city centres. *Spatial and Spatio-Temporal Epidemiology*, *29*, 85–96. https://doi.org/10.1016/j.sste.2019.02.003.

Levy, D.B., Redente, E.F., and Uphoff, G. D. (1999). Evaluating the phytotoxicity of Pb-Zn tailings to big bluestem (Andropogon gerardii vitman) and switchgrass (Panicum virgatum L.). *Soil Science*. https://doi.org/doi:10.1097/00010694-199906000-00001.

Losacco, C., & Perillo, A. (2018). Particulate matter air pollution and respiratory impact on humans and animals. In *Environmental Science and Pollution Research* (Vol. 25, Issue 34, pp. 33901–33910). Springer Verlag. https://doi.org/10.1007/s11356-018-3344-9.

Ministry of Housing and Human Settlements. (2013). Relieve del área GAM.

http://exnet.mivah.go.cr/Documentos/PlanGAM2013/03.CARTOGRAFIA/3_Ambiental/Relieve.pdf Ministry of Public Construction and Transportation. (2020). ANUARIO DE INFORMACIÓN DE TRÁNSITO 2019.

Mitchell, R., & Maher, B. A. (2009). Evaluation and application of biomagnetic monitoring of trafficderived particulate pollution. *Atmospheric Environment*, *43*(13), 2095–2103. https://doi.org/10.1016/j.atmosenv.2009.01.042.

Morrell, B. G., Lepp, N. W., & Phipps, D. A. (1986). Vanadium uptake by higher plants: Some recent developments. *Environmental Geochemistry and Health*, *8*(1), 14–18. https://doi.org/10.1007/BF02280116.

Muller, H. W., Schwaighofer, B., & Kalman, W. (1994). Heavy metal contents in river s e d i m e n t s. *Water, Air, and Soil Pollution 72:*, *72*, 191–203.

Nation State Program. (2020). *Capítulo 4 : Aspectos sobre la composición de las emisiones en la flota vehicular que afectan la salud y el ambiente [Informe Estado de la Nación 2020]*. 151–174.

Nielsen, F. H. (1987). Vanadium. In W. Mertz (Ed.), *Trace Elements in Human and Animal Nutrition* (Fifth Edit, pp. 275–300). Academic Press. https://doi.org/10.1016/B978-0-08-092468-7.50013-2

Ojekunle, Z., Adeboje, M., Taiwo, A., Sangowusi, R., Taiwo, A., & Ojekunle, V. (2015). Tree Leaves as Bioindicator of Heavy Metal Pollution in Mechanic Village, Ogun State. *Journal of Applied Sciences and Environmental Management*, *18*(4), 639. https://doi.org/10.4314/jasem.v18i4.12.

Peris, M. (2006). *Estudio de metales pesados en suelos bajo cultivos hortícolas de la provincia de Castellón* [Tesis Doctorals, Universidad de Valencia. Servei de Publicacions].

https://www.tesisenred.net/handle/10803/9504;jsessionid=D0C8EFEC5F512D9DBF2228566C2813 E6.

Polezer, G., Tadano, Y. S., Siqueira, H. V., Godoi, A. F. L., Yamamoto, C. I., de André, P. A.,

Pauliquevis, T., Andrade, M. de F., Oliveira, A., Saldiva, P. H. N., Taylor, P. E., & Godoi, R. H. M. (2018). Assessing the impact of PM2.5 on respiratory disease using artificial neural networks. *Environmental Pollution*, *235*, 394–403. https://doi.org/10.1016/j.envpol.2017.12.111.

Poveda, L., Publicaciones, P. De, & Rica, C. (2020). Calidad ambiental en Costa Rica : Análisis y perspectivas desde la UNA. *Ambientico*, *274*(3), 11–15. http://www.galeriaambientalista.una.ac.cr/pdfs/ambientico/274.pdf#page=34.

Reyes, Y., Vergara, I., Torres, O., Díaz, M., & González, E. (2016). Contaminación por Metales Pesados: Implicaciones en Salud, Ambiente y Seguridad Alimentaria. *Revista Ingeniería, Investigación y Desarrollo*, *16*(2). https://doi.org/10.19053/1900771x.v16.n2.2016.5447.

Romero, F., Elejalde, C., & Azpiazu, M. N. (1986). Metal Plant and Soil Pollution Indexes. *Water, Air, and Soil Pollution*, *34*, 347–352. https://doi.org/https://doi.org/10.1007/BF00282735.

Sanleandro, P. M., Navarro, A. S., Díaz-Pereira, E., Zuñiga, F. B., Muñoz, M. R., & Iniesta, M. J. D. (2018). Assessment of heavy metals and color as indicators of contamination in street dust of a city in SE Spain: Influence of traffic intensity and sampling location. *Sustainability (Switzerland)*, *10*(11). https://doi.org/10.3390/su10114105.

Simon-Hettich, B., Wagner, D., Tomaska, L., & Malcolm, H. (2001). Environmental Health criteria 221. In *Environmental Health Criteria*. https://doi.org/10.1016/s0031-3025(16)36534-5.

Solano, J., Villalobos, R., & Instituto Meteorológico Nacional de Costa Rica (IMN). (2020). Regionalización de Costa Rica. *Regiones y Subregiones Climáticas de Costa Rica*, *mapa 1*, 1–32. https://doi.org/10.15517/psm.v18i2.45179.

Tomašević, M., Aničić, M., Jovanović, L., Perić-Grujić, A., & Ristić, M. (2011). Deciduous tree leaves in trace elements biomonitoring: A contribution to methodology. *Ecological Indicators*, *11*(6), 1689– 1695. https://doi.org/10.1016/j.ecolind.2011.04.017.

U.S. EPA. (1996). *Method 3050b Acid Digestion of Sediments, Sludges, and Soils 1.0 Scope and Application*. https://www.epa.gov/esam/epa-method-3050b-acid-digestion-sediments-sludges-andsoils.

U.S. EPA. (2004). *A preliminary remediation goals table. Region 9: The Pacific southwest.* https://www.epa.gov/aboutepa/epa-region-9-pacific-southwest.

U.S. EPA. (2005). Ecological soil screening level for iron interim final. *US Environmental Protection Agency - Office of Solid Waste and Emergency*, *November*, 211. https://rais.ornl.gov/documents/ecossl_iron.pdf.

Wang, L., Liu, L. Y., Gao, S. Y., Hasi, E., & Wang, Z. (2006). Physicochemical characteristics of ambient particles settling upon leaf surfaces of urban plants in Beijing. *Journal of Environmental Sciences (China)*, *18*(5), 921–926. https://doi.org/10.1016/S1001-0742(06)60015-6.

Weissmannová, H. D., & Pavlovský, J. (2017). Indices of soil contamination by heavy metals – methodology of calculation for pollution assessment (minireview). *Environmental Monitoring and Assessment*, *189*(12). https://doi.org/10.1007/s10661-017-6340-5.

World Air Quality Index Team. (2020). *The World Air Quality Project*. World-Wide Air Quality Monitoring Data Coverage. https://aqicn.org/contact/.

World Health Organization, W. (1996). *Permissible limits of heavy metals in soil and plants*. https://www.omicsonline.org/articles-images/2161-0525-5-334-t011.html.

Zamudio, S., & Carranza, E. (1994). Cupressaceae. *Flora Del Bajío y de Regiones Adyacentes*, *29*.

Zhang, D., Harley, T., & Mabberley, D. (2009). *Flora of China, Chapter: Rutaceae*. Science Press.

4.2. Assessing Magnetic Properties of Biomonitors and Road Dust as a Screening Method for Air Pollution Monitoring

Salazar-Rojas, T., Cejudo-Ruiz, F. R., & Calvo-Brenes, G. (2022). Assessing magnetic properties of biomonitors and road dust as a screening method for air pollution monitoring. Chemosphere, 136795. https://doi.org/10.1016/j.chemosphere.2022.13679.

Assessing Magnetic Properties of Biomonitors and Road Dust as a Screening Method for Air Pollution Monitoring

Teresa Salazar-Rojas [1]*

Fredy Rubén Cejudo-Ruiz[2]

Guillermo Calvo-Brenes [3]

Abstract

Particulate matter (PM) pollution is one of the world's most serious environmental challenges. Among PM components, atmospheric heavy metals (HMs) are considered one of the main pollutants responsible for causing significant negative impacts on human health, and ecological quality. This study aimed to assess environmental magnetism as a simple and rapid method that can be used to evaluate heavy metal contamination in urban areas from the relationships between magnetic properties and heavy metal concentrations. For this purpose, road dust and leaf samples of two common evergreen species (*Cupressus lusitanica*/*Casuarina equisetifolia*) were sampled simultaneously for two years at sites with different levels of traffic pollution. The results found significant statistical correlations between the magnetic properties and the chemical substances of the plants studied, as Fe, Cr and V showed an $r \geq 0.9$ and Cr and Zn $r \geq 0.7$ with χlf in *C. equisetifolia*. The frequency-dependent magnetic susceptibility was found to be between 0% and 14% for plants, and 0% and 2% for road dust, suggesting a rather dissimilar particle size distribution for plants, and a less important contribution from the more hazardous ultrafine superparamagnetic magnetite for both. Confirming that magnetic analyses can be used to distinguish different degrees of urban air pollution.

Keywords: heavy metal, biomonitor, road dust, air pollution, magnetic properties, enrichment factor.

1* Doctorado en Ciencias Naturales para el Desarrollo (DOCINADE), Escuela de Química, Tecnológico de Costa Rica; Universidad Nacional, Universidad Estatal a Distancia, Costa Rica; tsalazar@itcr.ac.cr; Código ORCID 0000000223663638.
2 Instituto de Geofísica, Universidad Nacional Autónoma de México; Michoacán, México; ruben@geofisica.unam.mx, Código ORCID 0000-0003-1003-5664
3 . Escuela de Química, Tecnológico de Costa Rica; Cartago, Costa Rica; gcalvo@itcr.ac.cr, Código ORCID 00000002-7021-3509.
Corresponding author: tsalazar@itcr.ac.cr. Teresa Salazar Rojas, Escuela de Química, Tecnológico de Costa Rica, Cartago, Apartado postal: 159-7050, Costa Rica.

1. Introduction

In urban areas, traffic is a major source of both particulate matter and various HMs. Particulate matter (PM) pollution is one of the world's most serious environmental challenges (Li et al., 2017). Particulate matter is identified according to their aerodynamic diameter, either as PM_{10} (< 10 μm), $PM_{2.5}$, (< 2.5 μm) or $PM_{0.1}$ (< 0.1 μm), the smaller the size, the more hazardous they are (Hofman & Samson, 2014). Numerous source factors are involved in HMs emissions from traffic, such as combustion products from fossil-fuel engines, tire wear, pavement material, brake linings, corrosion material, and road maintenance activities (Limo et al., 2018).

Among PM components, atmospheric HMs are considered one of the main pollutants responsible for causing significant negative impacts on human health and ecological quality (Losacco & Perillo, 2018; Polezer et al., 2018; Yap et al., 2019). Its monitoring is relevant for the development of risk mitigation strategies. Traditional methods based on chemical analysis are slow and expensive; therefore, more convenient methods are needed (Leng et al., 2018). In addition, the use of fiberglass, quartz, and Teflon filter used for PM sampling, adds an economic cost to the already expensive installation and maintenance of air quality monitoring stations (Wilson et al., 2005).

Alternative methodologies have been tested worldwide for monitoring HMs concentrations in the environment in support of traditional monitoring; the use of biomonitors and magnetic properties of environmental samples (plants, soil, road dust), have proved to be effective (Cao et al., 2015;

Kawasaki et al., 2017; Kardel et al., 2018; Brignole et al., 2018; Wuyts et al., 2018; Gillooly et al., 2019). Moreover, biomagnetic monitoring could offer a fast, inexpensive, and non-destructive indicator to obtain a measure of the spatial and temporal variations of PM and HMs load on tree leaves (Hofman & Samson, 2014). In this sense, magnetic iron oxides and hydroxides comprise 10-70% of the Fe content in PM, which deposits in plans and other infrastructure close to the traffic (Priyanka et al., 2020).

The statistical relationship between magnetic variables and metal concentrations supports using a magnetic approach as a measurement tool that is simpler and more cost-effective than the traditional method as an indicator of airborne HMs (Li et al., 2017; Xiangzi Leng et al., 2017; Kardel et al., 2018). However the type of monitors and the relationships among their HMs content and magnetic properties has been determined are specific for a climatic and geographical area, because the variations in the magnetic behavior of a sample are a function of the mineralogical characteristics of the materials, which in turn are related to climatic variations, thus becoming calibrate indicators and quantifiers of the environmental processes of the local or regional climatic system of the study area (Maher et al., 1999). Besides, previous magnetic studies of tree leaves were carried out with species that are rare in a tropical country, *Platanus hispanica* (Davila et al., 2006); *Tilia platyphyllos* (Malvaceae) (Mitchell & Maher, 2009); Platanus acerifolia (Hofman et al., 2013); *Sambucus nigra* (Viburnaceae) (Aguilar et al., 2013); *Fraxinus Americana* ((Pétronille et al., 2013); *Chamaecyparis lawsoniana* (Cupressaceae), *Ligustrum japonicum* (Oleaceae) (Kardel et al., 2018) and *Pinus brutia* subsp. eldarica (Pinaceae) (Kardel et al., 2018; Khamesi et al., 2020).

Therefore, this study aimed to evaluate environmental magnetism as a simple and rapid method that can be used to assess heavy metal contamination in urban areas from the relationships between magnetic properties and heavy metal concentrations, in a tropical climate. Considering that traffic is one of the main sources of air pollution in urban areas, vehicle density was chosen as the criterion for selecting sampling points (Limo et al., 2018).

2. Material and methods Sampling site

Sampling was carried out in the Great Metropolitan Area (GMA) of Costa Rica, located in the central region of the country (Fig. 1). It was selected because, although it only comprises 3.8% of the national territory, it holds 70% of the automobile fleet, 60% of the population (3 097 823

inhabitants) and 85% of the industry (Briseño-Castillo et al., 2015; INEC, 2021). The climate of the GMA is variable from Tropical Rainforest (Af) to Tropical Monsoon (Am) depending on the region, according to Koppen-Geiger climate classification (Peel et al., 2007).

Fig. 1. Sampling sites for each plant and road dust, according to Table 1.

The sites were selected due to their vehicle density obtained from the Traffic Information Yearbook 2019 (Ministry of Public Construction and Transportation, 2020). Eight sampling sites were designated for each indicator, to ensure representativeness, the vehicle density range of the primary routes was identified and systematic sampling was considered with a value of k that allowed for the widest possible distribution (Table 1).

Table 1. Average daily number of vehicles of sampling sites.

Site	Daily average of vehicles[1]	Monitor
1	0	*C. lusitanica, C. equisetifolia*, road dust
2	17101	*C. lusitanica*, *C. equisetifolia*, road dust
3	32138	*C. equisetifolia*, road dust
3’	29198	*C. lusitanica*

4	45326	*C. lusitanica*, *C. equisetifolia*, road dust
5	62008	*C. lusitanica*, *C. equisetifolia*, road dust
6	77671	*C. lusitanica*
6’	73982	*C. equisetifolia*, road dust
7	88585	*C. lusitanica*, *C. equisetifolia*, road dust
8	104558	*C. lusitanica*, *C. equisetifolia*, road dust

[1]Ministry of Public Construction and Transportation, 2020.

The land use in all selected sites was residential with some commercial spots, to try to ensure a single source of HMs, traffic. All samples were taken as close as possible to the road, where most traffic pollutants accumulate (Kawasaki et al., 2017). For the selection of the background point, Site 1, a far distance from the sampled biomonitors and the road was considered. For the road dust sample, the background point was chosen at the end of a paved road, where there was practically no traffic.

2.1 Sampling

The plant species were selected, after carrying out a census in January 2020, considering criteria of abundance, accessibility, longevity, proximity to the road, and results obtained in a preliminary study. The selected bioindicators were: *Cupressus lusitanica* (Cupressaceae) (Zamudio & Carranza, 1994) and *Casuarina equisetifolia* (Casuarinaceae) (Rojas-Rodríguez & Torres-Córdoba, 2013), both of them perennials, with a foliage duration of 2 years or more.

A total of 160 plant leaf samples (10 samples × 2 plants x 8 sampling sites) were collected during dry the season, two campaigns from February to March one in 2020 and the other in 2021 (Table S1). Sampling was conducted during the dry season, although this is increasingly irregular due to climate change, but at least 5 days without rain were considered. Mature foliage was taken from the lateral canopy facing the side of the road, between 1 and 5 plants per site, at a height of 1.5 to 2.0 m, considering the normal height of human respiration and to avoid the influence of urban soil particles (Chaparro et al., 2015). The samples were stored in plastic bags and transferred into a cool box. In the laboratory, the samples were dried at (55 ±1) º C to obtain constant weight and then powdered with a mortar for subsequent analysis following Aguilar et al., (2012).

A total of 80 road dust samples (10 samples x 8 sampling sites) were collected at the same sampling sites and period time of the plants. The samples were collected at the ditch of the road, with a sweep of approximately one square meter. The road dust samples were stored in plastic bags and transferred into a cool box. In the laboratory, the samples were dried at environmental temperature and then sieved for subsequent analysis at the laboratory following Aguilar et al. (2012).

2.3 Chemical Methods

Unwashed leaf powder samples were used for the analysis, as some wash/unwashed experiments show that this is the optimal method for the HMs of interest and the objective of this study (Gillooly et al., 2019); (Khamesi et al., 2020). Duplicates of the samples were analyzed for metal content: Cu, Cr, Cu, Ni, Pb, V, Zn, Fe and, Cd. All plants and road dust samples were analyzed for HMs content by the Method EPA 3051 Microwave Assisted Acid Digestion of Solids using a Mars 6 (CEM) (U.S. EPA, 2007), and measurements were carried out in an Atomic Absorption Spectrophotometer (Perkin Elmer, model AAnalyst 800), supported by a graphite furnace and a hydride generator (Perkin Elmer, model FIAS 100), for the determination of concentrations at trace level.

The observations under the scanning electron microscope (SEM) were performed on selected samples using a SEM Hitachi (TM-1000) scanning electron microscope.

2.4 Magnetic measurements Magnetic susceptibility

The magnetic susceptibility of the samples was determined following the recommendations of (Dearing,

1999). Dry samples were crushed with a mortar and packed tightly in a 10 cm^3 plastic container. A Bartington MS2B single sample dual-frequency sensor and a Bartington MS3 Magnetic Susceptibility Meter were used to measure the susceptibility at low frequency (κ_{lf} at 0,46 kHz) and high frequency (κ_{hf} at 46,0 kHz). Results were also used to determine:

The value of mass specific susceptibility:

$$\chi lf = \frac{\kappa lf}{\rho} \quad (1)$$

Where ρ is the density of the material in kg m^{-3}.

The percentage of frequency-dependent magnetic susceptibility:

$$\chi df\% = ((\kappa lf - \kappa hf)/\kappa lf) \; x \; 100 \quad (2)$$

Through these magnetic parameters, the concentration of magnetic material and the presence of ultrafine particles (≤ 30 nm) of ferrimagnetic, superparamagnetic (SP) characteristics in the samples are identified.

2.5 Statistical Analysis

Statistical analyses of the magnetic and chemical data were carried out using RStudio software version 1.4.1717, including packages dplyr, lmtest, carData, tidyverse. Pearson's correlation coefficient test (r) was performed to evaluate the statistical relationship between the variables (RStudio Team, 2020).

2.6 Enrichment Factor

The default approach to assessing the anthropogenic impact of HMs is to calculate the enrichment factor (EF) for metal concentrations above uncontaminated background levels using the Equation (3).

$$EFi = (\frac{Ci}{Cie})/\left(\frac{Ci}{Cie}\right)_0 \quad (3)$$

with C_i concentration of studied metal and Cie the concentration of an immobile parameter (e.g., Al, Mn, and Fe); the subscript 0 indicates background values. With an scale of contamination: EF<2 (low), 2≤EF<5 (moderate), 5≤EF<20 (considerable), 20≤EF<40(very high) and EF>40 (extremely high) (Okedeyi et al., 2014; Cai et al., 2015).

3. Results and discussion

3.1 Metal concentrations and Magnetic properties

The concentration of each heavy metal was plotted as a function of sampling locations for the studied biomonitors, Fig. 2 and road dust, Fig. 3. All metals were identified at all sites except for Cd, which was not found at sites or studied monitors. Overall the sampling sites showed relatively high variability within and between different points, typical of environmental samples. Even when sampling considerations such as leaf age, plant height, and side are taken into account, plants are exposed to meteorological conditions such as wind (speed and direction) and rain, which

cause particles to concentrate differently within the plant, in addition to the inherent disparity of PM in the air and variation in the composition of particles emitted by the source. Showing high variability exhibited in heavy metal content measured in bioindicators such as the one used in this study *C. equisetifolia* (standard deviation (SD) from Cr = 0.56 to Fe = 150.70), *C. lusitanica* (SD from Cr = 0.67 to Fe = 87.04) , and as in *Chamaecyparis lawsoniana* (SD from Fe = 1.52 to Zn = 31.70), Ligustrum *japonicum* (SD from Fe = 1.96 to Zn = 79.05), and Pinus *brutia* (SD from Fe = 0.53, to Zn = 53.40) by Kardel et al., (2018). That variability is also reported in HMs content determined in PM collected through filters like quartz microfiber (SD from Ni = 2.99 to Fe = 257.0) by J. Wang et al., (2017) or Teflon filters (SD from Pb = 0.88 to Fe = 260.0) by Gillooly et al., (2019).

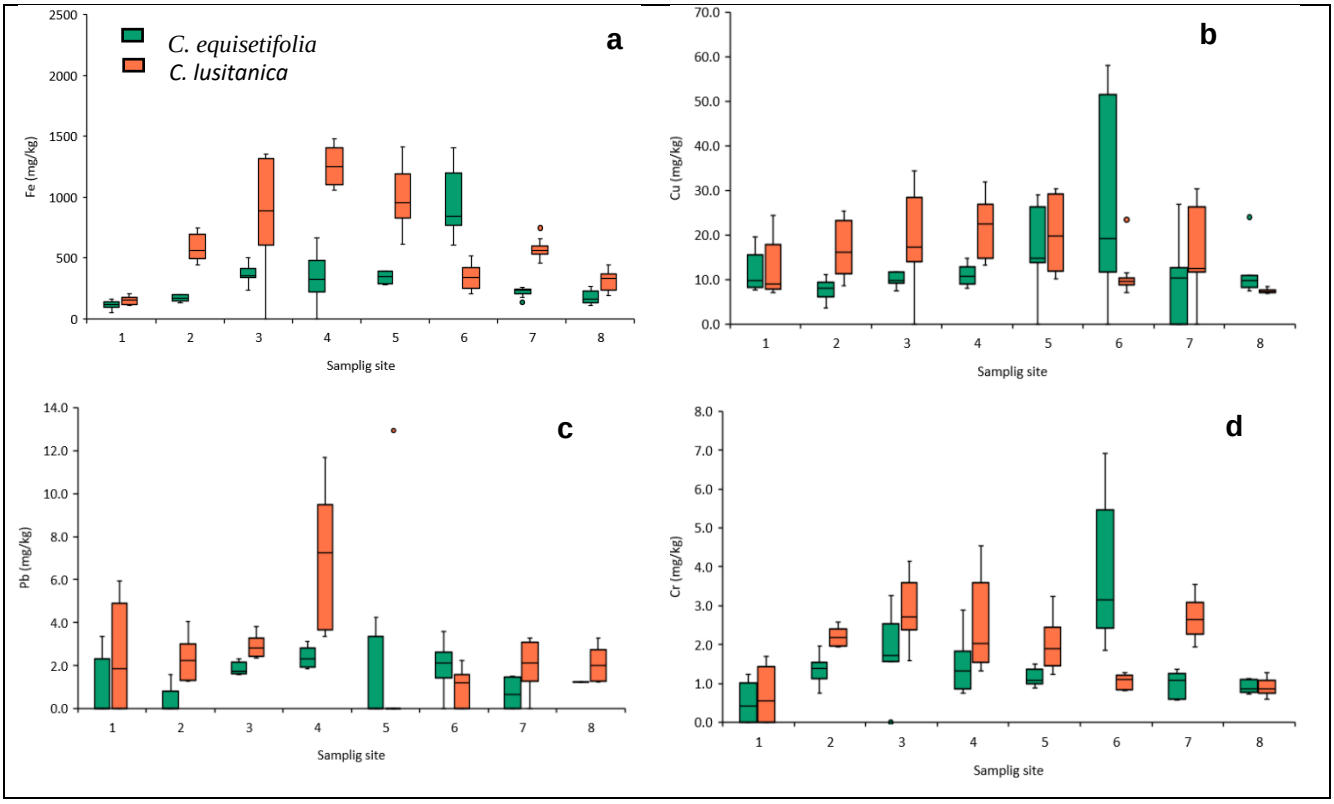

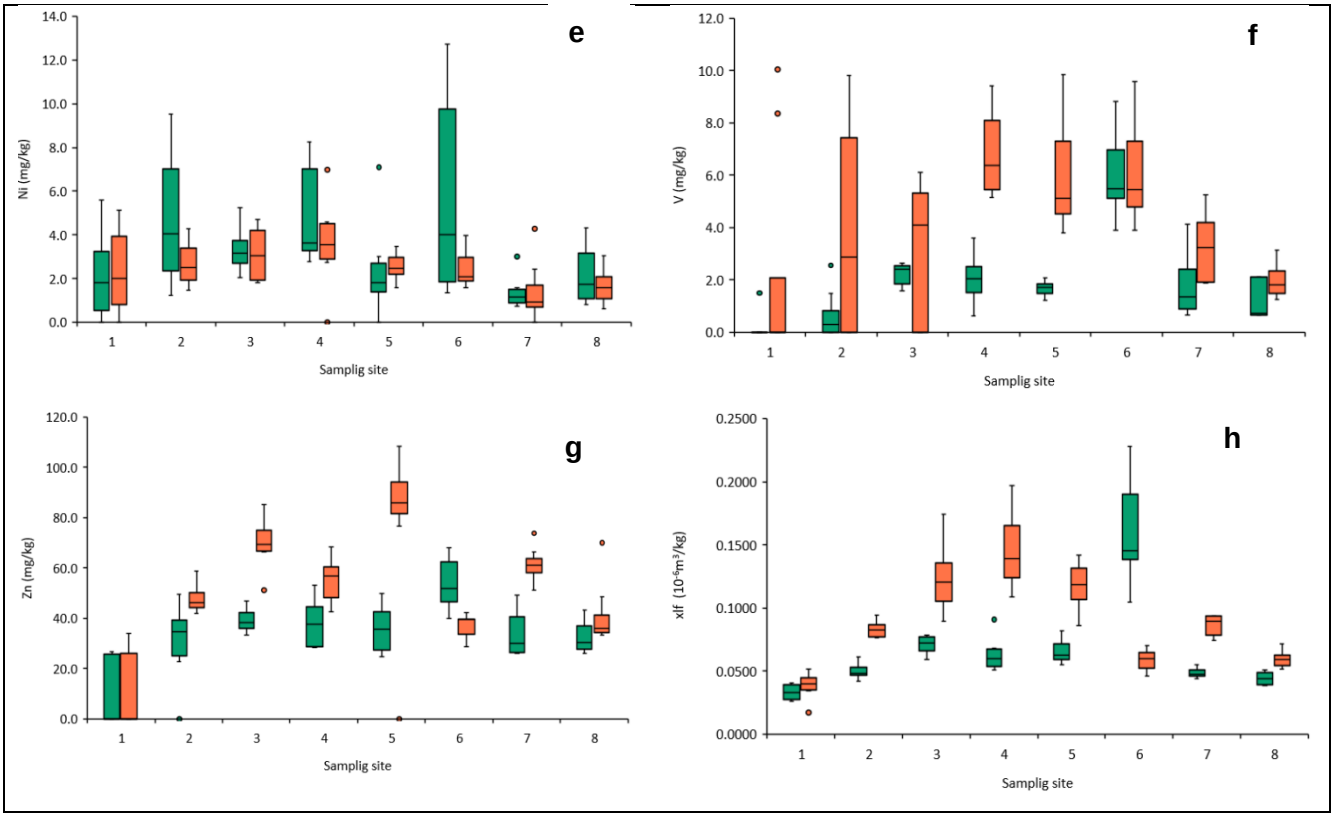

Fig. 2. Variation of HMs concentration and magnetic susceptibility at sampling sites for C. *equisetifolia* and *C. lusitanica.*

There is a tendency for the concentration of most of the HMs to increase as vehicle density increases, (Fig. 2). Similar results were obtained with higher amounts of HMs at high traffic sites identified in the PM deposited at the *Mora Alva* plant and on glass fiber filter paper sheets (Sharma et al., 2020). *C*. *equisetifolia*, presents a significant correlation between Fe, Cu, Pb, V, and Zn with vehicular density (Table 2). That tendency seems to decrease in concentration for C. *lusitanica* at sites 7, 8, and 6, where this plant had to be sampled a little further away from the road, confirming what has been shown in other studies, that the concentration of HMs is directly proportional to the distance from the road ((Hofman et al., 2013; Cao et al., 2015; Kawasaki et al., 2017).

In the case of street dust (Fig. 3), mean concentrations of HMs and magnetic susceptibility remained relatively similar among the different sites, denoting the possible accumulation of contaminants, due to different pollutant sources. This could be the result of sampling in the

roadside ditch, as no dust was found on the road, possibly because rainfall runoff, even in the dry season, increased due to the effects of climate change. It should be noted that metal debris accumulates in the ditch from traffic, gray sewage from nearby homes and businesses, and natural sources (dry and wet atmospheric deposition, surface soil resuspension) (Wang et al., 2019). Nevertheless, it presented a significant correlation between Fe, Cr and Zn, and vehicular density (Table 1 and 2).

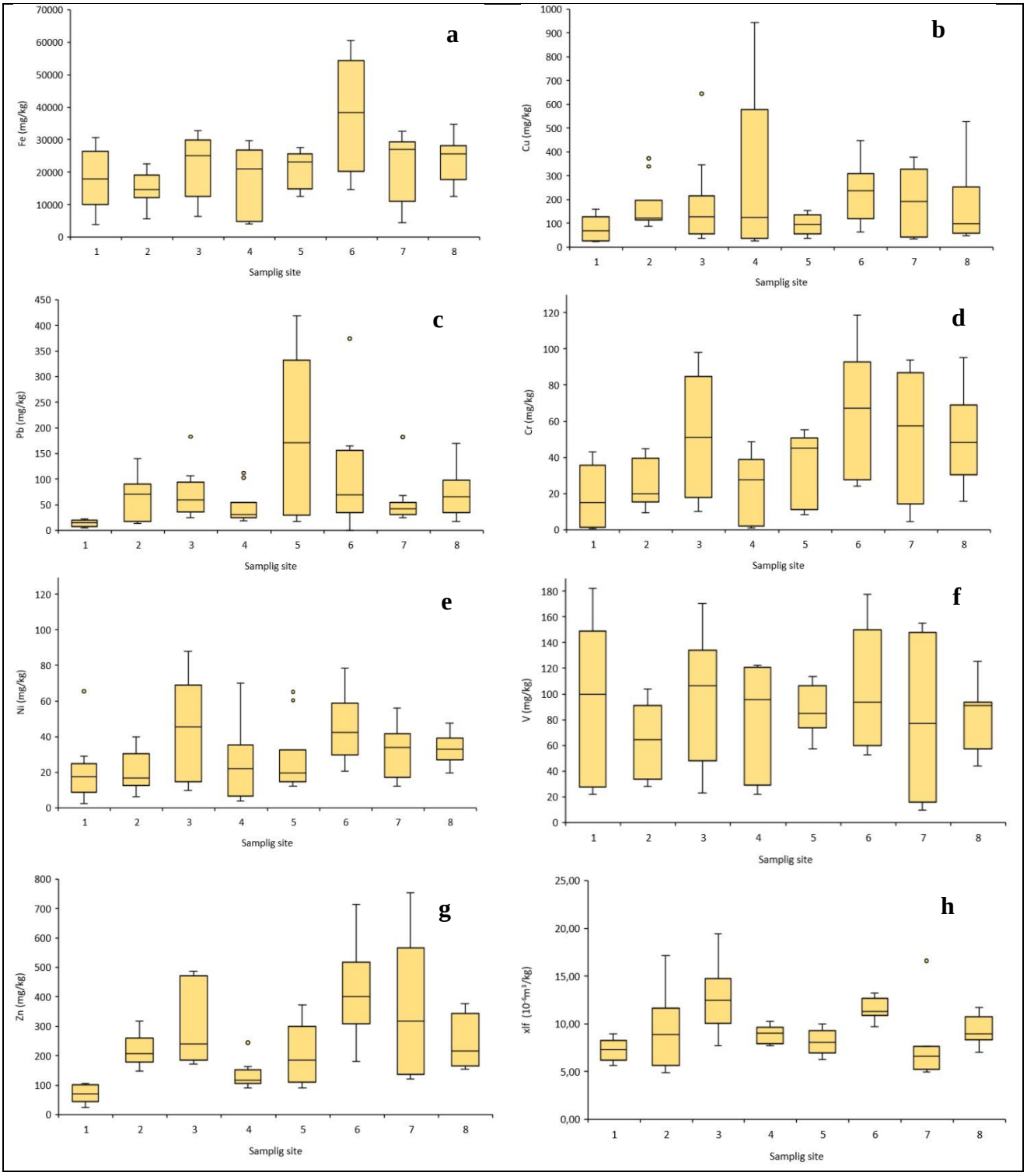

Fig. 3. Variation of HMs concentration and magnetic susceptibility at sampling sites in road dust.

Street dust samples are also exposed to meteorological conditions among other factors previously exposed which produces an important variability in data (SD from Ni = 20.35 to Fe = 9368) similar to street dust from a study in Murcia (Spain) (SD from V = 11 to Fe = 7249) (Sanleandro et al., 2018).

Additionally, the presence of HMs was also identified by SEM images (Fig. 3) on *C*. *equisetifolia* and *C*. *lusitanica*. One of the main assumptions related to the use of magnetic properties as an indicator for assessing heavy metal air contamination is that particle deposited on plants are trapped or encapsulated in the cuticle (Bussotti et al., 2014). In Fig. 3, the presence of anthropogenic particle was identified in the SEM images of both biomonitors, in their top layer and inside the cuticle of the plants, due to their regular shape and light reflections as identified in previous studies (Mariéa et al., 2018; Wang et al., 2019).

a) b)

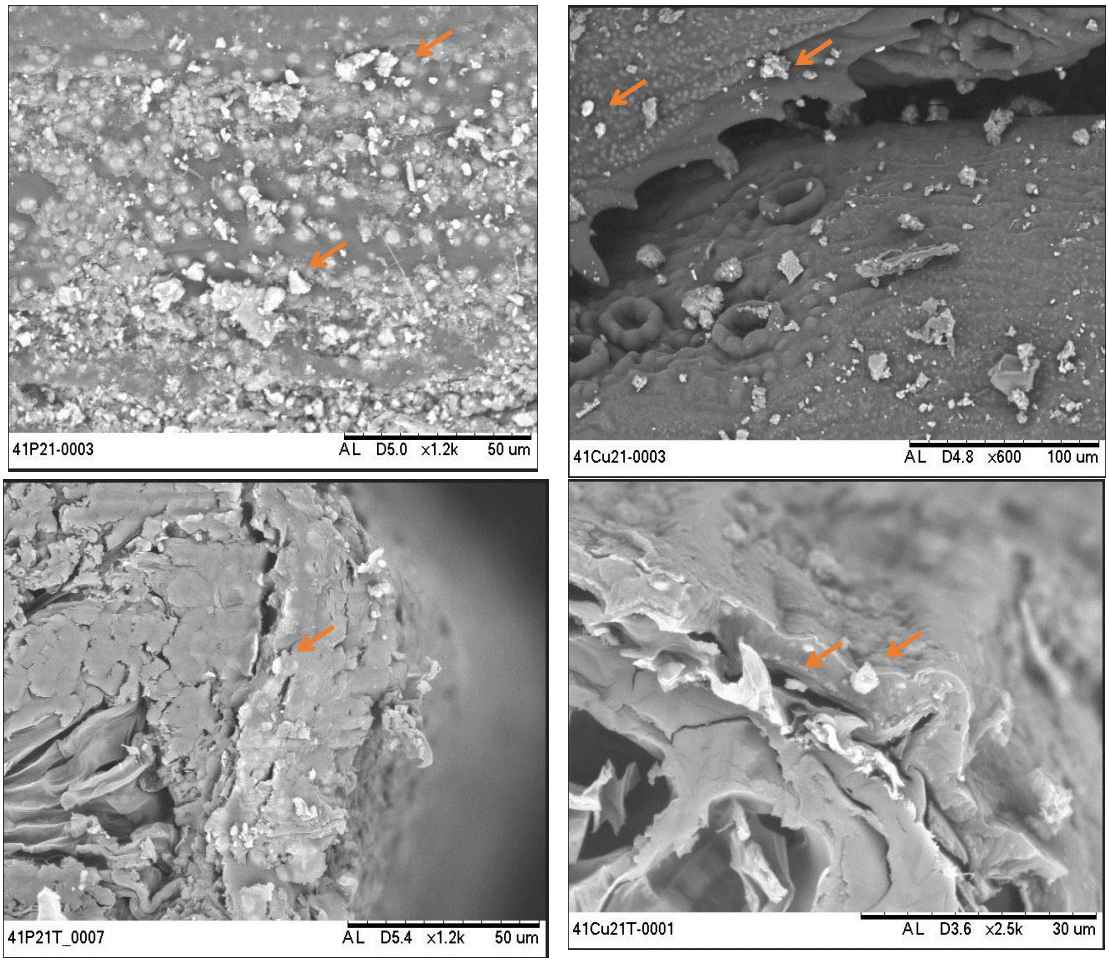

Fig. 4. SEM images of various a) C. *equisetifolia* b) C. *lusitanica* cuttings.

3.2 Correlations HM and the magnetic properties

Pearson's correlation coefficient (r) was calculated between the different HMs, vehicle quantity, and magnetic properties, Table 2. The usefulness of magnetic measurements as indicators of environmental contamination is based on the correlation between magnetic properties and iron concentrations, as well as the association between iron and HMs (Leng et al., 2017). For both biomonitors, all the HMs studied presented significant positive correlations with χlf. Thus, Fe, Cr, and V presented an $r \geq 0.9$ and Cr and Zn $r \geq 0.7$ with χlf in *C*. *equisetifolia*. For *C. lusitanica*, Fe, Zn, Cr, and Cu had $r > 0.8$, 0.7, 0.6, and 0.5 respectively with χlf.

About the road dust, Table 2 shows a poor correlation between HMs and χlf, being significant only for Fe, indicating a possible non-linear relationship between them, probably due to multiple contaminant sources, discussed earlier. As identified in previous works with multiple sources of HMs, in industrial and urban areas and using multiple magnetic properties (χlf, kdf, anhysteretic remanent magnetization (ARM), and saturation isothermal remanent magnetization (SIRM)) when there are multiple sources of especially domestic/commercial and natural processes, magnetic properties correlate poorly HMs. However, magnetic properties have a strong correlation with heavy metals derived from anthropogenic activities such as industrial and traffic activities content (Zhu et al., 2013; Li et al., 2014; Li et al., 2017).

The magnetic property, % kdf, on the other hand, showed significant correlations only with Fe for *C. equisetifolia* and with Zn and χlf for road dust.

Fe, which is the core of the use of magnetic properties, presented a strong significant correlation with all metals in the plants studied and for Cr, Cu, Ni, and Zn in the road dust Table 2.

Table 2. Pearson's Correlation Coefficient (r) among metals, vehicle amount and magnetic properties.

	Vehicules	Fe	Cu	Pb	Cr	Ni	V	Zn	xlf	kdf
C. equisetifolia										
Vehicules	1.00	0.24 [b]	0.24 [b]	0.31 [b]	0.2	-0.1	0.41 [a]	0.46 [a]	0.23 [b]	0.17
Fe		1.00	0.74 [a]	0.39 [a]	0.89 [a]	0.47 [a]	0.91 [a]	0.69 [a]	0.97 [a]	0.09 [a]
Cu			1.00	0.49 [a]	0.73 [a]	0.50 [a]	0.68 [a]	0.39 [a]	0.74 [a]	-0.18
Pb				1.00	0.45 [a]	0.35 [b]	0.27	0.52 [a]	0.36 [b]	-0.09
Cr					1.00	0.57 [a]	0.85 [a]	0.74 [a]	0.90 [a]	0.05
Ni						1.00	0.46 [a]	0.34 [a]	0.46 [a]	-0.04
V							1.00	0.70 [a]	0.93 [a]	0.22
Zn								1.00	0.70 [a]	0.15
xlf									1.00	0.14
kdf										1.00
C. lusitanica										
Vehicules	1.00	-0.07	-0.21	-0.05	-0.36 [b]	-0.28 [b]	-0.08	-0.24 [b]	-0.05	-0.03
Fe		1.00	0.55 [a]	0.57 [a]	0.48 [a]	0.44 [a]	0.49 [a]	0.67 [a]	0.86 [a]	0.18
Cu			1.00	0.51 [a]	0.16	0.16	0.42 [a]	0.44 [a]	0.51 [a]	-0.04
Pb				1.00	-0.03	0.06	0.22	0.27 [b]	0.48 [a]	0.11
Cr					1.00	0.26	0.14	0.45 [a]	0.65 [a]	0.04
Ni						1.00	0.44 [a]	0.19	0.45 [a]	0.07
V							1.00	0.37 [a]	0.45 [a]	0.11
Zn								1.00	0.71 [a]	0.15
xlf									1.00	0.16
kdf										1.00
Road dust										
Vehicules	1.00	0.29 [a]	0.11	0.21	0.38 [a]	0.21	0.01	0.39 [a]	0.01	0.27 [b]
Fe		1.00	0.34 [a]	-0.05	0.79 [a]	0.71 a	0.77	0.50 [a]	0.24 [b]	0.08
Cu			1.00	-0.04	0.44	0.4	0.36	0.36	-0.03	0.16
Pb				1.00	-0.08	-0.11	-0.12	0.28	0.17	0.16
Cr					1.00	0.73 a	0.74 [a]	0.63 [a]	0.11	0.29
Ni						1.00	0.57 [a]	0.47 [a]	0.16	0.28
V							1.00	0.41 [a]	0.08	-0.01
Zn								1.00	0.09	0.39 [a]
xlf									1.00	0.80 [a]
kdf										1.00

[a] $p < 0,01$; [b] $p < 0,05$

Fig. 5 gives examples of the most interesting of these correlations, and shows the varying responses of *C. equisetifolia* and *C. lusitanica*, to the absorption and adsorption to trace metals and their correlation with χlf for metals studied, denoting a positive linear relationship among them.

The largest R^2 values in the majority of the HMs were for *C. equisetifolia* (Fig 5). Comparing the R^2 obtained in this study with a similar study on lichen species *Evernia prunastri* (L.) in Milan for χlf, and Fe, Cu, Pb, and Zn, they obtained values for R^2 = 0.76, 0.7, 0.14 and 0.41 respectively. It is observed that *C. equisetifolia* presents higher R^2 values for Fe and Zn, a similar value for Pb, and a lower value for Cu. C. *lusitanica* presents higher values for Pb and Zn, similar for Fe, and lower for Cu as well (Winkler et al., 2020).

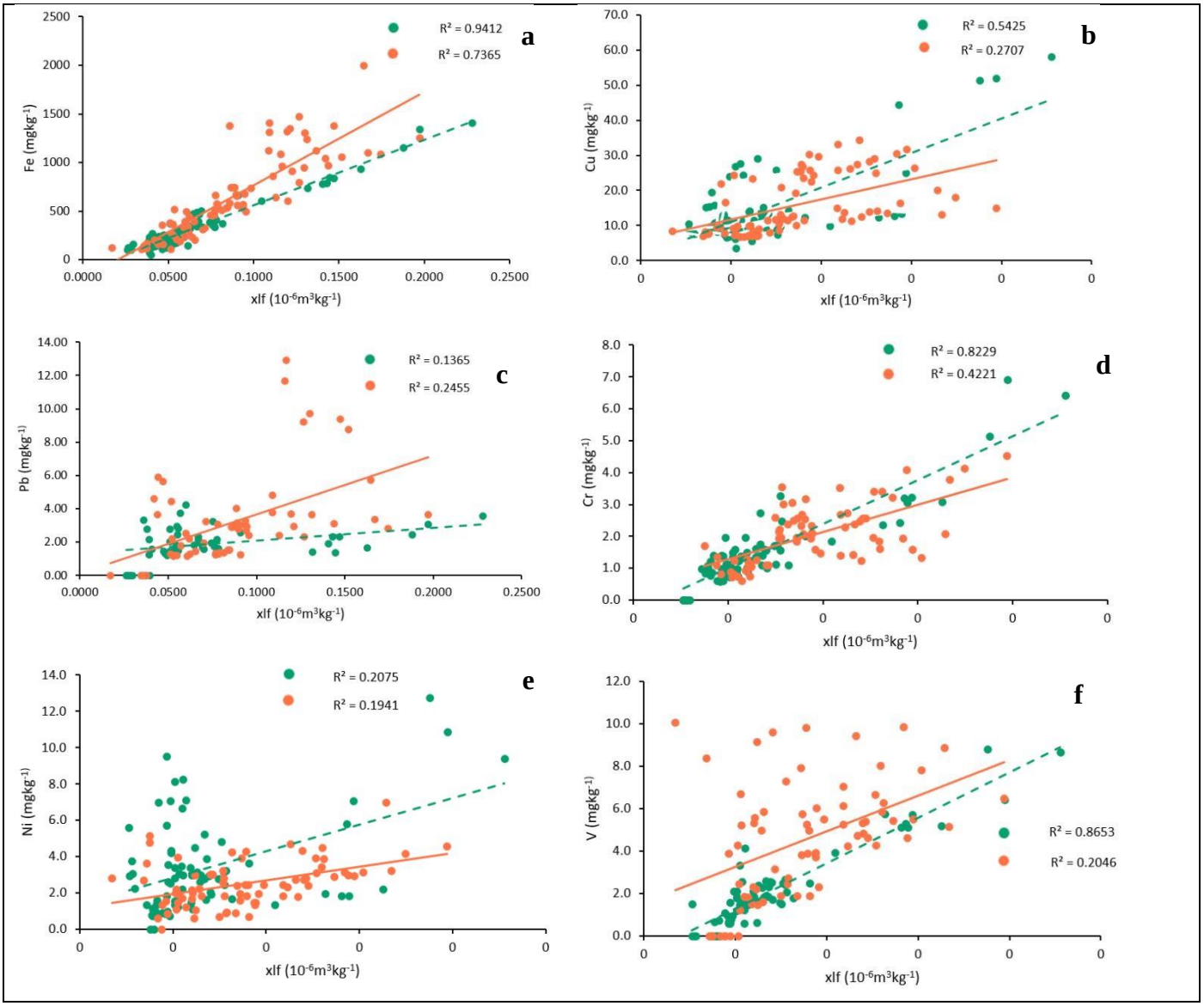

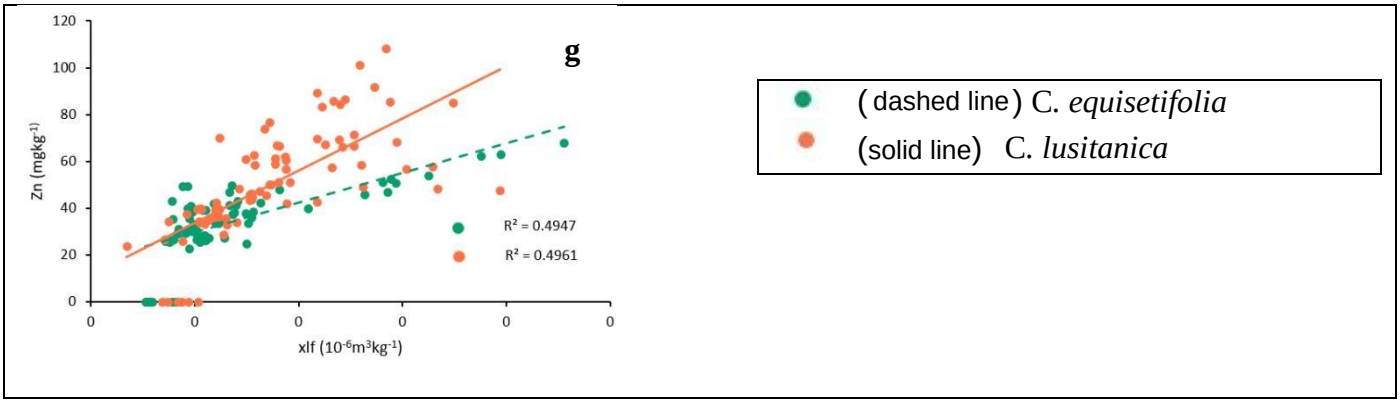

Fig. 5. Correlations between χlf with a) Fe, b) Cu, c) Pb, d) Cr, e) Ni, f) V, and d) Zn in biomonitors: *C. equisetifolia* and C. *lusitanica*. R^2 values for each line are given in the respective figure.

3.3 χlf and χfd%

The χlf and χfd% properties were plotted by sampling site (Fig. 6) and their correlation (Fig. 7) for the biomonitor and road dust samples. Fig.6a, shows a similar pattern in particle type (χfd%) for all sites for both *C. equisetifolia* and C. *lusitanica*, however it points to slightly higher χlf for *C. lusitanica* than for *C. equisetifolia*, with the exception of point 6, where the former was possibly more affected by the sampling distance from the road, because at that site *C. lusitanica* was found a little further away from the road. It should be noted that a higher χlf predicts a higher concentration of ferrimagnetic material probably of anthropogenic origin (Dearing, 1999).

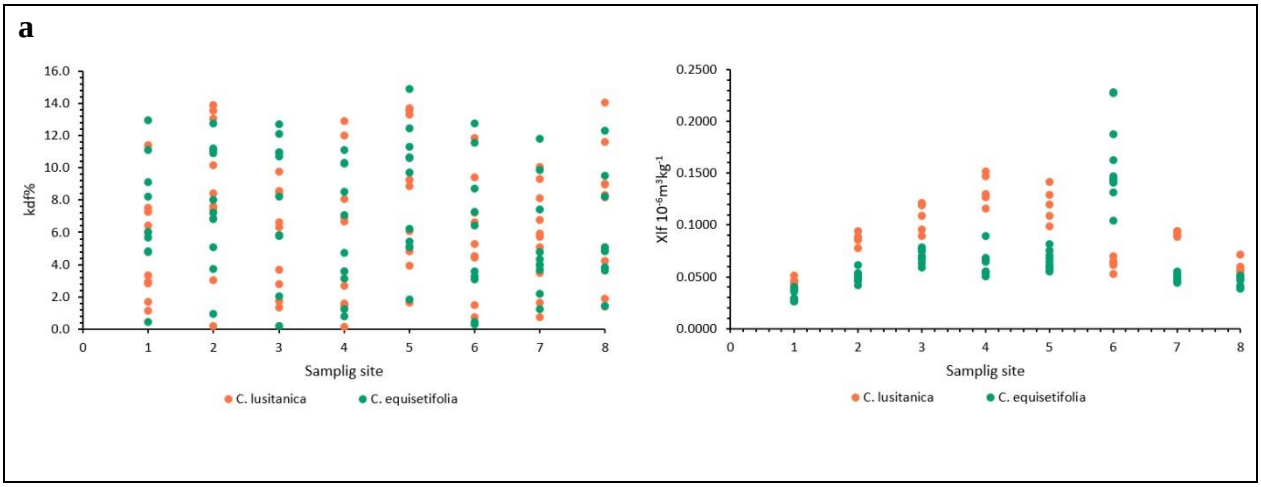

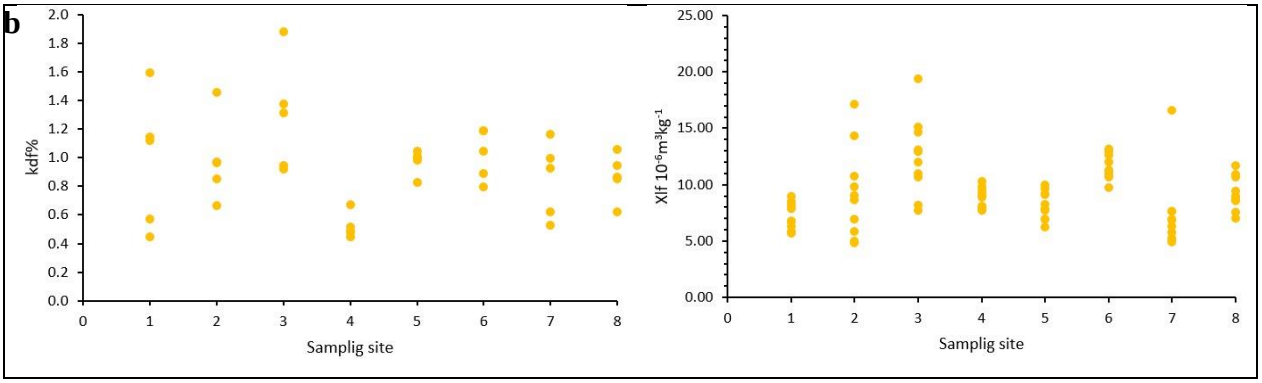

Fig. 6. Relationship between magnetic properties χlf and χfd% in a) C. *equisetifolia*, C. *lusitanica* and b) road dust.

Road dust samples (Fig. 6b), it was obtained values of χfd% < 2% for all sites, which denotes an insignificant contribution of SP grains (Muñoz et al., 2017).

Correlation between χlf and χfd% (Fig.7), in the biomonitor samples, the content of magnetic material was varied, χfd% values range from between 0-14 %, suggesting that the presence of different types of magnetic minerals, including some SP (when χfd% range from 10-14, virtually all (>75 %) are SP grains), with no predominance for any of them. However, the present of ferrimagnetic material is scarce hence the χlf values were low in both biomonitors (Dearing, 1999; Wang et al., 2019). These results are confirmed by the low levels of contamination found in the EF for these plants (Table 3).

For the road dust samples, χfd% denotes larger size of particle material of insignificant contribution of SP grains, as mention before. However, its χlf value range from 5 to 19 ($10^{-6}m^3/kg$) indicating the presence of more ferrimagnetic material than the one obtained by the plants, which also correlates with higher EF results (Table 3).

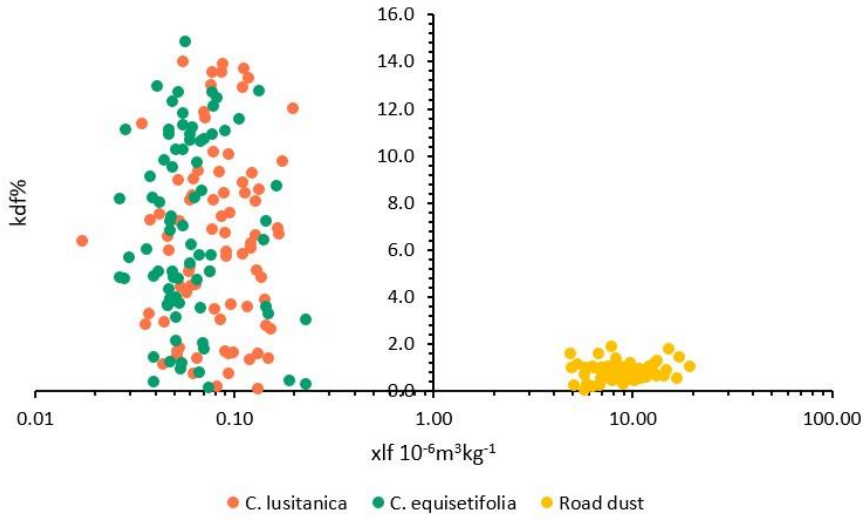

Fig. 7. Relationship between magnetic properties χlf and χfd% in *C. equisetifolia*, C. *lusitanica* and road dust.

3.4 Enrichment Factors

Enrichment factors were calculated by applying Equation 3, considering the mean metal concentrations, Table 3. Sampling Site 1 was considered as the uncontaminated or background point. Fe was used as the normalizing element due to its low variability (Okedeyi et al., 2014).

Evidence of metal contamination above background levels was observed in *C. equisetifolia,* a low level (EF <2) in most HMs and sites, only presented moderate contamination for V at all sites (EF = 3.4 to 5.4) and Zn (EF= 3.0, 2.3, 2.8) at sites 2, 7 and 8 respectively. *C. lusitanica* showed only low contamination in all HMs and sites. However, the highest EF were for V and Zn as well. In contrast to the plants, road dust showed more sites with different levels of pollution. Pb is the one that presented the highest values in all sites ranging from moderate (EF = 3.3 to 5.3) to considerable contamination (EF = 11.1). Follow for Zn with moderate contamination (EF = 2.0 to 4.3). Cu presented moderate contamination (EF = 2.1, 3.6, 2.1) in sites 2, 4 and 7 respectively.

The EFs obtained are lower for plants and road dust than those found for the plant *Struthanthus flexicaulis* in urban neighborhoods in Brazil with EF values in the region of 5 for Cr, 100 and 5 Pb, 75 for Cu and 150 for Zn or in a rural area with nearby traffic with EF values of 5 for Cr, 20 for Pb, 50 for Cu and 400 for Zn, however, the author used generals Earth's Crust data as a reference point (de Paula et al., 2015).

Table 3. Enrichment Factors from background values (Site 1).

	Site	Cu	Pb	Cr	Ni	V	Zn
Casuarina equisetifolia	2	0.4	1.1	**1.8**	**1.5**	**4.7**	**3.0**
	3	0.3	0.6	1.2	0.5	**4.1**	**1.5**
	4	0.3	0.7	0.8	0.7	**3.7**	**1.5**
	5	0.6	1.2	0.7	0.4	**3.4**	**1.5**
	6	0.3	0.3	0.9	0.3	**4.3**	0.8
	7	0.6	0.7	0.9	0.3	**5.4**	**2.3**
	8	0.6	0.8	1.2	0.7	**4.6**	**2.8**
Cupresses lusitanica	2	0.4	0.2	0.4	0.3	1.0	1.1
	3	0.3	0.2	0.3	0.2	0.4	1.0
	4	0.2	0.3	0.2	0.2	0.4	0.6
	5	0.2	0.8	0.2	0.2	0.5	1.2
	6	0.4	0.3	0.3	0.4	1.4	**1.5**
	7	0.4	0.2	0.5	0.2	0.5	1.4
	8	0.3	0.4	0.3	0.3	0.5	**1.7**
Road dust	2	**2.5**	**5.3**	**1.6**	1.2	0.8	**3.6**
	3	**1.9**	**4.1**	**2.2**	**1.7**	0.8	**3.5**
	4	**3.6**	**3.3**	1.3	1.3	0.8	**2.0**
	5	1.0	**11.1**	**1.6**	1.1	0.8	**2.4**
	6	1.4	**4.0**	**1.6**	1.0	0.5	**2.9**
	7	**2.1**	**3.3**	**2.3**	1.3	0.7	**4.3**
	8	**1.6**	**3.8**	**2.1**	1.2	0.6	**2.6**

4 **Conclusions**

In summary, this study provided several insights into the effective relationships between magnetic properties and HMs accumulated in biomonitors, that may allow their use in monitoring this type of pollution in a tropical area. It is concluded that *C. equisetifolia* and *C. lusitanica* leaves could be employed as a costeffective tool for the estimation of atmospheric heavy metals in urban areas.

According to the χlf-χfd% scatter plot results, the plant samples particles have wider ranges of size than those of the road dust, however, the latter has a higher concentration of ferrimagnetic material. The frequency-dependent magnetic susceptibility was found to be between 0 and 14%,

for plants and 0 and 2% for road dust. Suggesting for road dust samples, along with their high magnetic susceptibility, a less important contribution from the more size hazardous ultrafine superparamagnetic magnetite.

Besides, evidence of low metal contamination above background levels was observed in *C. equisetifolia* and *C. lusitanica*, only V and Zn showed some moderate pollution in some of the study sites. In contrast to road dust, where almost all sites showed considerable and moderate contamination in almost all HMs.

Declarations

Acknowledgements

The authors thank the Technological Institute of Costa Rica (ITCR) and the National Autonomous University of Mexico (UNAM), for their financial and administrative support. In addition, the Center for Research in Environmental Protection (CIPA), Center for Research and Chemical and Microbiological Services (CEQIATEC) and Institute of Geophysics (Morelia) for their support to the project.

Thanks to the Meteorological Guidance Department of the National Institute of Meteorology for the information provided.

Compliance with ethical standards Bioindicators were collected in compliance with the ethical standards of the Technological Institute of Costa Rica.

Consent to participate Consent for publication

Conflict of interest The authors declare that they have no conflict of interest.

Availability of data and material Code availability Not applicable

5. References

Aguilar, B., Cejudo, R., Martínez, J., Bautista, F., Goguitchaichvili, A., Carvallo, C., & Morales, J. (2012). Ficus benjamina leaves as indicator of atmospheric pollution: A reconaissance study. *Studia Geophysica et Geodaetica*, 56(3), 879–887. https://doi.org/10.1007/s11200-011-0265-1.

Aguilar, B., Mejía, V., Goguitchaichvili, A., Escobar, J., Bayona, G., Bautista, F., Morales, J., & Ihl, T. (2013). Reconnaissance environmental magnetic study of urban soils, dust and

leaves from Bogotá, Colombia. *Studia Geophysica et Geodaetica*, 57(4), 741–754. https://doi.org/10.1007/s11200-012-0682-9.

Brignole, D., Drava, G., Minganti, V., Giordani, P., Samson, R., Vieira, J., Pinho, P., & Branquinho, C. (2018). Chemical and magnetic analyses on tree bark as an effective tool for biomonitoring: A case study in Lisbon (Portugal). *Chemosphere*, 195, 508–514. https://doi.org/10.1016/j.chemosphere.2017.12.107.

Briseño-Castillo, J., Herrera-Murillo, J., Solórzano-Arias, D., Beita-Guerrero, V. H., & Rojas-Marin, J. F. (2015). VI Informe de Calidad del Aire Área Metropolitana de Costa Rica. MINAE.

Bussotti, F., Pollastrini, M., Killi, D., Ferrini, F., & Fini, A. (2014). Ecophysiology of urban trees in a perspective of climate change. *Agrochimica*, 58(3), 247–268. https://doi.org/10.12871/0021857201431.

Cai, C., Xiong, B., Zhang, Y., Li, X., & Nunes, L. M. (2015). Critical Comparison of Soil Pollution Indices for Assessing Contamination with Toxic Metals. *Water, Air, and Soil Pollution*, 226(10). https://doi.org/10.1007/s11270-015-2620-2.

Cao, L., Appel, E., Hu, S., Yin, G., Lin, H., & Rösler, W. (2015). Magnetic response to air pollution recorded by soil and dust-loaded leaves in a changing industrial environment. *Atmospheric Environment*, 119, 304–313. https://doi.org/10.1016/j.atmosenv.2015.06.017.

Chaparro, M., Chaparro, M., Castañeda Miranda, A. G., Böhnel, H. N., & Sinito, A. M. (2015). An interval fuzzy model for magnetic biomonitoring using the specie Tillandsia recurvata L. *Ecological Indicators*, 54, 238–245. https://doi.org/10.1016/j.ecolind.2015.02.018.

Davila, A. F., Rey, D., Mohamed, K., Rubio, B., & Guerra, A. P. (2006). Mapping the sources of urban dust in a coastal environment by measuring magnetic parameters of Platanus hispanica leaves. *Environmental Science and Technology*, 40(12), 3922–3928. https://doi.org/10.1021/es0525049.

de Paula, P. H. M., Mateus, V. L., Araripe, D. R., Duyck, C. B., Saint'Pierre, T. D., & Gioda, A. (2015). Biomonitoring of metals for air pollution assessment using a hemiepiphyte herb (Struthanthus flexicaulis). *Chemosphere*, 138, 429–437. https://doi.org/10.1016/j.chemosphere.2015.06.060.

Dearing, J. A. (1999). Using the Bartington MS2 System. Environmental Magnetic Susceptibility, 52.

Gillooly, S. E., Michanowicz, D. R., Jackson, M., Cambal, L. K., Shmool, J. L. C., Tunno, B. J., Tripathy, S., Bain, D. J., & Clougherty, J. E. (2019). Evaluating deciduous tree leaves as biomonitors for ambient particulate matter pollution in Pittsburgh, PA, USA. *Environmental Monitoring and Assessment*, 191(12). https://doi.org/10.1007/s10661-019-7857-6.

Hofman, J., & Samson, R. (2014). Biomagnetic monitoring as a validation tool for local air quality models: A case study for an urban street canyon. *Environment International*, 70(2014), 50–61. https://doi.org/10.1016/j.envint.2014.05.007.

Hofman, J., Stokkaer, I., Snauwaert, L., & Samson, R. (2013). Spatial distribution assessment of particulate matter in an urban street canyon using biomagnetic leaf monitoring of tree crown

deposited particles. *Environmental Pollution*, 183(2013), 123–132. https://doi.org/10.1016/j.envpol.2012.09.015.

INEC. (2021). Costa Rica en cifras 2021. www.inec.cr

Kardel, F., Wuyts, K., De Wael, K., & Samson, R. (2018). Biomonitoring of atmospheric particulate pollution via chemical composition and magnetic properties of roadside tree leaves. *Environmental Science and Pollution Research*, 25(26), 25994–26004. https://doi.org/10.1007/s11356-018-2592-z.

Kawasaki, K., Horikawa, K., & Sakai, H. (2017). Magnetic biomonitoring of roadside pollution in the restricted. *Environmental Science and Pollution Research*, 10313–10325. https://doi.org/10.1007/s11356-017-8702-5.

Khamesi, A., Khademi, H., & Zeraatpisheh, M. (2020). Biomagnetic monitoring of atmospheric heavy metal pollution using pine needles: the case study of Isfahan, Iran. *Environmental Science and Pollution Research*, 27(25), 31555–31566. https://doi.org/10.1007/s11356-020-09247-5.

Leng, Xiang, Qian, X., Yang, M., Wang, C., Li, H., & Wang, J. (2018). Leaf magnetic properties as a method for predicting heavy metal concentrations in PM2.5 using support vector machine: A case study in Nanjing, China. *Environmental Pollution*, 242, 922–930. https://doi.org/10.1016/j.envpol.2018.07.007.

Leng, Xiangzi, Wang, C., Li, H., Qian, X., Wang, J., & Sun, Y. (2017). Response of magnetic properties to metal deposition on urban green in Nanjing, China. *Environmental Science and Pollution Research*, 24(32), 25315–25328. https://doi.org/10.1007/s11356-017-0133-9.

Li, H., Qian, X., Wei, H., Zhang, R., Yang, Y., Liu, Z., Hu, W., Gao, H., & Wang, Y. (2014). Magnetic properties as proxies for the evaluation of heavy metal contamination in urban street dusts of Nanjing, Southeast China. *Geophysical Journal International*, 199(3), 1354–1366. https://doi.org/10.1093/gji/ggu253.

Li, H., Wang, J., Wang, Q., Tian, C., Qian, X., & Leng, X. (2017). Magnetic Properties as a Proxy for Predicting Fine-Particle-Bound Heavy Metals in a Support Vector Machine Approach. *Environmental Science and Technology,* 51(12), 6927–6935. https://doi.org/10.1021/acs.est.7b00729.

Limo, J., Paturi, P., & Mäkinen, J. (2018). Magnetic biomonitoring with moss bags to assess stop-and-go traffic induced particulate matter and heavy metal concentrations. *Atmospheric Environment*, 195, 187–195. https://doi.org/10.1016/j.atmosenv.2018.09.062.

Losacco, C., & Perillo, A. (2018). Particulate matter air pollution and respiratory impact on humans and animals. *Environmental Science and Pollution Research* (Vol. 25, Issue 34, pp. 33901–33910). Springer Verlag. https://doi.org/10.1007/s11356-018-3344-9.

Maher, B. A., Thompson, R., & Hounslow, M. W. (1999). Climates, Environments and Magnetism,. Cambridge University Press.

Mariéa, D. C., Chaparroa, M. A. E., Lavorniab, J. M., Sinitoa, A. M., Castañeda-Mirandaa, A. G., Gargiuloa, J. D., & Chaparrod, Mauro A.E. Böhnele, H. N. (2018). Atmospheric pollution

assessed by in situ measurement of magnetic susceptibility on lichens. *Ecological Indicators*, 95, 831–840.

Mitchell, R., & Maher, B. A. (2009). Evaluation and application of biomagnetic monitoring of traffic-derived particulate pollution. *Atmospheric Environment*, 43(13), 2095–2103. https://doi.org/10.1016/j.atmosenv.2009.01.042

MOPT. (2020). ANUARIO DE INFORMACIÓN DE TRÁNSITO 2019. https://www.mopt.go.cr/wps/wcm/connect/724c5cd7-31e8-415f-9e86-bd0571cfd9b9/AnuarioTransito2019.pdf?MOD=AJPERES.

Muñoz, D., Aguilar, B., Fuentealba, R., & Préndez, M. (2017). Environmental studies in two communes of Santiago de Chile by the analysis of magnetic properties of particulate matter deposited on leaves of roadside trees. *Atmospheric Environment*, 152(2017), 617–627. https://doi.org/10.1016/j.atmosenv.2016.12.047.

Okedeyi, O. O., Dube, S., Awofolu, O. R., & Nindi, M. M. (2014). Assessing the enrichment of heavy metals in surface soil and plant (Digitaria eriantha) around coal-fired power plants in South Africa. *Environmental Science and Pollution Research*, 21(6), 4686–4696. https://doi.org/10.1007/s11356-013-2432-0.

Peel, M. C., Finlayson, B. L., & McMahon, T. A. (2007). Updated world map of the Köppen-Geiger climate classification. *Hydrology and Earth System Sciences*, 11(5), 1633–1644. https://doi.org/10.5194/hess-11-1633-2007.

Pétronille, M., Sanchez Bettuci, L., Bautista, F., Aguilar Reyes, B., & Gogichaishvili, A. (2013). Rock-magnetic and scanning electron microscopy studies on leaves, soils and urban dusts from Montevide and Ririapolis (Uruguay). *Latinmag Letters*, 3(Special Issue), 1–6.

Polezer, G., Tadano, Y. S., Siqueira, H. V., Godoi, A. F. L., Yamamoto, C. I., de André, P. A., Pauliquevis, T., Andrade, M. de F., Oliveira, A., Saldiva, P. H. N., Taylor, P. E., & Godoi, R. H. M. (2018). Assessing the impact of PM2.5 on respiratory disease using artificial neural networks. *Environmental Pollution*, 235, 394–403. https://doi.org/10.1016/j.envpol.2017.12.111.

Priyanka, S., Yadav, P., Ghosh, C., & Singh, B. (2020). Heavy metal capture from the suspended particulate matter by Morus alba and evidence of foliar uptake and translocation of PM associated zinc using radiotracer (65Zn). *Chemosphere*, 254(126863).

Rojas-Rodríguez, F., & Torres-Córdoba, G. (2013). Casuarina. Revista Forestal Mesoamericana Kurú, 10(25), 32–33.

RStudio Team. (2020). RStudio: Integrated Development for R. RStudio, PBC. (1.4.1717). R Foundation for Statistical Computing. http://www.rstudio.com/.

Sanleandro, P. M., Navarro, A. S., Díaz-Pereira, E., Zuñiga, F. B., Muñoz, M. R., & Iniesta, M. J. D. (2018). Assessment of heavy metals and color as indicators of contamination in street dust of a city in SE Spain: Influence of traffic intensity and sampling location. *Sustainability* (Switzerland), 10(11). https://doi.org/10.3390/su10114105.

Sharma, P., Yadav, P., Ghosh, C., & Singh, B. (2020). Heavy metal capture from the suspended particulate matter by Morus alba and evidence of foliar uptake and translocation of PM

associated zinc using radiotracer (65Zn). *Chemosphere*, 254, 126863. https://doi.org/10.1016/j.chemosphere.2020.126863.

U.S. EPA. (2007). Method 3051A Microwave Assisted Acid Digestion of Sediments, Sludges, Soils, and Oils. (Issue February). USA.

Wang, G., Chen, J., Zhang, W., Ren, F., Chen, Y., Fang, A., & Ma, L. (2019). Magnetic properties of street dust in Shanghai, China and its relationship to anthropogenic activities. *Environmental Pollution*, 255, 113214. https://doi.org/10.1016/j.envpol.2019.113214.

Wang, J., Li, S., Li, H., Qian, X., Li, X., Liu, X., Lu, H., Wang, C., & Sun, Y. (2017). Trace metals and magnetic particles in PM2.5: Magnetic identification and its implications. *Scientific Reports*, 7(1), 1–11. https://doi.org/10.1038/s41598-017-08628-0.

Wilson, J. G., Kingham, S., Pearce, J., & Sturman, A. P. (2005). A review of intraurban variations in particulate air pollution: implications for epidemiological research. *Atmospheric Environment*, 39, 6444e6462.

Winkler, A., Contardo, T., Vannini, A., Sorbo, S., Basile, A., & Loppi, S. (2020). Magnetic emissions from brake wear are the major source of airborne particulate matter bioaccumulated by lichens exposed in Milan (Italy). *Applied Sciences* (Switzerland), 10(6). https://doi.org/10.3390/app10062073.

Wuyts, K., Hofman, J., Van Wittenberghe, S., Nuyts, G., De Wael, K., & Samson, R. (2018). A new opportunity for biomagnetic monitoring of particulate pollution in an urban environment using tree branches. *Atmospheric Environment*, 190, 177–187. https://doi.org/10.1016/j.atmosenv.2018.07.014.

Yap, J., Ng, Y., Yeo, K. K., Sahlén, A., Lam, C. S. P., Lee, V., & Ma, S. (2019). Particulate air pollution on cardiovascular mortality in the tropics: Impact on the elderly. *Environmental Health: A Global Access Science Source,* 18(34), 1–9. https://doi.org/10.1186/s12940-019-0476-4.

Zamudio, S., & Carranza, E. (1994). Cupressaceae. Flora Del Bajío y de Regiones Adyacentes, 29.

Zhu, Z., Sun, G., Bi, X., Li, Z., & Yu, G. (2013). Identification of trace metal pollution in urban dust from kindergartens using magnetic, geochemical and lead isotopic analyses. *Atmospheric Environment*, 77, 9–15. https://doi.org/10.1016/j.atmosenv.2013.04.053.

4.3. Comparison Between Machine Linear Regression (MLR) and Support Vector Machine (SVM) as Model Generators for Heavy Metal Assessment Captured in Biomonitors and Road Dust

Salazar-Rojas, T., Cejudo-Ruiz, F. R., & Calvo-Brenes, G. (2022). Comparison between machine linear regression (MLR) and support vector machine (SVM) as model generators for heavy metal assessment captured in biomonitors and road dust. *Environmental Pollution*, 314, 120227. https://doi.org/10.1016/j.envpol.2022.120227.

Comparison Between Machine Linear Regression (MLR) and Support Vector Machine (SVM) as Model Generators for Heavy Metal Assessment Captured in Biomonitors and Road Dust

Teresa Salazar-Rojas [1*]

Fredy Ruben Cejudo-Ruiz[2]

Guillermo Calvo-Brenes [3]

Abstract

Exposure to suspended particulate matter (PM), found in the air, is one of the most acute environmental problems that affects the health of modern society. Among the different airbone pollutants, heavy metals (HMs) are particularly relevant because they are bioaccumulated, impairing the functions of living beings. This study aimed to establish a method to predict heavy metal concentrations in leaves and road dust, through their magnetic properties measurements. For this purpose, machine learning, automatic linear regression (MLR), and support vector machine (SVM) were used to establish models for the prediction of airborne heavy metals based on leaves and road dust magnetic properties. Road dust samples and leaves of two common evergreen species (*Cupressus lusitanica / Casuarina equisetifolia*) were sampled simultaneously during two different years in the Great Metropolitan Area (GMA) of Costa Rica. MLR and SVM algorithms were used to establish the relationship between airborne heavy metal concentrations based on single (χlf) and multiple (χlf y χdf) leaf magnetic properties and road dust. Results showed that Fe, Cu, Cr, V, and Zn concentrations were well-simulated by SVM prediction models,

with adjusted R^2 values ≥ 0.7 in both training and test stages. By contrast, the concentrations of Pb and Ni were not well-simulated, with adjusted R2 values < 0.7 in both training and test stages. Heavy metal predicción models using magnetic properties of leaves from Casuarina equisetifolia, as collectors, yielded better prediction results than those based on the leaves of Cupressus lusitanica and road dust, showing relatively higher adjusted R2 values and lower errors (MAE and RMSE) in both training and test stages. SVM proved to be the best prediction model with variations between single (χlf) and multiple (χlf y χdf) magnetic properties depending on the element studied.

Keywords: heavy metal, biomonitors, air pollution, magnetic properties, machine linear regression, support vector machine.

1* Doctorado en Ciencias Naturales para el Desarrollo (DOCINADE), Escuela de Química, Tecnológico de Costa Rica; Universidad Nacional, Universidad Estatal a Distancia, Costa Rica; tsalazar@itcr.ac.cr; Código ORCID 0000000223663638.
2 Instituto de Geofísica, Universidad Nacional Autónoma de México; Michoacán, México; ruben@geofisica.unam.mx, Código ORCID 0000-0003-1003-5664
3 Escuela de Química, Tecnológico de Costa Rica; Cartago, Costa Rica; gcalvo@itcr.ac.cr, Código ORCID 00000002-7021-3509.
***** Corresponding author: tsalazar@itcr.ac.cr. Teresa Salazar Rojas, Escuela de Química, Tecnológico de Costa Rica, Cartago, Apartado postal: 159-7050, Costa Rica.

1. Introduction

One of the most serious environmental problems facing modern society is urban air pollution due to rapid economic and demographic growth (Goldizen et al., 2016; Lee et al., 2019; Li et al., 2020). The health effects associated with air pollution are related to respiratory problems, mainly correlated with temporary exposure to particulate matter (PM), especially the finest particles smaller than 2.5 μm ($PM_{2.5}$), which cause cardiopulmonary lesions and systemic diffusion (Weinmayr et al., 2015; Kulhánová et al., 2018; Losacco & Perillo, 2018; Polezer et al., 2018; Yap et al., 2019). Among the constituents of PM, heavy metals (HMs) are particularly relevant because they cannot be degraded or destroyed naturally; however, they can be diluted by

physicochemical agents and thus be leached, whereby they can then form soluble complexes, transported and distributed in ecosystems, and finally incorporated into trophic chains where they can be bioaccumulated, impairing the functions of living beings (Nagajyoti et al., 2010; Wu et al., 2016; Xiang Leng et al., 2018; Ahmad Bhat et al., 2019; Briffa et al., 2020; Xiao et al., 2021).

Due to the negative effects of air pollutants on health, their monitoring is important. Traditional methods of analysis require the use of monitoring stations that measure the different pollutants. However, their application in urban areas is reduced due to the high investment and maintenance costs of the necessary equipment, and chemical analysis is time-consuming and costly (Wilson et al., 2005; Xiang Leng et al., 2018).

Biomonitoring has proven to be an alternative method to study the impacts of air pollutants and a reliable method to discriminate between polluted and non-polluted areas (Sawidis et al., 2012; Serbula et al., 2013; Parmar et al., 2016; Nakazato et al., 2018). Biomonitoring has several advantages, such as lower cost, less ecological disruption and the production of reliable data related to the content of atmospheric pollutants and information on their effects on living systems (Markert et al., 2003; Burger, 2006; Hamza-Chaffai, 2014; Parmar, 2016; Leng et al., 2018). Likewise based on the relationship between elemental content and magnetic properties, the magnetic approach has been suggested as a simple and cost-effective tool to evaluate heavy metal pollution, captured by biomonitors, road dust and soil (Cejudo et al., 2015; Kawasaki et al., 2017; Li et al., 2017; Xiangzi Leng et al., 2017; Kardel et al., 2018; Gillooly et al., 2019).

The airborne HMs are usually trapped in suspended PM and these suspended particles are usually deposited on leaf surfaces and trapped in leaf waxes (Dzierzanowski et al., 2011). Morphological plant features like trichomes and grooves may enhance PM capture and absorption. The extent of plant foliar uptake on airborne particulates depends on foliar structure, particle size, load, and composition, besides plant morphological features; therefore, each biomonitor will exhibit different behavior and efficiency at capturing airborne particulates and HMs (Dzierzanowski et al., 2011; Bussotti et al., 2014; Sharma et al., 2020). It is difficult to distinguish between the amount of HMs taken up from the soil from the ones captured from the air; however, in the absence of industrial or agricultural activities, the airborne particulates and HMs are the result of vehicle combustion that eventually falls on the ground (Miri et al., 2016; Sharma et al., 2020).

Recently, the development of predictive air pollution models using machine learning approaches has been studied to expand and increase the effectiveness of air pollution monitoring programs

(Li et al., 2017; Leng et al., 2018; Li et al., 2020; Dai et al., 2020). Machine learning refers to any type of computer program that can "learn" on its own without having to be explicitly programmed by a human. It can be used in unsupervised machine learning, where the algorithms generate answers from unknown and unlabeled data to discover patterns in new data sets. Clustering algorithms, such as K-means, are often used in unsupervised machine learning and, in supervised learning, the user trains the program to generate a response based on a known and labeled data set. Examples of those are classification and regression algorithms, including random forests, decision trees, and support vector machines, the last one used in this study (Zhao et al., 2006; Wehle, 2017; Goodarzi et al., 2012).

Therefore, based on the need for alternative methodologies to expand, on a spatial and temporal scale, the monitoring of HMs contamination, this study aimed to establish a method to predict heavy metal concentrations based on magnetic properties measured on leaves and road dust. For this purpose, machine learning, automatic linear regression (MLR), and support vector machine (SVM) approaches were used.

2. Material and methods

2.1 Sampling Sites and plants

The Greater Metropolitan Area (GMA) is a very important geographic area because, although it covers only 3.8% of the national territory, it contains 70% of the automobile fleet, 62% of the population, 65% of the formal business park, and 82% of sales ((Nation State Program, 2019). Since most of the population, industry, and commerce are concentrated in specific sites in this area, people commute from one site to another, through public and private transportation, raising airborne pollutants levels in specific sites beyond WHO recommendations (World Health Organization, 1996; Castillo et al., 2015).

The sampling sites were selected considering their vehicle density obtained from the Traffic Information Yearbook 2019. To ensure representativeness of the sampling sites the vehicle density range of the primary routes was identified and systematic sampling was considered with a value of k that allowed the widest possible distribution, considering 8 sampling points (MOPT, 2020). Additionally, 4 sampling points were chosen to validate the model's results (Table 1). Ten samples were obtained from each sampling point for each monitor studied.

The land use in all selected sites was residential with some commercial spots. All the samples were taken nearby the road, where more traffic pollutants are accumulated (Mitchell & Maher, 2009; Hofman & Samson, 2014; Kawasaki et al., 2017).

The plants species were selected, after carrying out a census in January 2020, considering criteria of abundance, accessibility, longevity, proximity to the road and results obtained in previos study. The selected bioindicators were: *Cupressus lusitanica* (Cupressaceae) (Zamudio & Carranza, 1994) and *Casuarina equisetifolia* (Casuarinaceae) (Zamudio & Carranza, 1994), both of them perennials, with a foliage duration of 2 years or more (Table 1). Clarify that for some sites it was not possible to sample the two plants at exactly the same point, hence some sites such as 3, 6 and V2 have apostrophe indicating different vehicle density.

Table 1. Average daily number of vehicles of sampling sites.

Site	Daily average of vehicles	Monitor	Site	Daily average of vehicles	Monitor
1	0	Cl, Ce, rd	V1	3639	Cl, Ce, rd
2	17101	Cl, Ce, rd	V2	17866	Ce
3	32138	Ce, rd	V2’	23597	Cl, rd
3’	29198	Cl	V3	31999	Cl, Ce, rd
4	45326	Cl, Ce, rd	V4	44228	Cl, Ce, rd
5	62008	Cl, Ce, rd			
6	73982	Cl			
6’	77671	Ce, rd			
7	88585	Cl, Ce, rd			
8	104558	Cl, Ce, rd			

Cl=Cupressus *lusitanica,* Ce= *Casuarina equisetifolia,* rd= road dust

V = Validation point [1]Ministry of Public Construction and Transportation, 2020.

2.2 Sampling

A sum of 160 plant leaf samples was collected during two campaigns from February to March, one in 2020 and one in 2021. Mature foliage was taken from the lateral canopy facing the side of the road, among 1 and 5 plants per site, at a height of 1.5 to 2.0 m, considering the normal height of human respiration and to avoid the influence of urban soil particles (Chaparro et al., 2015).

The samples were stored in plastic bags and transferred into a coolbox. In the laboratory, the samples were dried at (55 ±1) ºC to constant weight and then ground for subsequent analysis at the laboratory following Aguilar et al., (2012).

A total of 80 road dust samples were collected at the same sampling sites and period time of the plants. The samples were collected on the road, a sweep of approximately one square meter was made to the edge of the road. The road dust samples were stored in plastic bags and transferred into a coolbox. In the laboratory, the samples were dried at environmental temperature and then sieved for subsequent analysis at the laboratory following Aguilar et al., (2012).

2.3 Chemical Methods

Replicates of unwashed leaf and road dust samples were tested for metal content: Cu, Cr, Cu, Ni, Pb, V, Zn, Fe, and Cd. All plant and road dust samples were examined for HMs content by EPA method 3051 Microwave-Assisted Acid Digestion of Solids using a Mars 6 (CEM) (U.S. EPA, 2007), and determinations were conducted on an Atomic Absorption Spectrophotometer (Perkin Elmer, model AAnalyst 800), backed by a graphite furnace and a hydride generator (Perkin Elmer, model FIAS 100), for determining trace-level detections. IV-Stock-10 from Inorganic Ventures was used as a reference standard.

2.4 Magnetic measurements Magnetic susceptibility

Magnetic susceptibility of the samples was determined following the recommendations of (Dearing, 1999). Dry samples were crushed with a mortar and packed tightly in a 10 cm^3 plastic container. A Bartington MS2B single sample dual frequency sensor and a Bartington MS3 Magnetic Susceptibility Meter were used to measure the susceptibility at low frequency (κ_{lf} at 0,46 kHz) and high frequency (κ_{hf} at 46,0 kHz).

Results were also used to determine: The value of specific susceptibility;

$$\chi lf = (\kappa lf/\rho) \quad (1)$$

Where ρ is the density of the material in kg m^{-3}.

And the percentage of frequency-dependent magnetic susceptibility;

$$\chi df\% = \left[\left(\frac{\kappa lf - \kappa hf}{\kappa lf}\right)\right] x\ 100 \quad (2)$$

The klf is the low-frequency magnetic susceptibility and khf is the high-frequency magnetic susceptibility. Through these magnetic parameters, the concentration of magnetic material and the presence of ultrafine particles (≤ 30 nm) of ferrimagnetic (SP) characteristics in the leaves of biomonitors were identified (Dearing, 1999; Bautista et al., 2014).

2.5 Model Formulation and Validation

The formulation and validation of the models were performed using RStudio software version 1.4.1717, packages; tidyverse, caret and e1071 (RStudio Team, 2020). Four types of models were developed for each of the biomonitors and road dust, obtaining for all of them, as output data, the concentration of HM, Table

2. Chosen models were selected for each HM and monitor among at least fifty models' trials.

Table 2. Type of model developed for obtaining HM concentration.

Model	Type	Input (Magnetic Property)
I	Machine linear regression -single (MLR-S)	χlf
II	Support vector machine - single (SVM-S)	χlf
III	Machine linear regression - multiple (MLR-M)	χlf y χdf
IV	Support vector machine - multiple (SVM-M)	χlf y χdf

Machine linear regression single and multiple

Single and multiple linear regression models were generated through machine learning based on magnetic parameters and heavy metal concentrations, of the type:

$$HM_c = (\beta_0 + \beta_1 Z_1 + \beta_2 Z_2 + \beta_3 Z_3) + e \quad (3)$$

Where, β_0 is the intercept, β_1, β_2, β_3 are the ratio coefficients for each magnetic parameter Zi and e is the error associated with the model (Acuña, 2015).

Support vector machine single and multiple

Support vector machine-generated models are supervised learning models with associated learning algorithms that analyze the data used for classification and regression analysis. In support vector regression, the straight line required to fit the data is called a hyperplane (Raj, 2020). In these the input variable is first mapped to a high-dimensional feature space by using

the Kernel function, after which feature mapping enables the treatment of nonlinear problems in a linear space. In this high-dimensional feature space, the
SVM approximates a dataset with a linear function through the function;

$$y = f(x, \omega) = \sum_{i=1}^{m} \omega_i \varnothing(x_i) + b \quad (4)$$

where ⌀(xi) presents the input variables after Kernel transformation and ωi and b are the coefficients that are estimated by minimizing the regularized hazard function (Li et al., 2017).

The validation of the models was carried out using two methods.

The first method consisted of performing cross-validation with a machine learning approach, Set Approach (or Data Split) of 80/20. Cross-validation is a technique in which the model is trained using the subset of the data set and then the model is evaluated using the complementary subset of the data set (Mishra, 2021). In cross-validation, the data are randomly divided into two sets, for the study 80% of the set was used for model training and 20% for the model test set (Li et al., 2017).

The second validation method corresponded to taking a sample for each biomonitor and road dust at 4 new sampling points, Table 1, following the same sampling procedures as the model construction samples.

The adjusted determination coefficient (R^2) was used to evaluate the model performance between predicted and observed elemental concentrations. The mean absolute error (MAE) and root mean square error (RMSE), were used to evaluate the predictive efficiency of the model. The MAE and RMSE measure the residual errors, both of which provide an overall estimate of the difference between observed and predicted data (Xiang Leng et al., 2018).

2.6 Statistical Analysis

Statistical analyses of the magnetic and chemical data were carried out using RStudio software version 1.4.1717, including packages dplyr, lmtest, car, carData, tidyverse (RStudio Team, 2020). The improvement in the models obtained by varying from the linear model (MLR, I and III) to the nonlinear model (SVM, II and IV) and including as input χdf (III and IV) was quantified by calculating the improvement rates (IRs) of models for the training adjusted R^2 of each metal. IR was calculated as follows (Dai et al., 2020):

$$IR = \frac{R^2\ model(I, III, II) - R^2\ model(II, IV)}{R\ model(I, III, II)}{}^2 \quad (5)$$

3. Results and discussion

3.1 Monitors assessment

The mass-related concentrations of heavy metals and single (χlf)/multiple (χlf y χdf) leaf magnetic properties and road dust were simulated using MLR and SVM models, Tables 3, 4, and 5. Casuarina equisetifolia presented adjusted R2 values >0.9 for Fe, >0.8 for Cr and V, ≥ 0.7 Cu, and Zn, and > 0.4 and 0.3 for Pb and Ni respectively. For the same biomonitor, the test values adjusted R2 were higher, with results > 0.9 for Fe, Cu, Cr, and V, > 0.7 for Zn and > 0.6 and 0.5 for Ni, and Pb, respectively (Table 3). The RMSE and MAE values obtained for training and test data were low, being <1 for Pb, Cr, and V, ≤ 2 for Ni and < 10 for Cr, and Zn, except for Fe. The results obtained in this biomonitor are greater in the number of well-modeled HMs than those obtained in a study conducted in China with three biomonitors whose best model results were for Fe and Pb with an R > 0.7 (Xiang Leng et al., 2018).

Table 3. Adjusted R-squared (R^2) mean absolute error (MAE) and root mean squared error (RMSE) for Casuarina equisetifolia models. Best model for each heavy metal in **bold.**

Prediction (mg/kg)	Model	Train data			Test data		
		R^2	RMSE	MAE	R^2	RMSE	MAE
Fe	I	0.917	64.84	50.55	0.973	73.87	52.69
	II	**0.938**	**74.57**	**54.05**	0.962	60.08	45.21
	III	0.918	64.59	49.88	0.974	70.91	50.89
	IV	0.922	86.69	56.30	0.942	67.41	48.10
Cu	I	0.520	7.199	5.322	0.837	5.993	4.102
	II	**0.739**	**5.747**	**3.716**	0.858	9.377	5.063
	III	0.548	6.337	4.635	0.879	7.233	4.957
	IV	0.663	6.870	4.005	0.900	11.73	6.183
Pb	I	0.126	1.013	0.781	0.202	0.516	0.437
	II	0.406	0.813	0.624	0.641	0.791	0.681

	III	0.178	0.885	0.670	0.438	1.144	0.860
	IV	**0.437**	**0.800**	**0.572**	0.491	0.959	0.748
Cr	I	0.823	0.551	0.409	0.863	0.517	0.386
	II	0.802	0.638	0.409	0.886	0.483	0.353
	III	0.829	0.542	0.400	0.902	0.465	0.341
	IV	**0.836**	**0.590**	**0.397**	0.865	0.344	0.271
Ni	I	0.193	2.394	1.820	0.393	1.585	1.410
	II	0.340	2.173	1.539	0.521	2.057	1.639
	III	0.218	2.359	1.813	0.287	1.686	1.410
	IV	**0.348**	**2.065**	**1.334**	0.438	2.398	1.795
V	I	0.855	0.734	0.546	0.934	0.727	0.567
	II	**0.862**	**0.762**	**0.534**	0.944	0.490	0.403
	III	0.854	0.713	0.523	0.922	0.684	0.547
	IV	0.813	0.716	0.502	0.858	1.941	1.033
Zn	I	0.491	10.19	7.276	0.494	12.60	8.193
	II	**0.654**	**9.662**	**7.110**	0.737	5.164	4.201
	III	0.477	10.97	7.848	0.572	8.373	5.506
	IV	0.549	9.762	6.510	0.598	12.34	9.110

In Table 4, the adjusted R2 for training data in Cupressus lusitanica, was > 0.7 for Fe, > 0.6 for Zn, > 0.5 for Cu and Cr, > 0.3 for Pb and Ni and the last one was V with an adjusted R^2 > 0.2. For the testing data adjusted R^2 presented also higher values, Fe > 0.9, Zn > 0.7, Cr > 0.6, Cu, Pb, and Ni > 0.5 and V > 0.4. For Cupressus lusitanica models the RMSE and MAE values obtained for training and test data could be considered quite low too, ≤1 for Cr, and Ni, ≤ 2 for Pb, and V, < 10 for C, < 15 and Zn, except for Fe as well.

Table 4. Adjusted R-squared (R^2) mean absolute error (MAE) and root mean squared error (RMSE) for Cupressus lusitanica models. Best model for each heavy metal in **bold.**

Prediction		Train data			Test data		
(mg/kg)	Model	R^2	RMSE	MAE	R^2	RMSE	MAE
Fe	I	0.713	229.9	166.8	0.894	110.0	81.33
	II	0.745	226.2	149.0	0.938	88.83	58.45

	III	0.752	220.1	146.8	0.907	102.8	73.05
	IV	**0.757**	**216.3**	**137.6**	0.899	131.4	114.4
Cu	I	0.290	6.797	5.860	0.302	7.851	6.540
	II	0.415	6.463	4.689	0.447	6.033	4.359
	III	0.290	6.797	5.860	0.393	7.658	6.318
	IV	**0.536**	**5.613**	**4.199**	0.587	5.535	4.078
Pb	I	0.243	2.122	1.499	0.390	3.254	2.077
	II	**0.377**	**2.278**	**1.380**	0.389	2.449	1.711
	III	0.245	2.120	1.487	0.315	2.107	2.107
	IV	0.338	2.303	1.385	0.532	2.553	1.583
Cr	I	0.432	0.723	0.585	0.462	0.595	0.482
	II	**0.588**	**0.585**	**0.457**	0.607	0.668	0.505
	III	0.435	0.722	0.582	0.489	0.576	0.477
	IV	0.479	0.680	0.471	0.497	0.726	0.583
Ni	I	0.215	1.010	0.790	0.266	1.650	1.142
	II	0.335	0.943	0.692	0.438	1.649	1.187
	III	0.168	1.176	0.911	0.532	0.872	0.692
	IV	**0.355**	**1.082**	**0.787**	0.359	0.839	0.630
V	I	0.174	2.497	1.976	0.381	2.203	1.976
	II	0.269	2.462	1.783	0.360	2.209	1.813
	III	0.192	2.512	2.031	0.290	2.104	1.628
	IV	**0.289**	**2.502**	**1.689**	0.411	2.234	1.859
Zn	I	0.498	17.49	12.71	0.768	12.53	8.813
	II	**0.670**	**14.83**	**11.04**	0.750	10.35	7.310
	III	0.195	2.475	1.997	0.286	2.296	1.839
	IV	0.329	2.381	1.666	0.370	2.086	1.829

Results showed, except for Fe, higher adjusted R^2 generally linked lower RMSE and MAE values, as in studies conducted in Nanjing, China (Xiang Leng et al., 2018). Fe presented the highest values of RMSE and MAE in all samples, including validation data (Table S1-S3), which could be a reflection of the small amount of data with high Fe concentration within the samples, also found in other studies (Schmidt et al.; 2005; Lu et al., 2007). Somehow normal because Fe has low variability in the environment, that is why it is used as normalizing element (Okedeyi et al., 2014).

Road dust samples presented the lowest adjusted R^2 of the monitors studied (Table 5). For training data adjusted R^2 was > 0.2 for Cr, Ni, V and Zn, > 0.1 for Fe and < 0.1 for Cu and Pb. Adjusted R^2 for testing data was higher than training data, with values ≥ 0.5 for Fe and Cr, > 0.4 for Ni and Zn, > 0.3 for V, > 0.2 for Pb and < 0.1 for Cu. The RMSE and MAE values obtained for road dust were much higher and more variable than those obtained by the plants for most of the HMs and even greater for Fe (Table 5).

Table 5. Adjusted R-squared (R^2) mean absolute error (MAE) and root mean squared error (RMSE) for Road dust models. Best model for each heavy metal in **bold.**

Prediction		Train data			Test data		
(mg/kg)	Model	R^2	RMSE	MAE	R^2	RMSE	MAE
Fe	I	0.029	10402	8235	0.299	12536	10735
	II	0.079	10164	7349	0.289	12533	9292
	III	0.040	11590	9291	0.496	8384	6942
	IV	**0.171**	**10080**	**7135**	0.423	10215	7511
Cu	I	0.002	148.2	110.1	0.000	224.5	138.2
	II	0.030	183.1	104.7	0.080	107.5	90.07
	III	0.026	169.9	117.7	0.095	137.6	118.7
	IV	**0.051**	**167.9**	**90.13**	0.068	183.8	106.3
Pb	I	0.021	85.35	56.96	0.078	79.77	58.80
	II	0.024	76.73	45.33	0.232	124.8	73.98
	III	0.029	85.01	55.99	0.163	78.09	55.14
	IV	**0.082**	**75.28**	**40.54**	0.102	125.1	71.81
Cr	I	0.003	30.49	24.86	0.091	25.35	21.61
	II	0.107	29.18	22.50	0.283	22.38	17.51
	III	0.086	29.19	24.29	0.087	25.21	21.65
	IV	**0.272**	**26.23**	**20.48**	0.572	17.28	14.46
Ni	I	0.025	19.93	15.84	0.053	14.52	12.68
	II	0.110	18.74	13.50	0.410	14.86	12.44
	III	0.057	17.98	14.47	0.224	20.33	15.19
	IV	**0.276**	**16.93**	**11.93**	0.331	15.30	12.99
V	I	0.002	45.03	37.96	0.062	43.99	34.22

	II	0.120	41.91	32.95	0.230	43.45	36.30
	III	0.004	44.02	37.01	0.029	47.96	38.22
	IV	**0.273**	**38.14**	**28.51**	0.344	38.69	33.25
Zn	I	0.002	163.1	129.2	0.090	145.5	121.1
	II	0.109	166.8	117.3	0.246	101.2	73.52
	III	0.137	145.9	117.2	0.257	156.4	126.1
	IV	**0.288**	**157.6**	**103.5**	0.402	104.8	77.39

It should be noted that the R^2s of the test data in Tables 3, 4, and 5 are greater than the R2s of the training data, as this is a criterion for the creation and selection of models with machine learning, to avoid overfitting the models and to ensure that the models work well data different from those used for their creation. A comparison of Tables 3, 4 and 5 shows that between the two biomonitors and the road dust, *Casuarina equisetifolia,* presented the highest adjusted R^2 values for all HMs for both training and test data. Although the leaves of different plant species have been shown to accumulate particles, only particles with a diameter of less than 10 μm are encapsulated in the cuticle. The degree of particle retention and encapsulation will vary depending on the type of plant, which points to the importance of leaf characteristics (roughness, smoothness, hairiness, petiole length and stiffness, orientation, etc.), cuticle chemical composition (amount of individual wax constituents responsible for cuticle hydrophobicity) and cuticle structure (thickness, morphology, alteration of the structure with age, presence of epicuticular wax crystals) (Bussotti et al., 2014). In the case of *Casuarina equisetifolia,*it*,* it has evergreen foliage, although they are not true leaves, these are reduced to small scales that perform the photosynthetic function in equal sections (hence its name *equisetifolia*) (Rojas-Rodríguez & Torres-Córdoba, 2013).

A factor that can affect the reliability of the models is the meteorological conditions, since they affect the magnetic properties, so the samples were taken at the same time of the year and under the same dry conditions. The results obtained showed to be comparable to those obtained by models in which meteorological conditions have been included. For example, in a study in which leaves of Osmanthus fragrans Lour was considered, training R and test R values were obtained for all the elements studied in the range of 0. 693-0.918 and 0.667-0.903, respectively, and in this study, the R2 values for Casuarina equisetifolia were in the range of 0.348-0.938 and 0.438 and 0.962 for metals, with Ni being the metal with the lowest value for both studies (Dai et al., 2020).

3.2 Models comparison

The comparison of the training adjusted R^2 and the IR obtained for each HM, according to the different models and monitors are plotted in Fig. 1, 2 and 3 (Dai et al., 2020).
Fig. 1 shows positive IR for 6 /7 HMs from the MLR-S to the SVM -S model, 4/7 HMs from the MLR-M to the SVM -M and 3/7 HMs from SVM -S to SVM -M for *Casuarina equisetifolia.*
As well in Table 3, it can be observed that the best adjusted R^2 results and the lowest RMSE and MAE values for Fe, Cu, V and Zn were obtained by model II (SVM -S) and for Pb, Cr Ni by model IV (SVM M) in *Casuarina equisetifolia*.

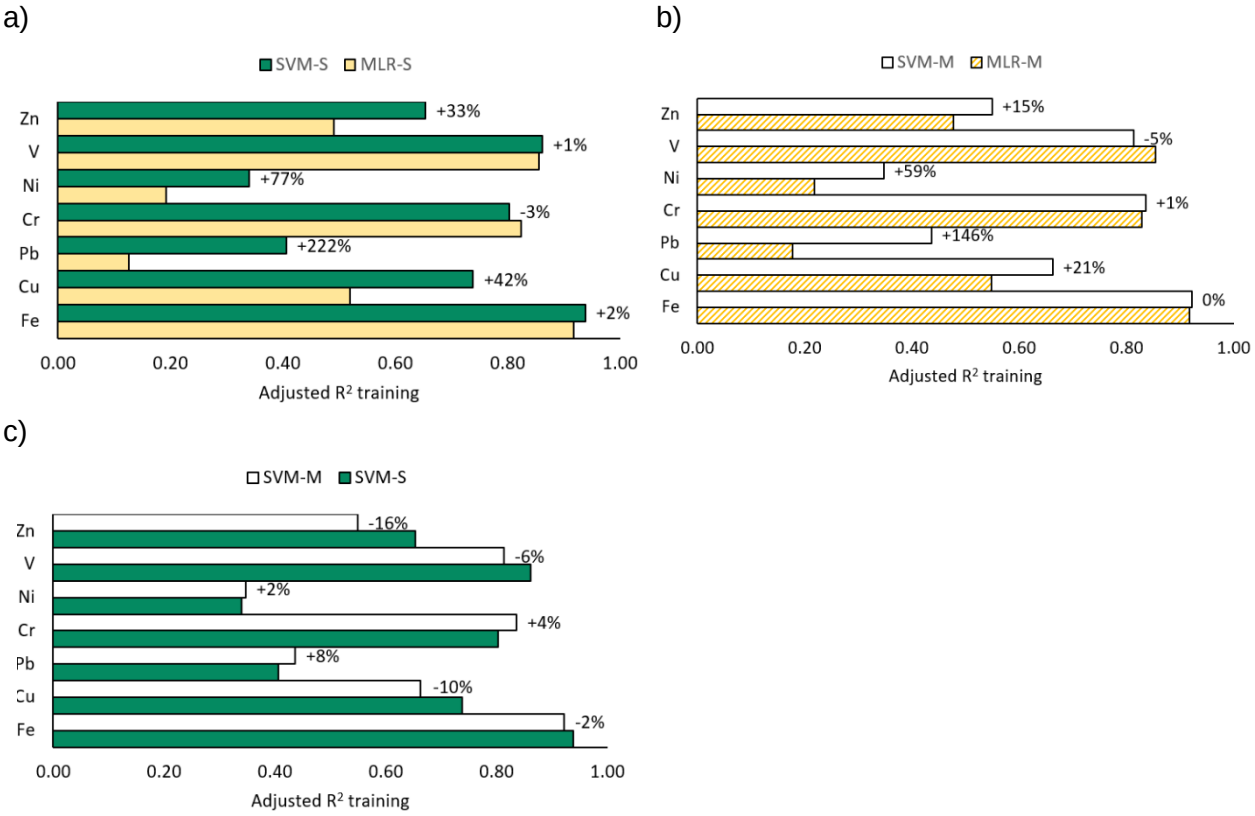

Fig. 1. Comparisons of the training adjusted R^2 and rate of improvement obtained by (a) models I (MLRS) and II (SVM -S), (b) models III (MLR-M) and IV (SVM -M), and models II and IV of the *Casuarina equisetifolia*.

For *Cupressus lusitanica*, Fig. 2, all HMs showed a positive IR from MLR to SVM in both simple and multiple and 4/7 HMs with a positive IR from SVM -S to SVM -M.

Likewise, in Table 4, it is shown that the best adjusted R^2 results and the lowest RMSE and MAE values for Pb, Cr and Zn are obtained with model II (SVM -S) and, for Fe, Cu, Ni and V with model IV (SVM -M).

a) b)

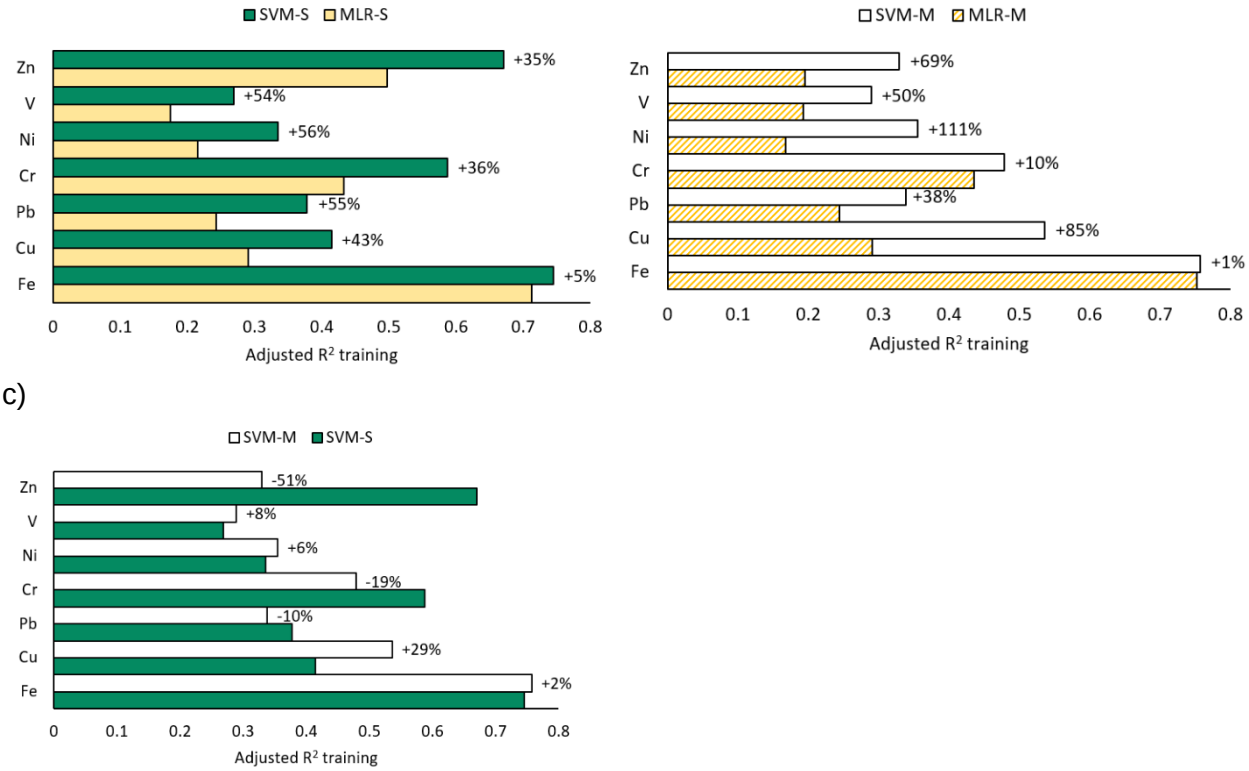

c)

Fig.2. Comparisons of the training adjusted R^2 and IR obtained by (a) models I (MLR-S) and II (SVM -S), (b) models III (MLR-M) and IV (SVM -M), and models II and IV for Cupressus *lusitanica*.

In Fig. 3, road dust showed the greatest positive IR among models, with values > 100% in the majority of them from MLR to SVM and from simple to multiple regression. All heavy metals analyzed presented the best adjusted R^2 results in model IV (SVM -M), as lower RMSE and MAE values, for most HMs, Table 5.

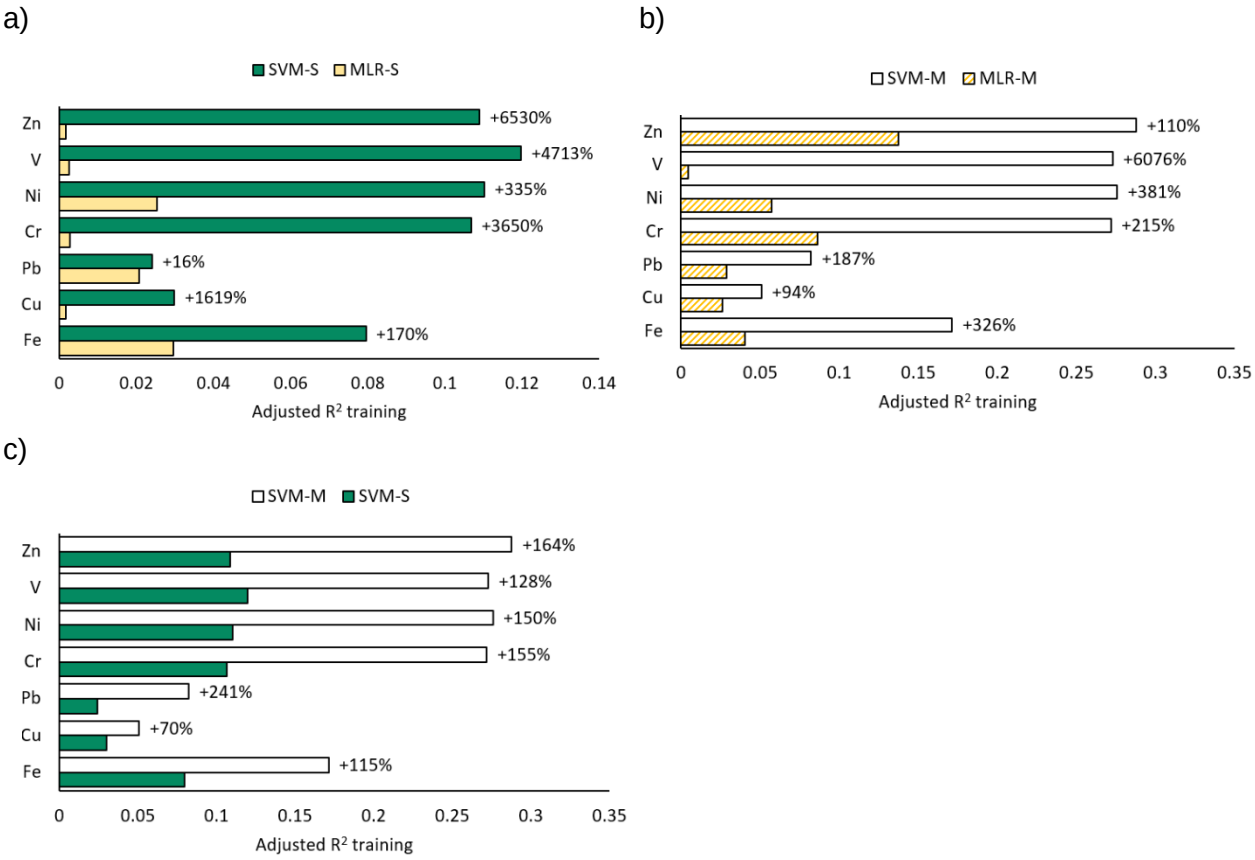

Fig. 3. Comparisons of the training adjusted R^2 and IR obtained by (a) models I (MLR-S) and II (SVM S), (b) models III (MLR-M) and IV (SVM -M), and models II and IV for road dust.

These results obtained by comparing the linear (MLR) with the nonlinear (SVM) approach showed a better nonlinear than linear relationship between metal concentrations and magnetic properties, especially for *Cupressus lusitanica* and road dust (Li et al., 2014).

In addition, similar results were obtained in which SVM showed a higher training correlation coefficient (R), and lower MAE and RMSE, than MLR, in the measurement of HMs in PM collected on quartz microfiber filters (Whatman, Maidstone, UK), proving the similarity of biomonitors with the use of filters used in traditional environmental monitoring. (Leng et al., 2017).

Comparing test data results, the adjusted R^2 for the test data, Fig. 4, shows a similar pattern to the training data, with the predominance of models II (SVM-S) and/or IV (SVM-M) for most of the HMs. For *Casuarina equisetifolia*, that pattern is shown by 5/7 HMs, Cu, Pb, Ni, V and Zn, only Fe and Cr present similar adjusted R^2 in all models. In *Cupressus lusitanica* and road dust, SVM

showed better results for 5/7 HMs with the exception of Ni and Zn in the former and Fe and Cu for road dust.

a) b)

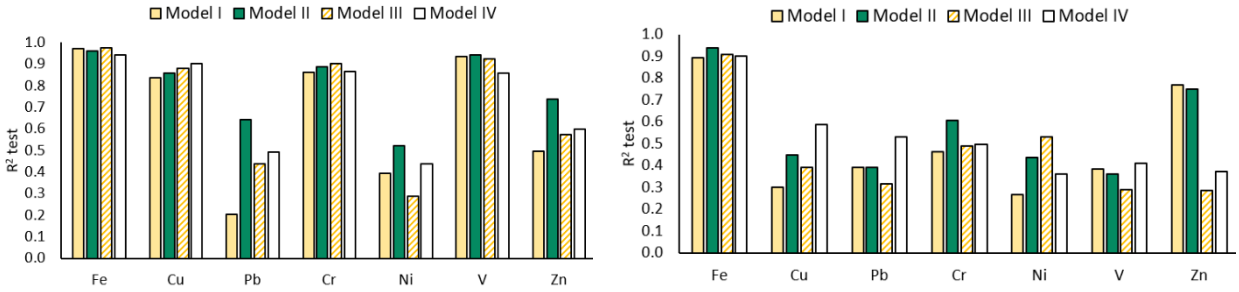

c)

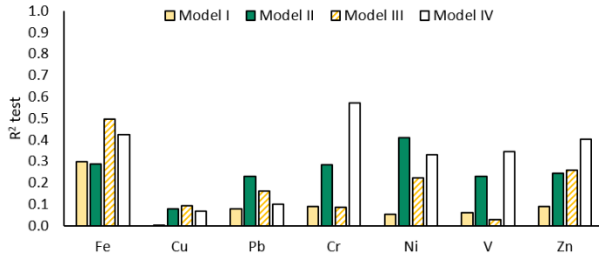

Fig. 4. Comparisons of test adjusted R^2 obtained by models I, II, III and IV for a) *Casuarina equisetifolia*, b) *Cupressus lusitanica* and c) Road dust.

Comparisons between estimated versus observed concentrations in the training and test phases were plotted for the 4 metals with the best adjusted R2 values in the different monitors, Fig. 5, 6, and 7. For Casuarina equisetifolia, the best models were for Fe, Cu, Cr, and V, and the values between HMs estimated and observed concentrations for the MLR and SVM models are quite similar (Fig. 5).

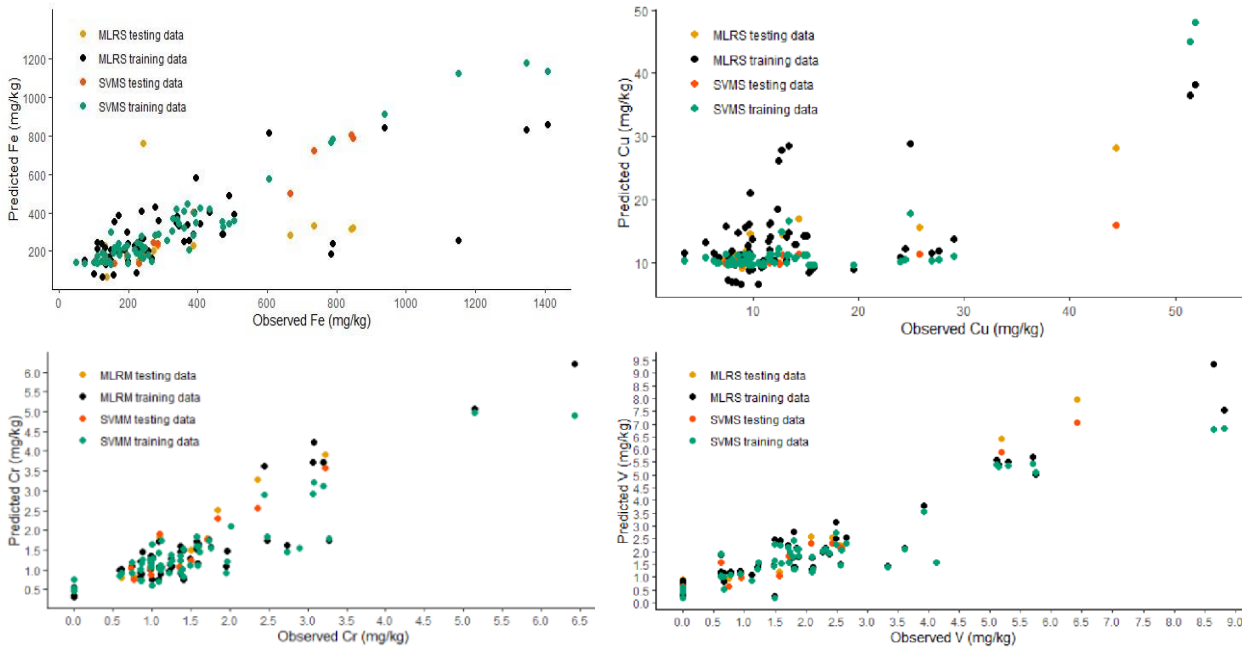

Fig. 5. Estimated compared to observed concentrations in the training and test phases of a) Fe, b) Cu, c) Cr y d) V, expressed as mass concentrations for models I and II for *Casuarina equisetifolia*.

For Cupressus lusitanica, the best modeled HMs were Fe, Cu, Cr, and, Zn, and it can be noticed a larger deviation between estimated and observed MLR values for the SVM models for both training and testing data (Fig. 6).

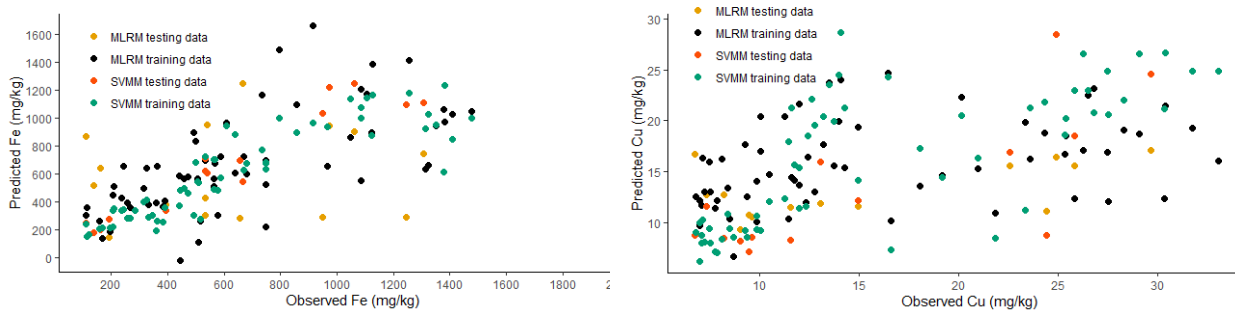

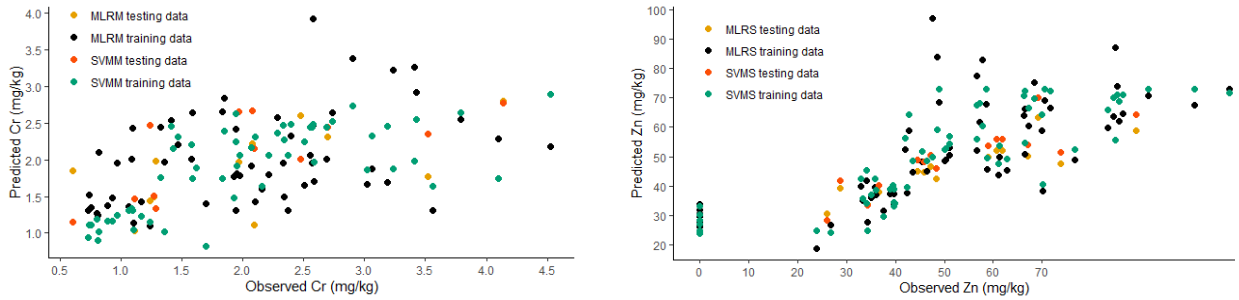

Fig.6. Estimated compared to observed concentrations in the training and test phases of a) Fe, b) Cu, c) Cr y d) Zn, expressed as mass concentrations for models I and II for *Cupressus lusitanica*.

Road dust the best modeled HMs were Cr, Ni, V, and, Zn, however those present an even greater deviation between the estimated and observed values for both MLR and SVM.

This shows that the greater the dispersion between the data, the better the SVM model maintains a certain degree of a linear relationship between the estimated and observed data, minimizing the error.

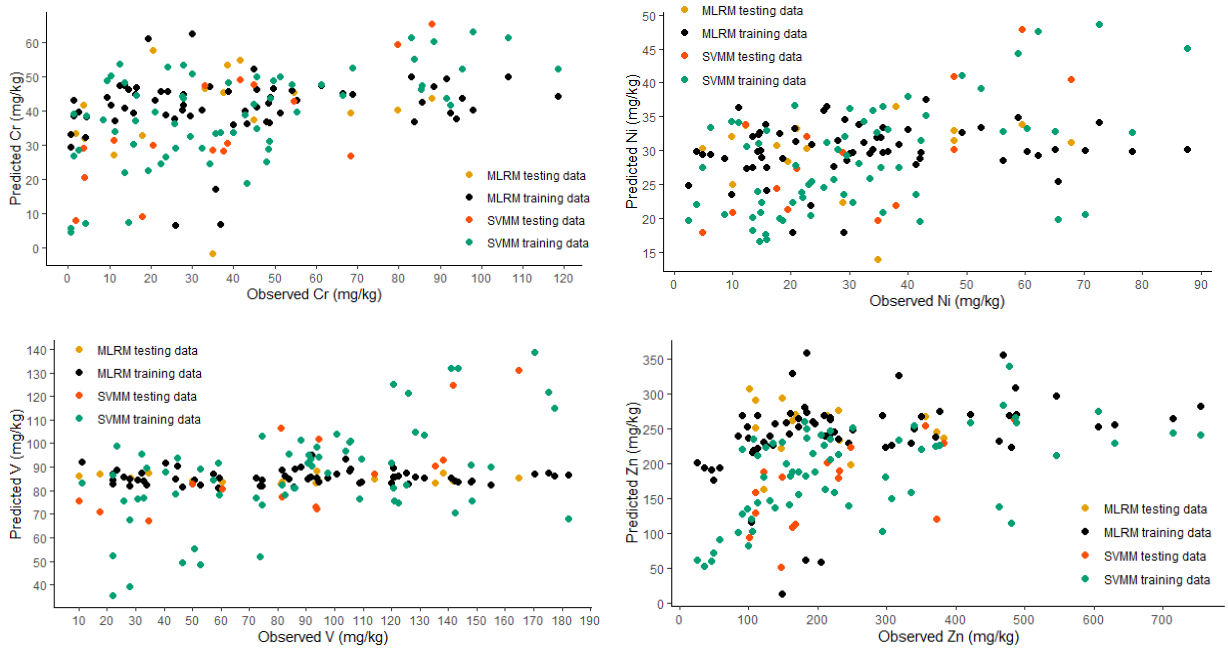

Fig. 7. Estimated compared to observed concentrations in the training and test phases of a) Fe, b) Cu, c) Cr y d) Zn, expressed as mass concentrations for models I and II for road dust.

Other model validation approach

The results of the second model validation method, in which new points were sampled and their HMs content determined, are shown in Tables S1, S2 and S3. They show the RMSE and MAE values of the residuals obtained by comparing the experimental data with those obtained by the different models.

Considering the models II and IV which showed the best adjusted R^2 in the training and test results for *Casuarina equisetifolia* (Table 3) Fe is the one that showed (Table S1) the highest values of RMSE (51.2159.25) and MAE (42.27-47.66), for the rest of metals the values of RMSE and MAE would be quite low, < 14.0 for Zn, <3.0 for Cu, < 2.0 for Pb, Ni, V and <0.5 for Cr.

For the same models, II and IV, Cupressus *lusitanica* showed the highest RMSE and MAE values for Fe and Zn, >100, followed by Pb, Cu, V, Ni and Cr with values of < 30, 10, 3,0, 1,0 and 0.5, respectively (Table S2). The values obtained would be quite acceptable for most of the HMs studied. For Fe and Zn, although the RMSE and MAE values may seem high, however, the fact that the concentration ranges are low (ppm) means that a good approximation can still be obtained.

As for road dust (Table S3), it presented the highest RMSE and MAE values for all HMs and models. With values in the model with the best training and test results, model IV (SVM -M), with values >1000, and 100, for Fe and Zn; < 50, for Cu, Pb, V, <20 for Cr and < 10 for Ni.

For the two biomonitors, in general terms, the error values (MAE and RMSE) were similar or lower for 5/7 of the heavy metals (Fe, Cu, Cr, Ni, V); only Pb and Zn presented errors higher than those obtained with the training and test data. As for road dust, the RMSE and MAE values were lower for all the heavy metals studied in 3 of the 4 models, except model III (MLR-M). These results demonstrate that the generated models, especially those of SVM, are valid models for the prediction of heavy metal content through magnetic properties in biomonitors.

3.4 Magnetic properties

Pearson's correlation coefficient (r) was calculated between the different heavy metals, vehicle quantity, and magnetic properties (Table S4). The usefulness of magnetic measurements as indicators of environmental contamination is based on the correlation between magnetic properties and iron concentrations, as well as the association between iron and heavy metals (Leng et al., 2017). Evidence of some of those significant correlations between magnetic properties and HMs concentration compared with results obtained for similar studies are shown in Table 6. For all the elements studied, except for Pb, the r-value obtained was higher for *Casuarina equisetifolia* compared to *Cupresses lusitanica,* and the results obtained for other studies (Table 6).

Table 6. Correlation between magnetic properties and HMs content in different biomonitors and studies.

Magnetic Property	**Significative correlation**	**Biomonitor**	**Reference**
χlf	r ≥ 0.9 for Fe, Cr, and, V, r ≥ 0.7 for Cu, and Zn, r > 0.4 for Ni, and r > 0.3 for Pb	*Casuarina equisetifolia*	This study
χlf	r > 0.8 for Fe, r >0.7 for Zn, >0.6 for Cr, and >0.5 for Cu, r > 0.4 for Ni, V, and Pb.	*Cupresses lusitanica*	This study
χlf	r >0.6 for Fe, r >0.4 for Mn, Ni, and Pb, r > 0.3 for V, Zn, As, and r >0.2 Cu)	*Osmanthus fragrans*	(Xiangzi Leng et al., 2017)
SIRM	r >0.7 for Fe, Zn, Mn, Co and Zr, r >0.6 for Ti, Ba, Ni, Cu, and V, r > 0.5 for Al, Si, and Cr	*Chamaecyparis lawsoniana*	(Kardel et al., 2018)
χlf	r >0.5 Fe, r >0.3 Zn, r >0.2 for Pb, Cu and Ni, r > 0.1 for Co)	*Pinus mugo*	(Khamesi et al., 2020)

SIRM: saturation isothermal remanent magnetisation

As for road dust, Table 9 shows a weak correlation between heavy metals and χlf, being significant only for Fe, indicating a possible non-linear relationship between them, probably due to multiple pollutant sources, since road dust had to be sampled in the ditch next to the road, where traces of metals accumulate from traffic, gray sewage from nearby houses and businesses and soil. As identified in previous works with multiple sources of heavy metals, in industrial and urban areas (Li et al., 2017; Li et al., 2014).

The magnetic property, kdf, on the other hand, showed significant correlations only with Fe for *Casuarina equisetifolia* and with Zn and χlf for road dust.

4. Conclusions

The best adjusted R^2 values in both training and test stages of the predictive model for *Casuarina equisetifolia, Cupressus lusitanica*, and road dust were obtained with the Support Vector Machine (SVM) model, with variations between single (χlf) and multiple (χlf y χdf) magnetic properties depending on the element studied.

The best adjusted R^2 results and the lowest RMSE and MAE for most of the elements studied were obtained for the *Casuarina equisetifolia*, making it the first among the monitors studied, follow by *Cupressus lusitanica* and last the road dust. Fe, Cu, Cr, V, and Zn concentrations were well-simulated by the prediction models (SVM S-M), with adjusted R^2 values ≥ 0.7 in both training and test stages for *Casuarina equisetifolia*. By contrast, the concentrations of Pb and Ni were not well-simulated, with most adjusted R^2 values < 0.7 in both training and test stages. Therefore, our current study provided an approach to predict heavy metals based on the magnetic properties of dust-laden tree leaves.

Our results showed that airborne heavy metals can be predicted from the magnetic properties of leaves based on a suitable nonlinear statistical method. However, since the measurement of magnetic properties is an indirect method to measure HMs content, in addition to other factors such as settling time, particle size distribution, and meteorological conditions can easily affect airborne heavy metal concentrations were not considered in this study. This method is proposed as a screening method to elucidate the HMs content in an easier, faster, and cheaper way and subsequently perform a more comprehensive analysis where and when needed.

Declarations

Acknowledgements

The authors thank the Technological Institute of Costa Rica (ITCR) and the National Autonomous University of Mexico (UNAM), for their financial and administrative support. In addition, the Center for

Research in Environmental Protection (CIPA), Center for Research and Chemical and Microbiological Services (CEQIATEC), and Institute of Geophysics (Morelia) for their support of the project.

Compliance with ethical standards Bioindicators were collected in accompliance with the ethical standards of the Technological Institute of Costa Rica.

Consent to participate Consent for publication

Conflict of interest The authors declare that they have no conflict of interest.

Availability of data and material Code availability Not applicable

5. References

Acuña, E. (2015). *Regresión Aplicada usando R*. https://www.researchgate.net/publication/335796371_REGRESION_APLICADA_USANDO_R.

Aguilar, B., Cejudo, R., Martínez, J., Bautista, F., Goguitchaichvili, A., Carvallo, C., & Morales, J. (2012). Ficus benjamina leaves as indicator of atmospheric pollution: A reconaissance study. *Studia Geophysica et Geodaetica*, *56*(3), 879–887. https://doi.org/10.1007/s11200-011-0265-1.

Ahmad Bhat, S., Hassan, T., & Majid, S. (2019). HEAVY METAL TOXICITY AND THEIR Harmful Effects on Living Organisms-A Review. *International Journal of Medical Science and Diagnosis Research (IJMSDR)*, *January*. https://doi.org/10.32553/JMSDR.

Bautista, F., Cejudo-Ruiz, R., Aguilar-Reyes, B., & Gogichaishvili, A. (2014). The potential of magnetism as a means for the classification of soils: A review. Boletin de La Sociedad Geologica Mexicana, 66(2), 365–376. https://doi.org/10.18268/BSGM2014v66n2a11.

Briffa, J., Sinagra, E., & Blundell, R. (2020). Heavy metal pollution in the environment and their toxicological effects on humans. *Heliyon*, *6*(9), e04691. https://doi.org/10.1016/j.heliyon.2020.e04691.

Burger, J. (2006). Bioindicators: Types, Development, and Use in Ecological Assessment and Research. *Environmental Bioindicators*, *1*(1), 22–39. https://doi.org/10.1080/15555270590966483.

Bussotti, F., Pollastrini, M., Killi, D., Ferrini, F., Fini, A., 2014. Ecophysiology of urban trees in a perspective of climate change. Agrochimica 58 (3), 247–268. https://doi.org/10.12871/0021857201431, 00021857.

Castillo, J. B., Murillo, J. H., Aias, D. S., Guerrero, V. H. B., & Marín, J. F. R. (2015). *Informe de Calidad del Aire 2013-2015*. https://www.ministeriodesalud.go.cr/images/stories/docs/DPAH/2016/DPAH_VI_informe_anual_cal idad_aire_GAM_2013_2014.pdf.

Cejudo, R., Bautista, F., Quintana, P., Delgado, M. del C., Aguilar, D., Goguitchaichvili, A., & Morales, J. J. (2015). Correlación entre elementos potencialmente tóxicos y propiedades magnéticas en suelos de la Ciudad de México para la identificación de sitios contaminados: definición de umbrales magnéticos. *Revista Mexicana de Ciencias Geológicas*, *32*(1).

Chaparro, M. A. E., Chaparro, M. A. E., Castañeda Miranda, A. G., Böhnel, H. N., & Sinito, A. M. (2015). An interval fuzzy model for magnetic biomonitoring using the specie Tillandsia recurvata L. *Ecological Indicators*, *54*, 238–245. https://doi.org/10.1016/j.ecolind.2015.02.018.

Dai, Q., Zhou, M., Li, H., Qian, X., Yang, M., & Li, F. (2020). Biomagnetic monitoring combined with support vector machine: a new opportunity for predicting particle-bound-heavy metals. *Scientific Reports*, *10*(1), 1–11. https://doi.org/10.1038/s41598-020-65677-8.

Dearing, J. A. (1999). Using the Bartington MS2 System. *Environmental Magnetic Susceptibility*, 52. Dzierzanowski, K., Popek, R., Gawrońska, H., Saebø, A., & Gawroński, S. W. (2011). Deposition of particulate matter of different size fractions on leaf surfaces and in waxes of urban forest species. *International Journal of Phytoremediation*, *13*(10), 1037–1046. https://doi.org/10.1080/15226514.2011.552929.

Dzierzanowski, K., Popek, R., Gawronska, ´ H., , Saebø, A., Gawronski, ´ S.W., 2011. Deposition of particulate matter of different size fractions on leaf surfaces and in waxes of urban forest species. Int. J. Phytoremediation 13 (10), 1037–1046. https://doi.org/10.1080/15226514.2011.552929.

Gillooly, S. E., Michanowicz, D. R., Jackson, M., Cambal, L. K., Shmool, J. L. C., Tunno, B. J., Tripathy, S., Bain, D. J., & Clougherty, J. E. (2019). Evaluating deciduous tree leaves as biomonitors for ambient particulate matter pollution in Pittsburgh, PA, USA. *Environmental Monitoring and Assessment*, *191*(12). https://doi.org/10.1007/s10661-019-7857-6.

Goldizen, F. C., Sly, P. D., & Knibbs, L. D. (2016). Respiratory effects of air pollution on children. In *Pediatric pulmonology* (Vol. 51, Issue 1, pp. 94–108). John Wiley and Sons Inc. https://doi.org/10.1002/ppul.23262 .

Goodarzi, M., Jensen, R., & Vander Heyden, Y. (2012). QSRR modeling for diverse drugs using different feature selection methods coupled with linear and nonlinear regressions. *Journal of Chromatography B: Analytical Technologies in the Biomedical and Life Sciences*, *910*, 84–94. https://doi.org/10.1016/j.jchromb.2012.01.012.

Hamza-Chaffai, Amel, 2014. Usefulness of Bioindicators and Biomarkers in Pollution Biomonitoring. Int. J. Biotechnol. Wellness Ind. 3 (1), 19–26. https://doi.org/ 10.6000/1927-3037.2014.03.01.4.

Hofman, J., & Samson, R. (2014). Biomagnetic monitoring as a validation tool for local air quality models: A case study for an urban street canyon. *Environment International*, *70*(2014), 50–61. https://doi.org/10.1016/j.envint.2014.05.007.

Kardel, F., Wuyts, K., De Wael, K., & Samson, R. (2018). Biomonitoring of atmospheric particulate pollution via chemical composition and magnetic properties of roadside tree leaves. *Environmental Science and Pollution Research*, *25*(26), 25994–26004. https://doi.org/10.1007/s11356-018-2592-z.

Kawasaki, K., Horikawa, K., & Sakai, H. (2017). Magnetic biomonitoring of roadside pollution in the restricted. *Environmental Science and Pollution Research*, 10313–10325. https://doi.org/10.1007/s11356-017-8702-5.

Kulhánová, I., Morelli, X., Le Tertre, A., Loomis, D., Charbotel, B., Medina, S., Ormsby, J. N., Lepeule, J., Slama, R., & Soerjomataram, I. (2018). The fraction of lung cancer incidence attributable to fine particulate air pollution in France: Impact of spatial resolution of air pollution models. *Environment International*, *121*(2), 1079–1086. https://doi.org/10.1016/j.envint.2018.09.055.

Lee, D., Robertson, C., Ramsay, C., Gillespie, C., & Napier, G. (2019). Estimating the health impact of air pollution in Scotland, and the resulting benefits of reducing concentrations in city centres. *Spatial and Spatio-Temporal Epidemiology*, *29*, 85–96. https://doi.org/10.1016/j.sste.2019.02.003.

Leng, Xiang'zi, Wang, J., Ji, H., Wang, Q., Li, H., Qian, X., Li, F., Yang, M., (2017). Prediction of size-fractionated airborne particle-bound metals using MLR, BP-ANN and SVM analyses. Chemosp.

Leng, Xiang, Qian, X., Yang, M., Wang, C., Li, H., & Wang, J. (2018). Leaf magnetic properties as a method for predicting heavy metal concentrations in PM2.5 using support vector machine: A case study in Nanjing, China. *Environmental Pollution*, *242*, 922–930. https://doi.org/10.1016/j.envpol.2018.07.007.

Leng, Xiangzi, Wang, C., Li, H., Qian, X., Wang, J., & Sun, Y. (2017). Response of magnetic properties to metal deposition on urban green in Nanjing, China. *Environmental Science and Pollution Research*, *24*(32), 25315–25328. https://doi.org/10.1007/s11356-017-0133-9.

Li, H., Dai, Q., Yang, M., Li, F., Liu, X., Zhou, M., & Qian, X. (2020). Heavy metals in submicronic particulate matter (PM1) from a Chinese metropolitan city predicted by machine learning models. *Chemosphere*, *261*(March). https://doi.org/10.1016/j.chemosphere.2020.127571.

Li, H., Qian, X., Wei, H., Zhang, R., Yang, Y., Liu, Z., Hu, W., Gao, H., & Wang, Y. (2014). Magnetic properties as proxies for the evaluation of heavy metal contamination in urban street dusts of Nanjing, Southeast China. *Geophysical Journal International*, *199*(3), 1354–1366. https://doi.org/10.1093/gji/ggu253.

Li, H., Wang, J., Wang, Q., Tian, C., Qian, X., & Leng, X. (2017). Magnetic Properties as a Proxy for Predicting Fine-Particle-Bound Heavy Metals in a Support Vector Machine Approach. *Environmental Science and Technology*, *51*(12), 6927–6935. https://doi.org/10.1021/acs.est.7b00729.

Losacco, C., & Perillo, A. (2018). Particulate matter air pollution and respiratory impact on humans and animals. In *Environmental Science and Pollution Research* (Vol. 25, Issue 34, pp. 33901–33910). Springer Verlag. https://doi.org/10.1007/s11356-018-3344-9.

Markert, B. A., Breure, A. M., & Zechmeister, H. G. (2003). Chapter 1 Definitions, strategies and principles for bioindication/biomonitoring of the environment. *Trace Metals and Other Contaminants in the Environment*, *6*(C), 3–39. https://doi.org/10.1016/S0927-5215(03)80131-5 Ministry of Public Construction and Transportation. (2020). *ANUARIO DE INFORMACIÓN DE TRÁNSITO 2019*.

Miri, M., Ehrampoush, M. H., Reza Ghaffari, H., Aval, H. E., Rezai, M., Najafpour, F., Abaszadeh Fathabadi, Z., Aval, M. Y., & Ebrahimi, A. (2016). Atmospheric Heavy Metals Biomonitoring Using a Local Pinus eldarica Tree. *Health Scope*, *6*(1). https://doi.org/10.17795/jhealthscope-39241.

Mishra, R. (2021). *Cross-Validation in R programming*. GeeksforGeeks. https://www.geeksforgeeks.org/cross-validation-in-r-programming/

Mitchell, R., & Maher, B. A. (2009). Evaluation and application of biomagnetic monitoring of trafficderived particulate pollution. *Atmospheric Environment*, *43*(13), 2095–2103. https://doi.org/10.1016/j.atmosenv.2009.01.042.

Nagajyoti, P. C., Lee, K. D., & Sreekanth, T. V. M. (2010). Heavy metals, occurrence and toxicity for plants: A review. *Environmental Chemistry Letters*, *8*(3), 199–216. https://doi.org/10.1007/s10311010-0297-8.

Nakazato, R. K., Esposito, M. P., Cardoso-Gustavson, P., Bulbovas, P., Pedroso, A. N. V., de Assis, P. I. L. S., & Domingos, M. (2018). Efficiency of biomonitoring methods applying tropical bioindicator plants for assessing the phytoxicity of the air pollutants in SE, Brazil. *Environmental Science and Pollution Research*, *25*(20), 19323–19337. https://doi.org/10.1007/s11356-018-2294-6.

Nation State Program, 2019. Seguimiento Al Desarrollo Humano Sostenible, pp. 27–92. https://estadonacion.or.cr/informes/.

Okedeyi, Olumuyiwa O., Dube, Simiso, Awofolu, Omotayo R., Nindi, Mathew M., 2014. Assessing the enrichment of heavy metals in surface soil and plant (Digitaria eriantha) around coal-fired power plants in South Africa. Environ. Sci. Pollut.

Parmar, T. K., Rawtani, D., & Agrawal, Y. K. (2016). Bioindicators: the natural indicator of environmental pollution. *Frontiers in Life Science*, *9*(2), 110–118. https://doi.org/10.1080/21553769.2016.1162753.

Polezer, G., Tadano, Y. S., Siqueira, H. V., Godoi, A. F. L., Yamamoto, C. I., de André, P. A., Pauliquevis, T., Andrade, M. de F., Oliveira, A., Saldiva, P. H. N., Taylor, P. E., & Godoi, R. H. M. (2018). Assessing the impact of PM2.5 on respiratory disease using artificial neural

networks. *Environmental Pollution*, *235*, 394–403. https://doi.org/10.1016/j.envpol.2017.12.111.

Raj, A. (2020). *Unlocking the True Power of Support Vector Regression*. Towards Data Science. https://towardsdatascience.com/unlocking-the-true-power-of-support-vector-regression847fd123a4a0.

Rojas-Rodríguez, F., & Torres-Córdoba, G. (2013). Casuarina. *Revista Forestal Mesoamericana Kurú*, *10*(25), 32–33.

RStudio Team. (2020). *RStudio: Integrated Development for R. RStudio, PBC.* (1.4.1717). R Foundation for Statistical Computing. http://www.rstudio.com/.

Sawidis, T., Krystallidis, P., Veros, D., & Chettri, M. (2012). A study of air pollution with heavy metals in Athens city and Attica basin using evergreen trees as biological indicators. *Biological Trace Element Research*, *148*(3), 396–408. https://doi.org/10.1007/s12011-012-9378-9

Schmidt, Armin, 2005. Magnetic susceptibility as proxy for heavy metal pollution: A site study. J. Geochem. Explor. 85 (3), 109–117. https://doi.org/10.1016/j. gexplo.2004.12.001, 03756742.

Serbula, S. M., Kalinovic, T. S., Ilic, A. A., Kalinovic, J. V., & Steharnik, M. M. (2013). Assessment of airborne heavy metal pollution using Pinus spp. and Tilia spp. *Aerosol and Air Quality Research*, *13*(2), 563–573. https://doi.org/10.4209/aaqr.2012.06.0153.

Sharma, P., Yadav, P., Ghosh, C., & Singh, B. (2020). Heavy metal capture from the suspended particulate matter by Morus alba and evidence of foliar uptake and translocation of PM associated zinc using radiotracer (65Zn). *Chemosphere*, *254*, 126863. https://doi.org/10.1016/j.chemosphere.2020.126863.

U.S. EPA. (2007). *Method 3051A Microwave Assisted Acid Digestion of Sediments, Sludges, Soils, and Oils.* (Issue February). USA.

Wehle, H., 2017. Machine Learning, Deep Learning and AI: What's the Difference?. Conference on Data scientist innovation day in Bruxelles, Belgium.

Weinmayr, G., Hennig, F., Fuks, K., Nonnemacher, M., Jakobs, H., M¨ohlenkamp,Weinmayr, G., Hennig, F., Fuks, K., Nonnemacher, M., Jakobs, H., Möhlenkamp, S., Erbel, R., Jöckel, K. H., Hoffmann, B., & Moebus, S. (2015). Long-term exposure to fine particulate matter and incidence of type 2 diabetes mellitus in a cohort study: Effects of total and traffic-specific air pollution. *Environmental Health: A Global Access Science Source*, *14*(1). https://doi.org/10.1186/s12940-0150031-x.

Wilson, J. G., Kingham, S., Pearce, J., & Sturman, A. P. (2005). A review of intraurban variations in particulate air pollution: implications for epidemiological research. *Atmospheric Environment*, *39*, 6444e6462.

World Health Organization, W. (1996). *Permissible limits of heavy metals in soil and plants*. https://www.omicsonline.org/articles-images/2161-0525-5-334-t011.html.

Wu, X., Cobbina, S. J., Mao, G., Xu, H., Zhang, Z., & Yang, L. (2016). A review of toxicity and mechanisms of individual and mixtures of heavy metals in the environment. *Environmental*

Science and Pollution Research, *23*(9), 8244–8259. https://doi.org/10.1007/s11356-016-6333-x.

Yap, J., Ng, Y., Yeo, K. K., Sahlén, A., Lam, C. S. P., Lee, V., & Ma, S. (2019). Particulate air pollution on cardiovascular mortality in the tropics: Impact on the elderly. *Environmental Health: A Global Access Science Source*, *18*(34), 1–9. https://doi.org/10.1186/s12940-019-0476-4.

Zamudio, S., & Carranza, E. (1994). Cupressaceae. *Flora Del Bajío y de Regiones Adyacentes*, *29*.

Zhao, C. Y., Zhang, H. X., Zhang, X. Y., Liu, M. C., Hu, Z. D., & Fan, B. T. (2006). Application of support vector machine (SVM) for prediction toxic activity of different data sets. *Toxicology*, *217*(2– 3), 105–119. https://doi.org/10.1016/j.tox.2005.08.019,2-3.

Supplementary material

Comparison Between Machine Linear Regression (MLR) and Support Vector Machine (SVM) as Model Generators for Heavy Metal Assessment Captured in Biomonitors and Road Dust

Teresa Salazar-Rojas [5]*

Fredy Ruben Cejudo-Ruiz[6]

Guillermo Calvo-Brenes [7]

1* Doctorado en Ciencias Naturales para el Desarrollo (DOCINADE), Escuela de Química, Tecnológico de Costa Rica; Universidad Nacional, Universidad Estatal a Distancia, Costa Rica; tsalazar@itcr.ac.cr; Código ORCID 0000000223663638.

2 Instituto de Geofísica, Universidad Nacional Autónoma de México; Michoacán, México; ruben@geofisica.unam.mx, Código ORCID 0000-0003-1003-5664

3 . Escuela de Química, Tecnológico de Costa Rica; Cartago, Costa Rica; gcalvo@itcr.ac.cr, Código ORCID 0000-0002-7021-3509.

***** Corresponding author: tsalazar@itcr.ac.cr. Teresa Salazar Rojas, Escuela de Química, Tecnológico de Costa Rica, Cartago, Apartado postal: 159-7050, Costa Rica.

Second model validation method

The results of the second validation of the models created using data from new sampling points are shown in tables S1, S2 and S3 for each biomonitor and monitor.

Table S1. Validation data of the different models considering data from new sampling points for *Casuarina equisetifolia.*

HM	Range (mg/kg)	Model							
		I		II		III		IV	
		RMSE	MAE	RMSE	MAE	RMSE	MAE	RMSE	MAE
Fe	128-240	65.23	56.53	59.25	47.66	66.86	60.04	51.21	42.27
Cu	7.04-13.86	2.597	2.234	2.689	2.542	3.249	2.802	2.221	1.991
Pb	0.00- 3.22	1.666	1.663	1.667	1.649	1.691	1.682	1.672	1.655
Cr	0.69-1.82	0.445	0.362	0.454	0.342	0.392	0.308	0.477	0.365
Ni	0.79-1.37	1.815	1.807	1.360	1.350	1.803	1.793	1.299	1.197
V	0.00 -0.78	1.200	1.063	11.48	1.025	1.175	1.075	1.244	1.167
Zn	28.7-57.1	13.94	9.341	13.92	10.98	13.98	8.94	13.25	8.806

Table S2. Validation data of the different models considering data from new sampling points for Cupressus *lusitanica.*

HM	Range (mg/kg)	Model							
		I		II		III		IV	
		RMSE	MAE	RMSE	MAE	RMSE	MAE	RMSE	MAE
Fe	347-700	127.1	105.6	110.2	99.63	129.0	109.1	103.2	86.98
Cu	8.95-13.35	4.365	3.958	6.037	4.847	4.463	3.968	8.658	7.740
Pb	1.20-9.56	27.16	15.93	27.37	16.06	27.16	15.91	27.58	16.21

Cr	1.40-2.14	0.429	0.371	0.589	0.473	0.444	0.383	0.554	0.466
Ni	0.96-1.33	1.105	1.050	0.753	0.741	1.347	1.333	0.777	0.738
V	0.00-2.21	3.311	3.185	2.759	2.593	3.244	3.114	2.445	2.243
Zn	35.4-466.7	208.3	113.5	206.4	111.6	207.4	111.9	207.5	116.5

Table S3. Validation data of the different models considering data from new sampling points for road dust.

HM	**Range (mg/kg)**	**Model**							
		I		**II**		**III**		**IV**	
		RMSE	**MAE**	**RMSE**	**MAE**	**RMSE**	**MAE**	**RMSE**	**MAE**
Fe	20119-27515	4161	3877	3366	3127	7632	6541	7632	6541
Cu	117.7-193.5	28.2	23.47	51.71	44.92	375.1	287.8	48.00	45.07
Pb	0.00-79.07	54.3	47.31	40.56	34.93	118.1	111.8	43.55	37.04
Cr	20.21-32.61	14.2	13.39	9.66	8.57	132.4	102.9	18.06	13.54
Ni	16.21-26.09	10.2	9.53	4.89	3.93	42.50	34.94	9.30	6.99
V	65.32-147.8	33.1	25.93	29.65	21.78	31.39	21.28	31.57	27.54
Zn	35.89-160.7	170.0	162.7	124.8	106.1	657.2	551.8	134.3	119.7

Magnetic properties and HMs content correlations

Table S4. Pearson's Correlation Coefficient (r) among metals, vehicles amount and magnetic properties.

	Vehicules	Fe	Cu	Pb	Cr	Ni	V	Zn	xlf	kdf
Casuarina										
Vehicules	1,00									
Fe	0,24[b]	1,00								
Cu	0,24 [b]	0,74 [a]	1,00							
Pb	0,31 [b]	0,39 [a]	0,49[a]	1,00						
Cr	0,20	0,89 [a]	0,73 [a]	0,45 [a]	1,00					
Ni	-0,10	0,47 [a]	0,50 [a]	0,35 [b]	0,57 [a]	1,00				

V	0,41 [a]	0,91 [a]	0,68 [a]	0,27	0,85 [a]	0,46 [a]	1,00			
Zn	0,46[a]	0,69 [a]	0,39 [a]	0,52 [a]	0,74 [a]	0,34 [a]	0,70 [a]	1,00		
xlf	0,23 [b]	0,97 [a]	0,74 [a]	0,36 [b]	0,90 [a]	0,46 [a]	0,93 [a]	0,70 [a]	1,00	
kdf	0,17	0,09[a]	-0,18	-0,09	0,05	-0,04	0,22	0,15	0,14	1,00
Cupressus										
Vehicules	1,00									
Fe	-0,07	1,00								
Cu	-0,21	0,55 [a]	1,00							
Pb	-0,05	0,57 [a]	0,51 [a]	1,00						
Cr	-0,36 [b]	0,48 [a]	0,16	-0,03	1,00					
Ni	-0,28 [b]	0,44 [a]	0,16	0,06	0,26	1,00				
V	-0,08	0,49 [a]	0,42 [a]	0,22	0,14	0,44 [a]	1,00			
Zn	-0,24 [b]	0,67 [a]	0,44 [a]	0,27 [b]	0,45 [a]	0,19	0,37 [a]	1,00		
xlf	-0,05	0,86 [a]	0,51 [a]	0,48 [a]	0,65 [a]	0,45 [a]	0,45 [a]	0,71 [a]	1,00	
kdf	-0,03	0,18	-0,04	0,11	0,04	0,07	0,11	0,15	0,16	1,00
Road dust										
Vehicules	1,00									
Fe	0,29[a]	1,00								
Cu	0,11	0,34 [a]	1,00							
Pb	0,21	-0,05	-0,04	1,00						
Cr	0,38 [a]	0,79 [a]	0,44	-0,08	1,00					
Ni	0,21	0,71 [a]	0,40	-0,11	0,73 [a]	1,00				
V	0,01	0,77	0,36	-0,12	0,74 [a]	0,57 [a]	1,00			
Zn	0,39 [a]	0,50 [a]	0,36	0,28	0,63 [a]	0,47 [a]	0,41 [a]	1,00		
xlf	0,01	0,24 [b]	-0,03	0,17	0,11	0,16	0,08	0,09	1,00	
kdf	0,27[b]	0,08	0,16	0,16	0,29	0,28	-0,01	0,39 [a]	0,80 [a]	1,00

[a] $p < 0,01$; [b] $p < 0,05$

4.4. Assessing Heavy Metals Pollution Load Index (PLI) in Plants and Road Dust from Vehicular Emission by Magnetic Properties Modeling

Salazar-Rojas, T; Cejudo-Ruiz, F. R.; Gutierrez-Soto, M. V; Calvo-Brenes; G., (2022, en revisión) Assessing Heavy Metals Pollution Load Index (PLI) in Plants and Road Dust from Vehicular Emission by Magnetic Properties Modeling. Presentado a Revista *Environmental Science and Pollution Reseach.*

Assessing Heavy Metals Pollution Load Index (PLI) in Plants and Road Dust from Vehicular Emission by Magnetic Properties Modeling

Teresa Salazar-Rojas [1]*
Fredy Rubén Cejudo-Ruiz [2]
Marco V. Gutierrez-Soto [3]
Guillermo Calvo-Brenes [4]

Abstract

Vehicular traffic occupies a significant place among the sources of air pollution, due to population and urban growth that has led to an excessive increase in the vehicle fleet worldwide, and in Costa Rica as well. Vehicle emissions generate greenhouse gases (GHG), suspended particles (PM), heavy metals (HMs), due to combustion products from fossil-fuel engines, tire wear, and brake linings. HMs are important because they cannot be degraded or destroyed naturally; however, they can be diluted by physicochemical agents and be incorporated into trophic chains where they can be bioaccumulated causing significant negative effects on human well-being and ecological quality. This study aimed to assess the HMs pollution load in plants and road dust from vehicular emissions. For this purpose, chemical and magnetic property analyses were carried out on samples of road dust and leaves of *Cupressus lusitanica* and *Casuarina equisetifolia,* which were sampled during two different

years in the Greater Metropolitan Area (GMA) of Costa Rica. Contamination Factor (CF) and PLI results showed significant metal pollution in some

1* Doctorado en Ciencias Naturales para el Desarrollo (DOCINADE), Escuela de Química, Tecnológico de Costa Rica; Universidad Nacional, Universidad Estatal a Distancia, Costa Rica; tsalazar@itcr.ac.cr; Código ORCID 0000000223663638.

2 Instituto de Geofísica, Universidad Nacional Autónoma de México; Michoacán, México; ruben@geofisica.unam.mx,
Código ORCID 0000-0003-1003-5664.

3 . Escuela de Agronomía. Universidad de Costa Rica. Costa Rica; marcovgutierrez82@gmail.com, Código ORCID 0000-0002-8264-0129.

4. Escuela de Química, Tecnológico de Costa Rica; Costa Rica; gcalvo@itcr.ac.cr, Código ORCID 0000-0002-70213509.

Corresponding author: tsalazar@itcr.ac.cr. Teresa Salazar Rojas, Escuela de Química, Tecnológico de Costa Rica, Cartago, Apartado postal: 159-7050, Costa Rica.

of the study sites. Contamination by the metals V, Cr, and Zn was the most commonly present in the biomonitors, and Cr, Zn, and Pb in road dust. PLI estimates obtained with the support vector machine (SVM) models were consistent (accuracy and specificity) with those obtained by chemical analysis, proving to be viable for the identification of different levels of contamination by HMs.

Keywords: potentially toxic elements, confusion matrix, biomonitors, road dust, pollution load index, magnetic properties.

1. Introduction

Vehicular traffic occupies a significant place among the sources of air pollution, due to population and urban growth that has led to an excessive increase in the vehicle fleet worldwide. The production growth from 2000 to 2018 was 34% for cars and 128% for trucks (Davis & Robert, 2021). The vehicle fleet increase is a problem that affects many countries and Costa Rica not the exception, since the country's annual vehicle fleet growth 6% average,

each year from 1980 to 2019. In addition, the vehicle fleet is mostly based on fuel-fossile combustion engines, in 2019 the distribution of fuel types was; 82% gasoline vehicles, 17.3% diesel, and the remaining 0.7% to hybrid electric or gas vehicles (Nation State Programme, 2020). Vehicle emissions generate GHG, suspended particles matter with different sizes (PM_{10} with a particle diameter ≤ 10 μm and $PM_{2.5}$ with a particle diameter ≤ 2.5 μm), HMs (Cr, Cd, Cu, Ni, Pb, V and Zn), due to combustion products from fossil-fuel engines, tire wear, and brake linings. (Miri et al., 2017). Within the fine fraction of PM_{10} and $PM_{2.5}$, several chemical species such as nitrates, sulfates, HMs, organic compounds, and elemental carbon can be found (Kelly & Fussell, 2012; Castañeda-Miranda et al., 2020). Heavy metals are considered one of the most important components of particulate matter, causing significant negative effects on human health and ecological quality (LosaccoMH & Perillo, 2018; Polezer et al., 2018; Yap et al., 2019). Heavy metal is defined for US-EPA as “a common hazardous waste; can damage organisms at low concentrations and tends to accumulate in the food chain” (US-EPA, 2022). These may reach urban soils by different routes 1) aerial deposition from industries, vehicles, and volcanoes, 2) paints, 3) use of pesticides and fertilizers, 4) waste utilization, 5) dredged sediments, and 6) river and irrigation water (Ihl et al., 2015). HMs accumulate in the food chain because they cannot be degraded or destroyed naturally; however, they can be diluted by physicochemical agents, and thus be leached and can form soluble complexes, be transported and distributed in ecosystems, and get incorporated into trophic chains where they can be bioaccumulated (Leng et al., 2018).

A common way of assessing heavy metal contamination in the environment is by using pollution indices, which have been used to identify metal pollution in soil (Ihl et al., 2015; Hołtra & Zamorska-Wojdyła, 2020; Olusegun et al., 2021), sediments (Sukri et al., 2018; Maurya & Kumari, 2021ª; Guzeva et al., 2021), road dust (Nazzal et al., 2013; Bourliva et al., 2018; Wahab & Razak, 2019; Bisht et al., 2022) and plants (Daud et al., 2011; Norouzi et al., 2016; 2018; Badawy et al., 2022). However, to our knowledge, this is the first study to use predictive model estimates based on magnetic properties of plants and road dust to calculate the pollutant loading index (PLI).

This study aimed to evaluate heavy metal pollution load from vehicular emission in plants and road dust by chemical and magnetic properties modeling. Considering that traffic is one of the main sources of contamination, the Greater Metropolitan Area of Costa Rica (GAM in Spanish)

was selected as the study area and vehicle density used as criteria to select the sampling points.

2. Material and methods

2.1 Sampling site

The GAM is located in the central region of Costa Rica, 9°55′59″N 84°04′59″W (Fig. 1). This comprises part of the 4 provinces with the largest population, San Jose, Cartago, Heredia, and the capital San Jose. The average temperature of the GAM is 22.0°C, the average annual precipitation is 2300 mm and the climate is temperate. It presents altitudinal variations from 500 to 3400 masl. This region is affected by the climatic conditions of the Pacific (equatorial winds and the Intertropical Confluence Zone (ITCZ)), and the Caribbean (trade winds from the northeast, with cloudiness and weak rains). It has a two-period climate: dry from December to April and rainy from May to November; however, as a result of climatic oscillations due to the effects of climate change, these periods have been affected in their periodicity (Solano et al., 2020).

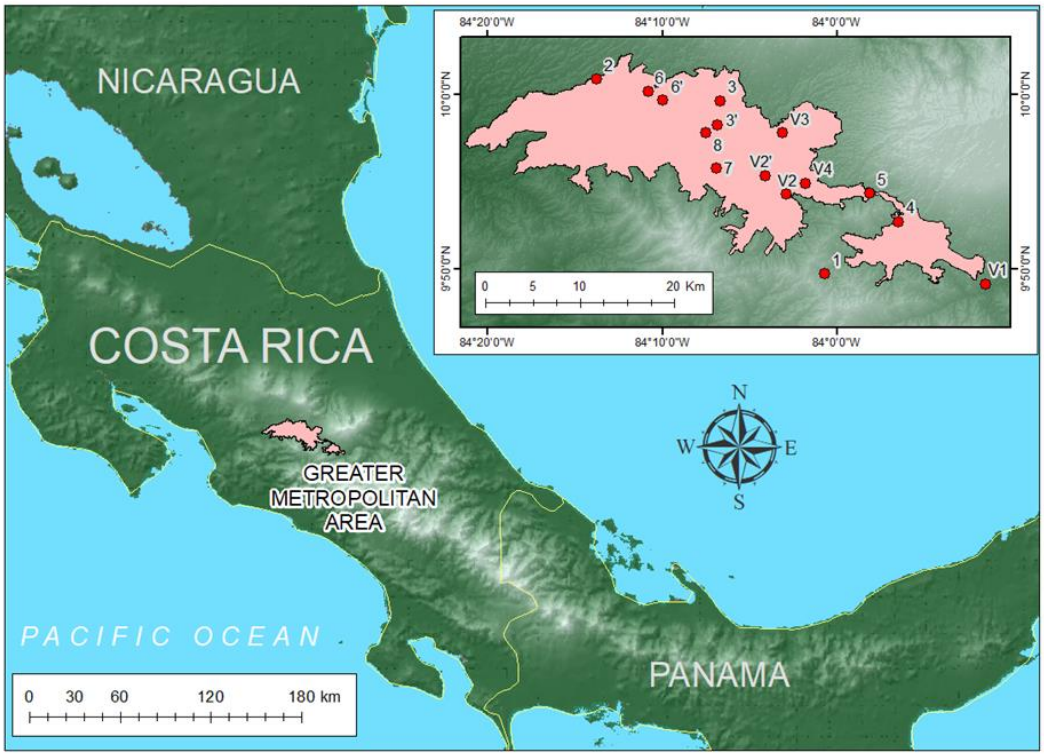

Fig. 1. Study domain in the Great Metropolitan Area of Costa Rica

Eight sampling sites were selected along the primary roads of the GAM, using vehicle density as a selection criterion, numbered from 1 to 8, some with apostrophes such as 3 and 6 as some monitors were found on the same road but in different sites, Fig. 1 Salazar-Rojas et al. (2022). Traffic ranged in average vehicles per day from zero for plants, and near zero for road dust (end of a paved road) at site 1 to 104500 at site 8 (Table 4).

In order for traffic to be the main source of HMs, samples were taken close to the road and locations were sought where the land use was primarily residential, although there were also some commercial locations nearby.

2.2 Sampling

Sampling was carried out in the dry season (February-March) for the years 2020 and 2021. The sample site's meteorological conditions during sampling were added as supplementary material (Table S1). Three monitors were selected, two plant species (Cupressus lusitanica (Cupressaceae) (Zamudio & Carranza, 1994) and Casuarina equisetifolia (Casuarinaceae), both perennials, with a foliage duration of 2 years or more (Rojas-Rodríguez & Torres-Córdoba, 2013), and road dust. Plants were taken in the side canopy facing the roadside at a height of 1.5 to 2.0 m, considering the normal height of human respiration and to avoid the influence of urban soil particles (Chaparro et al., 2015). A total of 240 samples (10 samples for each monitor x each of the 8 sites) were collected in plastic bags and transferred to a coolbox to the laboratory. Plant samples were dried at (55 ±1) ºC to constant weight and then crushed and road dust samples were air dried and then sieved for subsequent chemical and magnetic analysis at the laboratory following Aguilar et al., (2012).

2.3 Chemical and Magnetic Measurements

Heavy metal Cu, Cr, Cu, Ni, Pb, V, Zn, Fe and, Cd were analyzed in monitors samples using Method EPA 3051 Microwave Assisted Acid Digestion of Solids using a Mars 6 (CEM)) (U.S. EPA, 2007), and an Atomic Absorption Spectrophotometer (Perkin Elmer, model AAnalyst 800), supported by a graphite furnace and a hydride generator (Perkin Elmer, model FIAS 100).

Magnetic measurements were made in monitor´s samples packed tightly in a 10 cm3 plastic containers. Two magnetic properties were analyzed; magnetic susceptibility and the

percentage of frequency-dependent magnetic susceptibility measured at low frequency (κLF, 0.46 kHz) and high frequency (κHF, 46.0 kHz) using a Bartington MS2B single-sample dual-frequency meter and a Bartington MS3 magnetic susceptibility meter.
, the concentration of magnetic material and the presence of ultrafine Where ρ is the density of the material in kg m^{-3}.

2.5 Statistical Analysis

Statistical analyses of the magnetic and chemical data for model building and Pearson correlation were carried out using R version 4.0.2 (2020-06-22), including the packages dplyr, lmtest, car, carData, tidyverse, ggplot2, lattice, caret and e1071 (RStudio Team, 2020).

Support vector machine- single and multiple

Estimated values of each HMs concentrations from magnetic properties were obtained from single (χlf) and multiple (χlf and χdf %) support vector machine (SVM) predictive validated models generated for the monitors within this same study (Salazar-Rojas et al., 2022). The models generated by support vector machines are supervised learning models and associated learning algorithms that analyze the data feed for classification and regression analysis (Raj, 2020). The estimates of HMs concentrations obtained with the models were used to calculate the PLI and its subsequent evaluation by constructing a confusion matrix.

2.6 Heavy metal assessment

Contamination indices are used to quantify pollution. They exist as a single index for a metal, as contamination factor (CF), as well as an integrated index as a combination of several elements, such as pollution load index (PLI) (Ihl et al., 2015).

Contamination factor

The contamination factor for each metal was calculated using:

$$CF = Cm/Cb \quad (1)$$

Where Cm refers to the metal content in the sample, and Cb is the background level of the metal.

Since no background values have been established for HMs in the country for either the plant species analyzed or for road dust, the average of the two sites with the lowest values for each metal is proposed (Table 3). The contamination factor is categorized into four classes (Table 1) (Maurya & Kumari, 2021; Bisht et al., 2022).

Table 1. Classification of classes of contamination factors.

Contamination factor (CF)	Description value
CF < 1	Low contamination
1 ≤ CF < 3	Moderate contamination
3 ≤ CF < 6	Considerable contamination
CF ≥ 6	Very high contamination

Pollution load index

This index is determined by calculating the nth root of the product of the CF, where n is the total number of metals analyzed.

$$PLI = \sqrt[n]{CF_1 \; X \;\; CF^8 \; X \; CF_3 \ldots . . XCF_n} \qquad (2)$$

The interpretation of the PLI is as follows: a value of 0 indicates good quality of the site, a value of 1 indicates the presence of only baseline levels of pollutants, and a value greater than 1 indicates a progressive deterioration in the quality of the site (Ihl et al., 2015; Olusegun et al., 2021).

3. Results and discusión

3.1 Metal concentrations and Magnetic properties

The samples were analyzed chemically and magnetically, finding results for all metals except Cd which values found were below the detection limit of the equipment (Table 2). The HMs values from road dust are distinctly higher than those from plants. This could be the result of sampling in the roadside gutter, as no road dust was found on the roads. It should be noted

that metal debris from traffic, gray wastewater from nearby homes and businesses, and natural sources (dry and wet atmospheric deposition, surface soil resuspension) accumulate in the roadside ditch (Wang et al., 2019).

Table 2. HMs values for each biomonitor and road dust at the sampling sites.

Monitor	Site		Fe (mg/kg)	Cu (mg/kg)	Pb (mg/kg)	Cr mg/kg)	Ni (mg/kg)	V (mg/kg)	Zn (mg/kg)	χlf ($10^{-6}m^3$/kg)	kfd%
C. equisetifolia	1	Mean	113	11.85	0.99	0.51	2.07	0.17	7.8	0.0332	8.34
		SD	34	4.26	1.35	0.55	1.80	0.50	12.6	0.0059	5.50
	2	Mean	169	7.66	0.16	1.22	4.58	1.18	35.2	0.0499	7.78
		SD	25	2.20	0.50	0.54	2.69	0.86	8.0	0.0054	3.79
	3	Mean	368	10.06	1.31	2.07	3.33	2.24	39.3	0.0711	7.95
		SD	71	1.48	0.93	0.61	0.99	0.38	4.1	0.0066	4.35
	4	Mean	377	11.00	2.37	1.43	4.68	2.03	34.7	0.0624	6.16
		SD	160	2.25	0.45	0.67	2.13	0.83	15.3	0.0121	4.02
	5	Mean	338	19.74	2.84	1.14	2.53	1.70	35.5	0.0651	8.82
		SD	47	6.73	1.66	0.20	1.81	0.24	8.4	0.0086	4.01
	6	Mean	945	31.00	2.02	3.77	5.50	6.00	53.5	0.1586	6.65
		SD	268	20.13	1.00	1.76	4.30	1.57	8.6	0.0360	4.67
	7	Mean	220	13.13	0.57	0.66	1.08	1.74	27.0	0.0489	5.33
		SD	38	6.49	0.74	0.53	0.86	1.16	17.1	0.0034	3.36
	8	Mean	175	10.71	0.25	0.64	2.16	0.35	29.6	0.0443	5.38
		SD	52	4.81	0.52	0.46	1.28	0.68	12.2	0.0049	3.71
C. lusitanica	1	Mean	150	12.11	2.44	0.59	2.30	1.84	11.1	0.0390	5.05
		DS	34	6.12	2.50	0.70	1.70	3.70	13.8	0.0089	3.05
	2	Mean	590	16.99	2.28	2.21	2.70	7.37	47.4	0.0830	8.42
		DS	107	6.06	0.97	0.22	0.85	1.46	4.6	0.0058	4.26
	3	Mean	961	21.68	2.89	2.87	3.12	4.57	70.3	0.1225	5.51
		DS	307	7.77	0.50	0.78	1.00	1.15	9.2	0.0232	2.84
	4	Mean	1304	21.52	7.01	2.53	3.99	6.73	55.3	0.1439	5.60
		DS	266	6.50	2.92	1.11	1.23	1.42	7.9	0.0255	4.25
	5	Mean	999	20.19	12.94	2.02	2.53	5.81	89.7	0.1172	8.04
		DS	241	8.43	0.00	0.58	0.54	1.81	9.1	0.0161	4.16
	6	Mean	344	10.70	1.05	0.84	2.37	6.06	37.4	0.0585	5.60
		DS	99	4.38	0.76	0.45	0.70	1.82	4.0	0.0070	3.19
	7	Mean	573	18.61	2.07	2.70	1.52	3.27	61.4	0.0866	5.69

		DS	74	7.54	1.06	0.48	1.10	1.21	5.6	0.0068	2.93
	8	Mean	312	7.34	1.24	0.90	1.30	1.96	40.3	0.0595	7.27
		DS	77	0.50	1.15	0.19	0.90	0.54	10.8	0.0056	3.88
Road dust	1	Mean	17714	77.15	13.98	18.76	20.55	95.60	70.3	7.2829	0,60
		SD	9141	53.89	5.99	17.94	17.89	61.46	31.2	1.1683	0,51
	2	Mean	15135	168.04	63.23	25.01	20.77	64.62	217.7	9.2554	0,99
		SD	5312	101.17	42.62	12.89	11.12	30.14	54.2	4.0222	0,37
	3	Mean	21873	179.38	70.93	51.49	44.06	98.96	303.9	12.4851	1,18
		SD	9619	186.97	47.21	35.09	28.16	48.16	130.6	3.4419	0,39
	4	Mean	17057	270.19	44.26	22.87	39.00	77.55	132.9	8.8465	0,60
		SD	11075	326.38	33.83	19.09	46.31	43.92	44.9	0.8935	0,14
	5	Mean	20991	95.09	184.29	34.93	26.71	87.79	200.4	8.1977	0,80
		SD	5680	42.61	152.96	19.14	19.38	17.98	98.2	1.2585	0,20
	6	Mean	36844	226.60	116.82	64.03	44.72	106.59	418.4	11.5762	0,91
		SD	16369	123.25	108.58	36.36	17.87	48.24	163.7	1.0956	0,18
	7	Mean	21177	189.16	54.93	51.63	32.09	80.86	358.6	7.3204	0,71
		SD	10852	142.54	46.58	34.20	13.71	66.12	241.8	3.4087	0,32
	8	Mean	23703	160.64	71.12	51.68	32.96	82.35	242.0	9.2373	0,73
		SD	6895	149.93	45.61	26.07	8.35	24.57	86.5	1.4749	0,19

The proposed values of HMs limits were obtained as a result of a multi-rank test, choosing for each element the two sites with the lowest heavy metal concentration because the country has no limit values for the HMs studied in plants and road dust (Table 3). From these values, the CF and PLI were calculated for each site in 2020 and 2021 separately.

Table 3. Proposed limit values for the content of HMs.

Monitor	Fe (mg/kg)	Cu (mg/kg)	Pb (mg/kg)	Cr (mg/kg)	Ni (mg/kg)	V (mg/kg)	Zn (mg/kg)
C. *equisetifolia*	129	13.13	1.61	0.99	1.88	1.05	24.4
C. *lusitanica*	208	11.80	3.54	1.03	1.38	1.16	21.6
Road dust	8517	95.17	37.32	4.07	15.65	41.32	93.5

3.2 Heavy metal assessment

Contamination factor

Different degrees of contamination are reflected in the variations of CF of heavy metal in all sites, being in general terms the lowest at Site 1 for both biomonitors and road dust (Table 4 and Fig. 2).

Table 4. Daily average of vehicles and mean CF values at each site.

Site	Daily average of vehicles	Mean CF					
		C. *equisetifolia*		C. *lusitanica*		Road dust	
		2020	2021	2020	2021	2020	2021
1	0	0.7	0.5	0.8	1.5	0.6	2.8
2	17101	1.3	0.5	2.5	1.3	2.1	2.8
3/3'	32138/29198	1.5	1.7	2.4	2.6	2.1	6.2
4	45326	1.5	1.7	**3.0**	**2.8**	1.4	3.5
5	62008	1.7	1.1	2.8	**2.8**	3.3	3.5
6/6'	73982/77671	**4.0**	**2.0**	2.1	1.6	**3.4**	**7.0**
7	88585	1.3	0.9	2.3	1.6	1.9	6.1
8	104558	1.3	0.8	1.2	1.0	2.7	5.0

Among sites, *C. equisetifolia* showed the highest mean CF values at Site 6 in both years, CF ranging from considerable contamination (CF = 4.0) in 2020 to moderate contamination (CF = 2.0) in 2021; *C. lusitanica*, CF highest mean value was for Site 4 varying from considerable contamination (CF = 3.0) in 2020 to moderate contamination (CF = 2.8) in 2021 and road dust highest mean value was for Site 6 varying from considerable contamination (CF = 3.4) in 2020 to very high contamination (CF = 7.0) in 2021. In biomonitors, there was a decrease in CF values at most sites between 2020 and 2021, possibly due to vehicle restrictions imposed by the pandemic after the 2020 sampling and by 2021. This effect was not observed in road dust samples, suggesting that biomonitors better reflect atmospheric pollution and road dust reflects cumulative pollution from various sources.

Among metals, the highest CF values in both years were for V, and Cr for *C. equisetifolia* (Fig. 2a and 2b); V, and Zn for *C. lusitanica* (Fig.2c and 2d), and Cr and Zn for road dust (Fig. 2e and 2f).

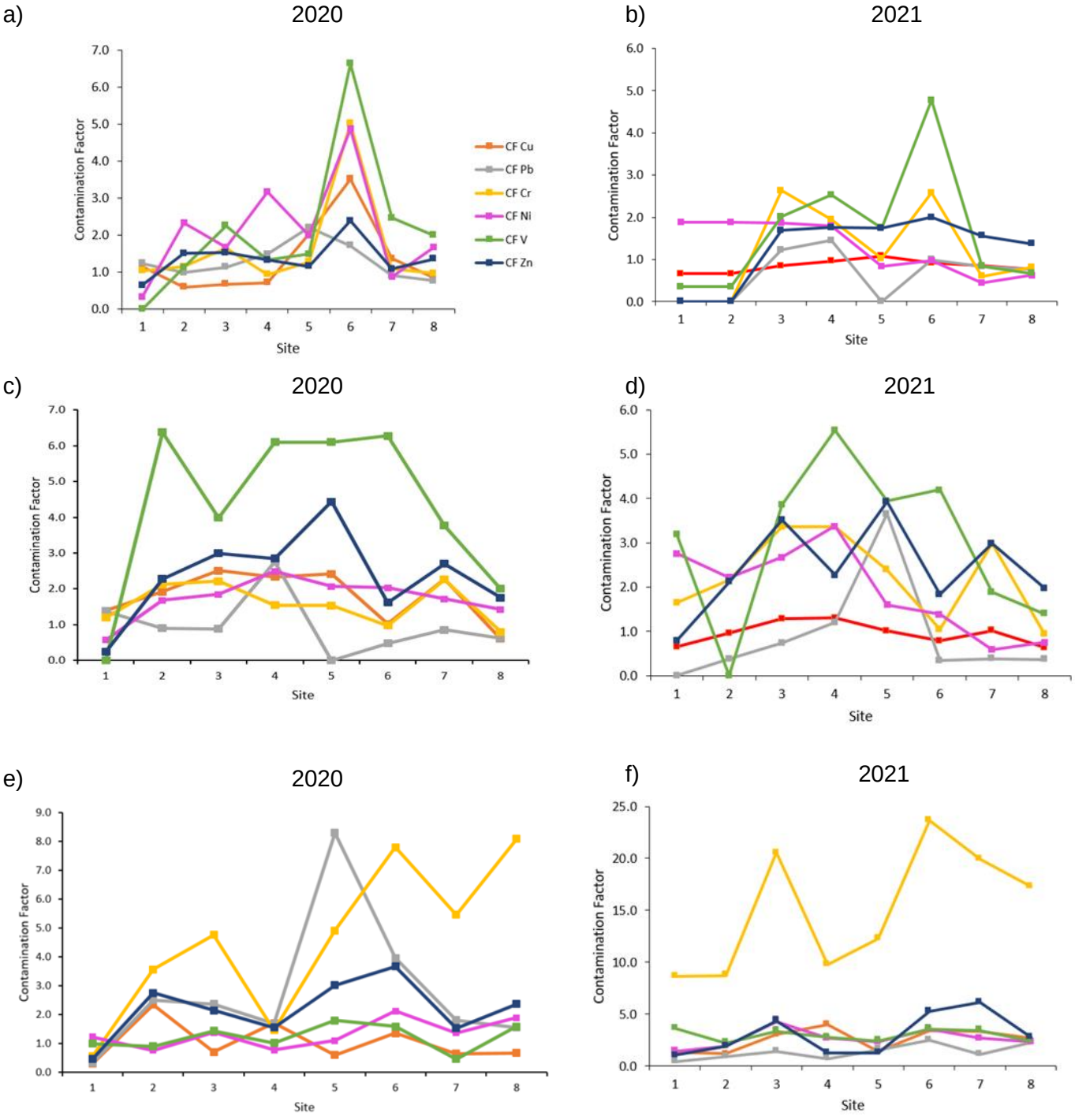

Fig. 2. Calculated contamination factor for years 2020 and 2021 respectibely for; *C. equisetifolia* (a and b), *C. lusitanica* (c and d), and road dust (e and f).

Pollution load index

Overall, among biomonitors, there was a decrease in some sites among PLI values between 2020 and 2021, which could be due to vehicle restrictions imposed by the pandemic after the 2020 sampling and for 2021 (Fig. 3). In some sites, the PLI value was zero because according to Equation 2) when the site has a CF of zero in some metal its PLI value cancels out. PLI highest value was 3.6 (2020) and 2.0 (2021) for C. equisetifolia, and 2.7 (2020) and 2.5 (2021) for C. lusitanica, similar PLI values (highest 2.5) were obtained for dustfall collected in cylindrical glass vessels in a high traffic and industrial area in Hunshandake Sandy Land, China (Qiao et al., 2013), however low compared with PLI values obtained in moss bags with the highest PLI value of 21.8 for crossing streets and 20.5 for middle streets in highly trafficked main roads in Turku, Finland for which traffic was lower than in this study (Limo et al., 2018), demonstrating that the biomonitors used are good airborne particulate matter samplers, although the distance to the source has an important effect on the results obtained. As observed with Site 6 in which the *C*. *lusitanica* sample had to be sampled further away from the road than the others giving lower CF and PLI values.

Road dust samples showed an increase in PLI values from 2020 to 2021, evidencing accumulation of HMs in this monitor. PLI values in road dust samples ranged from 0.6 to 2.8 for 2020 and 1.7 to 4.2 for 2021 (Fig. 3). A similar study conducted in Uttarakhand, India, obtained a comparable PLI range (1.1 to 1.7) a highway with 30000 vehicles average per day (Bisht et al., 2022) and a study conducted on road dust in Toronto (Canada) obtained a higher PLI range from 2 to 8 for four roads which together, have an estimated average traffic flow of 750,000 vehicles per day (Nazzal et al., 2013), data which could be consistent if compares with the highest value of this study of 104558 vehicles average per day (Table 4), considering that the country vehicle fleet tend to be older.

PLI values in 2020 (Fig. 3) showed a greater agreement at most sites and monitors studied than in 2021, sites 2, 3, 4, 6, 7, and 8 for monitors in 2020, and sites 3, 4, and 6 in 2021. Additionally, the highest PLI values were observed at Site 6, in both years, for road dust and *C. equisetifolia*. The consistencies among PLI values allow the use of *C. lusitanica, C. equisetifolia*, and road dust for the identification of pollution load.

a) b)

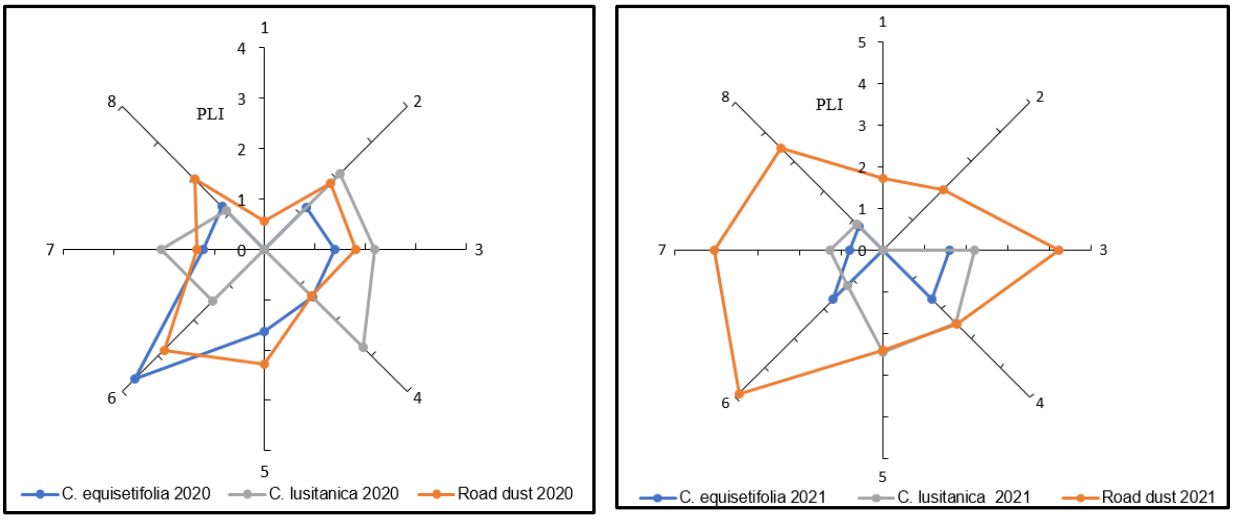

Fig. 3. Pollution load index (PLI) for years a) 2020 and b) 2021 for *C. equisetifolia*, *C. lusitanica* and road dust at each site.

Differences found between the PLI values of plants and road dust might be explained due to the multiple of sources of pollution in the case of the latter, however concerning plants, considering that their degree of retention and encapsulation of particles depends on several factors such as leaf characteristics, cuticle chemical composition, and cuticle structure, more detailed phytochemical studies would be required to explain with certainty the differences found between the plants studied (Bussotti et al., 2014).

Correlations among vehicles density, average HMs, average magnetic properties (χlf and χdf%) and PLI were calculated (Table 5). Results showed a significant correlation among all HMs, χlf, and PLI for *C.* equisetifolia, except χlf and Pb. *C.* lusitanica presented significant correlation between χlf and HMs (Fe, Cu, Cr, Ni, V, and Zn) and correlation PLI with HMs (Fe, Pb, Cr, V), and χlf. PLI of road dust was significantly correlated with HMs (Fe, Cu, Cr, Ni, V and Zn). Comparable results were obtained by a study conducted in Isfahan, Iran in which a significant correlation between χlf, HMs (Cu, Fe, Mn, Ni, Zn and Pb) and PLI was obtained in a tree (*Platanus orientalis L.*, Platanaceae) and for χlf, HMs (Cu, Fe, Zn and Pb) and PLI in atmospheric dust (Norouzi et al., 2016).

Table 5. Person's correlation and p-value among vehicles density, average HMs, average magnetic properties (χlf and χfd) and PLI for each site and monitor.

		Vehicles	Fe	Cu	Pb	Cr	Ni	V	Zn	χlf	kfd%
C. equisetifolia	Fe	0,246									
		0,359									
	Cu	0,267	0,711								
		0,318	0,002								
	Pb	0,145	0,432	0,534							
		0,592	0,095	0,033							
	Cr	0,117	0,898	0,719	0,448						
		0,665	0,000	0,002	0,082						
	Ni	-0,148	0,530	0,547	0,325						
		0,585	0,035	0,028	0,219	0,010					
	V	0,386	0,940	0,694	0,408	0,856	0,488				
		0,140	0,000	0,003	0,117	0,000	0,055				
	Zn	0,445	0,740	0,389	0,312	0,745	0,341	0,714			
		0,084	0,001	0,137	0,240	0,001	0,197	0,002			
	xlf	0,246	**0,975**	**0,702**	**0,349**	**0,912**	**0,514**	**0,944**	**0,747**		
		0,359	0,000	0,002	0,185	0,000	0,042	0,000	0,001		
	kdf%	-0,451	-0,320	-0,358	-0,007	-0,248	-0,328	-0,389	-0,288	-0,261	
		0,079	0,227	0,174	0,978	0,354	0,215	0,136	0,280	0,330	
	PLI	0,360	**0,824**	**0,704**	**0,715**	**0,825**	**0,632**	**0,861**	**0,677**	**0,779**	-0,423
		0,171	0,000	0,002	0,002	0,000	0,009	0,000	0,004	0,000	0,103
C. lusitanica	Fe	-0,060									
		0,825									
	Cu	-0,193	0,590								
		0,474	0,016								
	Pb	-0,073	0,534	0,190							
		0,788	0,033	0,482							
	Cr	-0,237	0,587	0,202	0,168						
		0,378	0,017	0,453	0,535						
	Ni	-0,375	0,506	0,189	0,052	0,410					

		0,152	0,046	0,484	0,850	0,115					
	V	0,034	0,548	0,493	0,173	0,115	0,521				
		0,901	0,028	0,052	0,521	0,671	0,038				
	Zn	0,279	0,714	0,472	0,270	0,465	0,183	0,425			
		0,296	0,002	0,065	0,313	0,070	0,498	0,100			
	xlf	-0,056	**0,940**	**0,567**	**0,417**	**0,680**	**0,529**	**0,485**	**0,738**		
		0,837	0,000	0,022	0,108	0,004	0,035	0,057	0,001		
	kdf	0,070	0,041	-0,411	0,222	0,287	0,146	0,065	0,168	0,106	
		0,797	0,880	0,114	0,409	0,281	0,589	0,810	0,534	0,695	
	PLI	0,189	**0,684**	0,343	**0,598**	**0,464**	0,284	**0,551**	**0,426**	**0,640**	0,203
		0,484	0,004	0,193	0,014	0,071	0,286	0,027	0,100	0,008	0,452
Road dust	Fe	0,328									
		0,215									
	Cu	0,162	0,629								
		0,549	0,009								
	Pb	0,272	-0,045	-0,226							
		0,309	0,868	0,400							
	Cr	0,406	0,889	0,714	-0,121						
		0,119	0,000	0,002	0,655						
	Ni	0,266	0,826	0,680	-0,197	0,895					
		0,320	0,000	0,004	0,465	0,000					
	V	0,012	0,824	0,634	-0,192	0,815	0,736				
		0,966	0,000	0,008	0,476	0,000	0,001				
	Zn	0,440	0,623	0,551	0,257	0,739	0,601	0,490			
		0,088	0,010	0,027	0,337	0,001	0,014	0,054			
	xlf	0,022	0,244	-0,046	0,180	0,140	0,259	0,102	0,168		
		0,937	0,362	0,867	0,504	0,605	0,333	0,708	0,535		
	kdf	-0,117	0,374	0,303	-0,046	0,509	0,412	0,466	0,393	0,386	
		0,666	0,154	0,254	0,866	0,044	0,113	0,069	0,133	0,140	
	PLI	0,436	**0,870**	**0,738**	0,114	**0,948**	**0,862**	**0,737**	**0,861**	0,243	0,506
		0,091	0,000	0,001	0,673	0,000	0,000	0,001	0,000	0,365	0,046

Line 1 Correlation

Line 2 p-value

Although the average data per site of HMs and magnetic properties, used for the calculation of CF and PLI, did not show a significant correlation with the number of vehicles (Table 5), it was obtained among the individual data of the variables in this study (Salazar-Rojas et al., 2023).

3.3 Confusion Matrix

The confusion matrix is an n x n matrix, where n is the number of classes, to describe the performance of the classifier (Salmon et al., 2015). For its construction, SVM models were performed from the magnetic properties of each monitor, and estimates of the content of HMs were obtained (Salazar-Rojas et al., 2022), and based on the proposed values in Table 3, and Equation 2, estimated PLI values were calculated for each site, Fig 4. Estimated PLI values, based on magnetic properties, also reflected a decrease from 2020 to 2021 for plants and an increase for road dust.

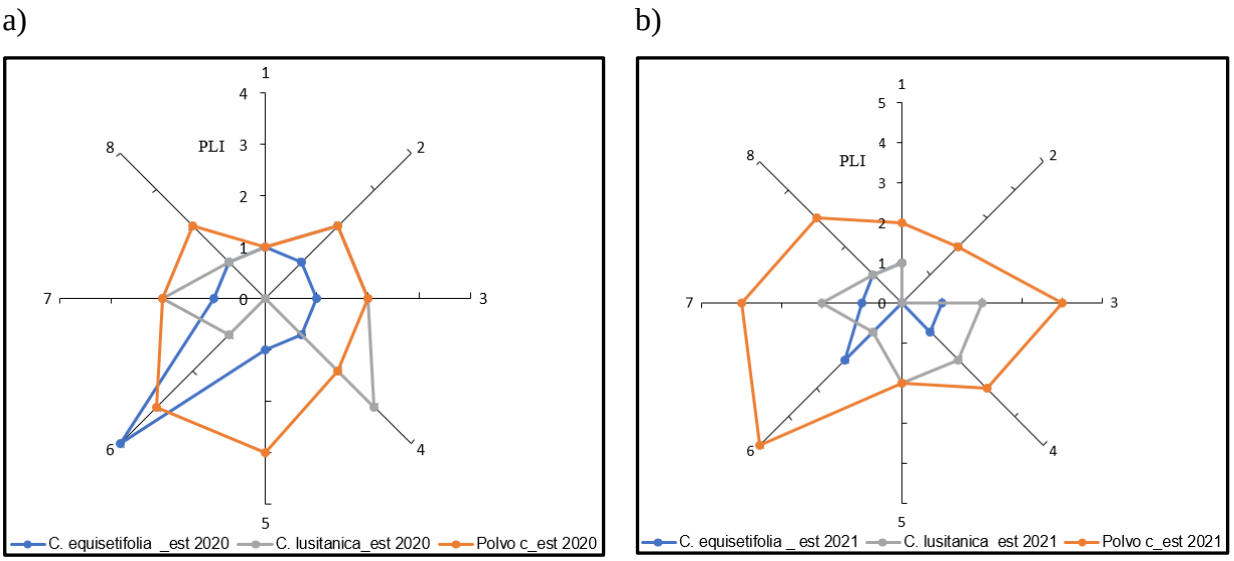

Fig. 4. Estimated values of PLI for for years a) 2020 and b) 2021 for *C. equisetifolia, C. lusitanica,* and road dust at each site.

The confusion matrix (Table 6) and individual results for each monitor (Tables 7, 8, and 9) were attained using the PLI values obtained from the chemical analyses as a reference (Fig. 3), and the estimated PLI values obtained from the models (Fig. 4).

Table 6. Confusion matrix for reference and estimated PLI for monitors.

	a. *C. equisetifolia*						b. *C. lusitanica*						c. Road dust						
	Estimated						Estimated						Estimated						
Reference value		0	1	2	3	4		0	1	2	3		0	1	2	3	4	5
	0	2	2	0	0	0	0	2	2	0	0	0	0	0	0	0	0	0
	1	0	7	0	0	0	1	0	4	0	0	1	0	1	2	0	0	0
	2	0	3	1	0	0	2	0	0	6	0	2	0	0	5	1	0	0
	3	0	0	0	0	0	3	0	0	0	1	3	0	0	2	2	0	0
	4	0	0	0	1	0						4	0	0	1	1	0	0
												5	0	0	0	1	0	0
	Accuracy = 63%						Accuracy = 75%					Accuracy = 50%						

Considering the PLI values according to the classes identified by the chemical analyses, which denote various degrees of contamination, 5 classes (from 0 to 4) for C. equisetifolia, 4 classes (from 0 to 3) for C. lusitanica and 6 classes (from 0 to 5) for road dust, compared with the estimated PLI values obtained by the models, it was obtained overall accuracy percentages of 63%, 75% and 50% for C. equisetifolia, C. lusitanica and road dust, respectively, Table 6. However, if data are grouped only in the 3 classes mentioned in the literature for PLI are considered (a value of 0 indicates good quality, a value of 1 indicates the presence of basic levels of contaminants, and a value higher than 1 indicates a progressive deterioration of the quality of the site) the % accuracy obtained improves considerably for all monitors (69%, 81% and 81% accuracy respectively). Obtaining good accuracy by using validated SVM models of the magnetic properties of biomonitors to determine the different degrees of MHs contamination at a site, and the existence of MHs contamination for road dust.

Table 7. Results of the confusion matrix by class for *C. equisetifolia*.

Class:	0	1	2	3	4
Sensitivity	1	0.5833	1	0	NA
Specificity	0.8571	1	0.8	1	0.9375
Pos Pred Value	0.5	1	0.25	NA	NA
Neg Pred Value	1	0.4444	1	0.9375	NA
Prevalence	0.125	0.75	0.0625	0.0625	0
Detection Rate	0.125	0.4375	0.0625	0	0

Detection Prevalence	0.25	0.4375	0.25	0	0.0625
Balanced Accuracy	0.9286	0.7917	0.9	0.5	NA

Table 8. Results of the confusion matrix by class for *C. lusitanica*.

Class:	0	1	2	3
Sensitivity	1	0.6667	0.75	NA
Specificity	0.8571	0.9	1	0.9375
Pos Pred Value	0.5	0.8	1	NA
Neg Pred Value	1	0.8182	0.8	NA
Prevalence	0.125	0.375	0.5	0
Detection Rate	0.125	0.25	0.375	0
Detection Prevalence	0.25	0.3125	0.375	0.0625
Balanced Accuracy	0.9286	0.7833	0.875	NA

It is noteworthy that although the road dust samples presented a significant correlation only with two HMs (Cr and V) for the kfd and none for the χlf. Their correlation was significant between PLI values and HMs and kdf (Table 5), which is probably why the validated SVM models predicted accurate PLI values to determine the existence of possible contamination by HMs, according to the confusion matrix, Table 9.

Table 9. Results of the confusion matrix by class for road dust.

Class:	0	1	2	3	4	5
Sensitivity	NA	1	0.5	0.4	NA	NA
Specificity	1	0.8667	0.8333	0.8182	0.875	0.9375
Pos Pred Value	NA	0.3333	0.8333	0.5	NA	NA
Neg Pred Value	NA	1	0.5	0.75	NA	NA
Prevalence	0	0.0625	0.625	0.3125	0	0
Detection Rate	0	0.0625	0.3125	0.125	0	0
Detection Prevalence	0	0.1875	0.375	0.25	0.125	0.0625
Balanced Accuracy	NA	0.9333	0.6667	0.6091	NA	NA

4. Conclusions

The CF and PLI results show significant metal pollution in some of the studied sites, especially for road dust. Contamination by the metals V, Cr, and Zn was the most present in the biomonitors

and Cr, Zn, and Pb in road dust. The plants studied demonstrate to be good monitors of air pollution and road dust from accumulated pollution with significant correlations between PLI and HMs.

The PLI results obtained with the SVM magnetic properties models were consistent (accuracy and specificity) with those obtained by chemical analysis, which gives validity to the methodology to be used for estimations of contamination by HMs.

The significant and positive correlation between the average content of nearly all HMs studied, PLI, and magnetic properties, and the fact that the HMs limits for each of the samples in this study have a magnetic property value associated with them, demonstrate that the magnetic properties themselves could also serve as a reference limit for identifying possible contamination at a site.

Acknowledgements

The authors thank the Technological Institute of Costa Rica (ITCR) and the National Autonomous University of Mexico (UNAM), for their financial and administrative support. In addition, the Center for Research in Environmental Protection (CIPA), Center for Research and Chemical and Microbiological Services (CEQIATEC) and Institute of Geophysics (Morelia) for their support to the project.

Compliance with ethical standards Bioindicators were collected in compliance with the ethical standards of the Technological Institute of Costa Rica.

Consent to participate Consent for publication

Conflict of interest The authors declare that they have no conflict of interest.

Availability of data and material Code availability Not applicable

5. References

Aguilar, B., Cejudo, R., Martínez, J., Bautista, F., Goguitchaichvili, A., Carvallo, C., & Morales, J. (2012). Ficus benjamina leaves as indicator of atmospheric pollution: A reconaissance study. Studia Geophysica et Geodaetica, 56(3), 879–887. https://doi.org/10.1007/s11200-011-0265-1.

Badawy, W. M., Sarhan, Y., Duliu, O. G., Kim, J., Yushin, N., Samman, H. El, Hussein, A. A., Frontasyeva, M., & Shcheglov, A. (2022). Monitoring of air pollutants using plants and

co-located soil—Egypt: characteristics, pollution, and toxicity impact. Environmental Science and Pollution Research, 29(14), 21049–21066. https://doi.org/10.1007/s11356-021-17218-7.

Bisht, L., Gupta, V., Singh, A., Gautam, A. S., & Gautam, S. (2022). Heavy metal concentration and its distribution analysis in urban road dust: A case study from most populated city of Indian state of Uttarakhand. Spatial and Spatio-Temporal Epidemiology, 40(October 2021), 100470. https://doi.org/10.1016/j.sste.2021.100470.

Bourliva, A., Kantiranis, N., Papadopoulou, L., Aidona, E., Christophoridis, C., Kollias, P., Evgenakis, M., & Fytianos, K. (2018). Seasonal and spatial variations of magnetic susceptibility and potentially toxic elements (PTEs) in road dusts of Thessaloniki city, Greece: A one-year monitoring period. Science of the Total Environment, 639, 417–427. https://doi.org/10.1016/j.scitotenv.2018.05.170.

Briffa, J., Sinagra, E., & Blundell, R. (2020). Heavy metal pollution in the environment and their toxicological effects on humans. Heliyon, 6(9), e04691. https://doi.org/10.1016/j.heliyon.2020.e04691.

Bussotti, F., Pollastrini, M., Killi, D., Ferrini, F., & Fini, A. (2014). Ecophysiology of urban trees in a perspective of climate change. Agrochimica, 58(3), 247–268.

https://doi.org/10.12871/0021857201431.

Castañeda-Miranda, A. G., Chaparro, M., Pacheco-Castro, A., Chaparro, M., & Böhnel, H. (2020). Magnetic biomonitoring of atmospheric dust using tree leaves of Ficus benjamina in Querétaro (México). Environmental Monitoring and Assessment, 192(6). https://doi.org/10.1007/s10661-020-8238-x.

Chaparro, M., Chaparro, M., Castañeda Miranda, A. G., Böhnel, H. N., & Sinito, A. M. (2015). An interval fuzzy model for magnetic biomonitoring using the specie Tillandsia recurvata L. Ecological Indicators, 54, 238–245. https://doi.org/10.1016/j.ecolind.2015.02.018.

Daud, M., Khalid, N., Waheed, S., Wasim, M., Arif, M., & Zaidi, J. H. (2011). Morus nigra plant leaves as biomonitor for elemental air pollution monitoring. Radiochimica Acta, 99(4), 243–252. https://doi.org/10.1524/ract.2011.1814.

Davis, S. C., & Robert, G. B. (2021). Transportation Energy Data Book (39th ed.). Oak Ridge National Laboratory. https://tedb.ornl.gov/wp-content/uploads/2021/02/TEDB_Ed_39.pdf.

Guzeva, A., Slukovskii, Z., Dauvalter, V., & Denisov, D. (2021). Trace element fractions in sediments of urbanised lakes of the arctic zone of Russia. Environmental Monitoring and Assessment, 193(6), 1–17. https://doi.org/10.1007/s10661-021-09166-z.

Hołtra, A., & Zamorska-Wojdyła, D. (2020). The pollution indices of trace elements in soils and plants close to the copper and zinc smelting works in Poland's Lower Silesia. Environmental Science and Pollution Research, 27(14), 16086–16099. https://doi.org/10.1007/s11356-020-08072-0.

Ihl, T., Bautista, F., Cejudo Ruíz, F. R., Delgado, M. del C., Quintana Owen, P., Aguilar, D., & Goguitchaichvili, A. (2015). Concentración de elementos tóxicos en suelos del área metropolitana de la Ciudad de México: análisis espacial utilizando kriging ordinario y kriging indicador. Revista Internacional de Contaminación Ambiental, 31(1), 47–62. http://www.scielo.org.mx/scielo.php?script=sci_arttext&pid=S0188-49992015000100004&lng=es&nrm=iso&tlng=en.

Kawasaki, K., Horikawa, K., & Sakai, H. (2017). Magnetic biomonitoring of roadside pollution in the restricted. Environmental Science and Pollution Research, 10313–10325. https://doi.org/10.1007/s11356-017-8702-5.

Kelly, F. J., & Fussell, J. C. (2012). Size, source and chemical composition as determinants of toxicity attributable to ambient particulate matter. Atmospheric Environment, 60, 504–526. https://doi.org/10.1016/j.atmosenv.2012.06.039.

Leng, X., Qian, X., Yang, M., Wang, C., Li, H., & Wang, J. (2018). Leaf magnetic properties as a method for predicting heavy metal concentrations in PM2.5 using support vector machine: A case study in Nanjing, China. Environmental Pollution, 242, 922–930. https://doi.org/10.1016/j.envpol.2018.07.007.

Limo, J., Paturi, P., & Mäkinen, J. (2018). Magnetic biomonitoring with moss bags to assess stop-and-go traffic induced particulate matter and heavy metal concentrations.

Atmospheric Environment, 195, 187–195. https://doi.org/10.1016/j.atmosenv.2018.09.062.

Losacco, C., & Perillo, A. (2018). Particulate matter air pollution and respiratory impact on humans and animals. In Environmental Science and Pollution Research (Vol. 25, Issue 34, pp. 33901–33910). Springer Verlag. https://doi.org/10.1007/s11356-018-3344-9

Maurya, P., & Kumari, R. (2021a). Toxic metals distribution, seasonal variations and environmental risk assessment in surficial sediment and mangrove plants (A. marina), Gulf of Kachchh (India). Journal of Hazardous Materials, 413(January), 125345. https://doi.org/10.1016/j.jhazmat.2021.125345.

Maurya, P., & Kumari, R. (2021b). Toxic metals distribution, seasonal variations and environmental risk assessment in surficial sediment and mangrove plants (A. marina), Gulf of Kachchh (India). Journal of Hazardous Materials, 413(October 2020), 125345. https://doi.org/10.1016/j.jhazmat.2021.125345.

Miri, M., Ehrampoush, M. H., Reza Ghaffari, H., Aval, H. E., Rezai, M., Najafpour, F., Abaszadeh Fathabadi, Z., Aval, M. Y., & Ebrahimi, A. (2017). Atmospheric Heavy Metals Biomonitoring Using a Local Pinus eldarica Tree. Health Scope, 6(1), 1–9. https://doi.org/10.17795/jhealthscope-39241.

Nation State Program. (2020). Capítulo 4 : Aspectos sobre la composición de las emisiones en la flota vehicular que afectan la salud y el ambiente [Informe Estado de la Nación 2020]. 151–174.

Nazzal, Y., Rosen, M. A., & Al-Rawabdeh, A. M. (2013). Assessment of metal pollution in urban road dusts from selected highways of the Greater Toronto Area in Canada. Environmental Monitoring and Assessment, 185(2), 1847–1858. https://doi.org/10.1007/s10661-012-2672-3.

Norouzi, S., Khademi, H., Cano, A. F., & Acosta, J. A. (2016). Biomagnetic monitoring of heavy metals contamination in deposited atmospheric dust, a case study from Isfahan, Iran. Journal of Environmental Management, 173, 55–64. https://doi.org/10.1016/j.jenvman.2016.02.035.

Olusegun, O. A., Osuntogun, B., & Eluwole, T. A. (2021). Assessment of heavy metals concentration in soils and plants from electronic waste dumpsites in Lagos metropolis. Environmental Monitoring and Assessment, 193(9), 1–19. https://doi.org/10.1007/s10661-021-09307-4.

Polezer, G., Tadano, Y. S., Siqueira, H. V., Godoi, A. F. L., Yamamoto, C. I., de André, P. A., Pauliquevis, T., Andrade, M. de F., Oliveira, A., Saldiva, P. H. N., Taylor, P. E., & Godoi, R. H. M. (2018). Assessing the impact of PM2.5 on respiratory disease using artificial neural networks. Environmental Pollution, 235, 394–403. https://doi.org/10.1016/j.envpol.2017.12.111.

Qiao, Q., Huang, B., Zhang, C., Piper, J. D. A., Pan, Y., & Sun, Y. (2013). Assessment of heavy metal contamination of dustfall in northern China from integrated chemical and magnetic investigation. Atmospheric Environment, 74(5), 182–193. https://doi.org/10.1016/j.atmosenv.2013.03.039.

Raj, A. (2020). Unlocking the True Power of Support Vector Regression. Towards Data Science. https://towardsdatascience.com/unlocking-the-true-power-of-support-vector-regression-847fd123a4a0.

Rojas-Rodríguez, F., & Torres-Córdoba, G. (2013). Casuarina. Revista Forestal Mesoamericana Kurú, 10(25), 32–33.

RStudio Team. (2020). RStudio: Integrated Development for R. RStudio, PBC. (1.4.1717). R Foundation for Statistical Computing. http://www.rstudio.com/.

Salazar-Rojas, T., Cejudo-Ruiz, F. R., & Calvo-Brenes, G. (2022). Comparison Between Machine Linear Regression (MLR) and Support Vector Machine (SVM) as Model Generators for Heavy Metal Assessment Captured in Biomonitors and Road Dust. Environmental Pollution, 314, 120227. https://doi.org/https://doi.org/10.1016/j.envpol.2022.120227.

Salazar-Rojas, T., Cejudo-Ruiz, F. R., & Calvo-Brenes, G. (2023). Assessing magnetic properties of biomonitors and road dust as a screening method for air pollution monitoring. Chemosphere, 310(September 2022). https://doi.org/10.1016/j.chemosphere.2022.136795.

Salmon, B. P., Kleynhans, W., Schwegmann, C. P., & Olivier, J. C. (2015). School of Engineering and ICT , University of Tasmania , Australia Remote Sensing Research Unit , Meraka Institute , CSIR , South Africa Department of Electrical , Electronic and Computer Engineering , University of Pretoria , South Africa. 3057–3060.

Solano, J., Villalobos, R., & Instituto Meteorológico Nacional de Costa Rica (IMN). (2020). Regionalización de Costa Rica. Regiones y Subregiones Climáticas de Costa Rica, mapa 1, 1–32. https://doi.org/10.15517/psm.v18i2.45179.

Sukri, N. S., Aspin, S. A., Kamarulzaman, N. L., Jaafar, N. F., Mohd Ghazi, R., Shafiee @ Ismail, N. S., Yaacob, S. H., Kedri, F. K., & Zakaria, M. P. (2018). Assessment of metal pollution using enrichment factor (EF) and pollution load index (PLI) in sediments of selected Terengganu rivers, Malaysia. Malaysian Journal of Fundamental and Applied Sciences, 14(2), 235–240. https://doi.org/10.11113/mjfas.v14n2.1065.

U.S. EPA. (2007). Method 3051A Microwave Assisted Acid Digestion of Sediments, Sludges, Soils, and Oils. (Issue February). USA.

U.S. EPA. (2022). IRIS. United States, Environmental Protection Agency, Integrated Risk Information System. https://www.epa.gov/iris.

Wahab, M. I. A., & Razak, W. M. A. A. (2019). Assessment of trace elements concentration in road dust around the city of Kuala Lumpur. IOP Conference Series: Materials Science and Engineering, 572(1). https://doi.org/10.1088/1757-899X/572/1/012116.

Wang, G., Chen, J., Zhang, W., Ren, F., Chen, Y., Fang, A., & Ma, L. (2019). Magnetic properties of street dust in Shanghai, China and its relationship to anthropogenic activities. Environmental Pollution, 255, 113214. https://doi.org/10.1016/j.envpol.2019.113214.

Yap, J., Ng, Y., Yeo, K. K., Sahlén, A., Lam, C. S. P., Lee, V., & Ma, S. (2019). Particulate air pollution on cardiovascular mortality in the tropics: Impact on the elderly. Environmental Health: A Global Access Science Source, 18(34), 1–9. https://doi.org/10.1186/s12940-019-0476-4.

Zamudio, S., & Carranza, E. (1994). Cupressaceae. Flora Del Bajío y de Regiones Adyacentes, 29.

5. Discusión General

La contaminación del aire es una de las problemáticas ambientales más importantes de la sociedad moderna, que afecta directamente la calidad de vida de todas las especies que habitan nuestro planeta (Organización Mundial de la Salud, 2018). Debido a su importancia se realizan tanto a nivel mundial como a nivel de país esfuerzos importantes para la mejora y el monitoreo de la calidad del aire. Sin embargo, debido a los costos de instalación, mantenimiento y operación de las estaciones de monitoreo, la cuantía existente no es suficiente ni en escala de espacio ni de tiempo, ya que las mediciones se realizan solo en ciertas partes de las áreas metropolitanas y no con la frecuencia necesaria como para contar un monitoreo efectivo. Por ejemplo, en Costa Rica el número de estaciones de monitoreo de la calidad del aire es reducido (11 equipos de medición con 8 estaciones manuales de REMCA y una estación en Pavas de la Embajada de USA) y ubicadas únicamente en el GAM. Además de que los reportes de REMCA no están ni fácilmente disponibles ni actualizados al público (Poveda et al., 2020).

Es por ello que han surgido a nivel mundial metodologías alternativas a las tradicionales como el uso de biomonitores, debido a que estos, son capaces de captar partículas contaminantes. Existen varios estudios que muestran la posibilidad de emplear diferentes tipos de plantas, polvo de carreteras o suelo para estimar la presencia de metales pesados que provienen de emisiones que producen los vehículos, industrias y otras actividades antrópicas. Algunos métodos de monitoreo también están explorando el uso de propiedades magnéticas para establecer relaciones de concentración de elementos, la ventaja de esta técnica resulta en una disminución de costos-tiempo y no genera desechos contaminantes, por lo que resulta amigable con el ambiente. Aunque se ha logrado establecer que estas relaciones entre las propiedades magnéticas y las concentración de MPs en el PM son especificas en cada lugar, por lo que no es posible establecer una homologación entre ciudades, esto representa una desventaja, ya que las relaciones en cada lugar deben de pasar por un proceso de ajuste (Cejudo et al., 2015; Kawasaki et al., 2017; Kardel et al., 2018; Gillooly et al., 2019;).

Los resultados obtenidos en este trabajo demuestran la factibilidad de utilizar biomonitores en vez de los filtros usados en las metodologías tradicionales para la deposición del material particulado y por ende de los MPs. Se logró identificar la presencia de los MPs; Fe, Cu, Cr, Ni,

Pb, Zn y V en las hojas de los biomonitores estudiados tanto a nivel cuantitativo por medio de los análisis químicos y de análisis de propiedades magnéticas como a nivel cualitativo mediante la identificación de partículas minerales con forma de espinela, típica de las partículas ferrimagnéticas en imágenes SEM (Maher & Thompson, 1999). Además, los resultados obtenidos para el cálculo de los FE permitieron identificar diferentes niveles de contaminación en las muestras obtenidas. Para lo cual se consideró las concentraciones medias de metales y el sitio de muestreo 1 como el sitio de control y el Fe como elemento normalizador debido a su baja variabilidad (Okedeyi et al., 2014). Se observaron niveles de contaminación desde bajos a considerable para las muestras de *C. equisetifolia* y niveles bajos para *C. lusitanica*, siendo los valores más altos para metales V y Zn. El uso de biomonitores como filtros pasivos colectores de los MPs en el material particulado representó una alternativa, más simple de muestrear, al uso de los filtros tradicionales de cuarzo, teflón o fibra de vidrio, los cuales además de su propio impacto ambiental de producción implican costos adicionales en el monitoreo de la calidad del aire. Obteniendose resultados de concentración de MPs con desviaciones estándar similares a otros estudios realizados tanto en otras plantas como en los filtros tradicionales (Salazar-Rojas et al., 2023). Si se debe considerar adicional a la propia especie, ciertas precauciones en la selección de las hojas a muestrear en los biomonitores, cuestiones tales como edad, posible contaminación por excretas de animales, altura del suelo. Tratando de evitar por ejemplo hojas o muy jóvenes o muy maduras, y contaminaciones diferentes a las analizadas (Aguilar et al., 2012).

En contraste con los biomonitores, el polvo de la carretera mostró más sitios con diferentes niveles de contaminación, desde contaminación moderada hasta muy alta para algunos de los MPs estudiados, siendo los valores de FE más altos para Pb y Zn. Estos valores más altos de FE encontrados en el polvo de la carretera pueden explicarse por las posibles múltiples fuentes de MPs en las muestras de polvo de la carretera. El muestreo de polvo de carretera obtenido en cunetas presentó una diversidad de concentraciones en los elementos, este resultado está asociado a que no se encontró polvo en las carretera, posiblemente debido a la escorrentía de las lluvias incluso en la estación seca. Se debe observar que en la cuneta se acumulan restos metálicos procedentes del tráfico, aguas residuales grises de las viviendas y negocios cercanos y fuentes naturales, deposición atmosférica seca y húmeda, resuspensión del suelo superficial (Wang et al., 2019). Prueba de esta acumulación es el plomo, cuya fuente principal se esperaría

que fuera el combustible, sin embargo, en Costa Rica no se vende gasolina con plomo desde 1996, así el contenido de metal identificado podría ser producto de acumulaciones anteriores (RECOPE, 2016).

Mediante las correlaciones estadísticas significativas obtenidas, se comprobó que las propiedades magnéticas, en especial χlf, medidas en las hojas de los biomonitores permiten realizar una aproximación bastante certera del contenido de MPs incluidos en el PM suspendido en el aire y depositado en los bioindicadores, logrando ser utilizadas en vez del método de análisis químico para hacer un cribado (screening en inglés) bastante más rápido, barato y menos contaminante del contenido de MPs presentes. La utilidad de las mediciones magnéticas como indicadores de contaminación ambiental se basa en la correlación entre las propiedades magnéticas y las concentraciones de hierro, así como en la relación entre el hierro y los MPs (Li et al., 2017). Este trabajo muestra que todos los metales presentaron correlaciones positivas significativas entre la susceptibilidad magnética (χlf) y los MPs para ambos biomonitores. *C. equisetifolia* obtuvo para la χlf un $r \geq 0{,}9$ para el Fe, Cr y V, un $r \geq 0.7$ para el Cu y Zn y un $r > 0.4$ para el Ni. *C. lusitánica* alcanzó para la misma propiedad magnética un $r > 0.8$, 0.7, 0.6 y 0.5 para la el Fe, Zn, Cr y Cu respectivamente y un $r > 0.4$ para el Pb, Ni y V. Los valores obtenidos de correlación entre χlf y los MPs fueron inclusive iguales o superiores que estudios similares realizados en otros países con otras especies (Salazar-Rojas et al., 2023)

El polvo de la carretera presentó una pobre correlación entre los MPs y χlf , siendo significativa sólo para el Fe, indicando una posible relación no lineal entre estos parámetros, probablemente debido a las múltiples fuentes de contaminantes, como se ha identificado también en trabajos anteriores con múltiples fuentes de metales pesados, en zonas industriales y urbanas (Li et al., 2014; Li et al., 2017). La propiedad magnética, kdf%, por otro lado, mostró correlaciones significativas solo con el Fe para la *C. equisetifolia* y con el Zn y χlf para el polvo de la carretera.

Asimismo, recientemente, se ha estudiado el desarrollo de modelos de predicción de la contaminación atmosférica mediante enfoques de aprendizaje automático para ampliar y aumentar la eficacia de los programas de vigilancia de la contaminación atmosférica (Li et al., 2017; Leng et al., 2018; Li et al., 2020; Dai et al., 2020). Para este trabajo se utilizó el enfoque de aprendizaje automático supervisado, en el cual se entrenó el programa para que generara modelos de predicción de contenidos de MPs de tipo SVM y MLR partiendo de las propiedades

magnéticas de monitores (plantas y polvo de carretera) (Zhao et al., 2006; Wehle, 2017; Goodarzi et al., 2012).

Con este enfoque se obtuvo para los datos de entrenamiento, que el modelo de predicción del contenido de MPs a partir de las propiedades magnéticas, mostraron una mejor relación no lineal (SVM) que el lineal (MLR) entre las concentraciones de metales y las propiedades magnéticas, especialmente para la *C. lusitanica* y el polvo de la carretera, similares resultados de no linealidad entre estos parámetros fue obtenido por Li et al., (2014).

Además, con la excepción del Fe, los valores un R^2 ajustado más altos fueron obtenidos con valores más bajos de RMSE y MAE, como en los estudios realizados en Nanjing, China en el cual se realizaron modelos predictivos que incluyeron las propiedades magnéticas en hojas de *Ligustrum lucidum Ait*, *Osmanthus fragrans Lour* y *Cedar deodara G. Don ,* contaminantes en el aire y parámetros meteorológicos (Leng et al., 2018). Por otro parte, el Fe presentó los valores más altos de RMSE y MAE en todas las muestras, incluyendo los datos de validación, eso sería un reflejo de la pequeña cantidad de datos con alta concentración de Fe entre las muestras, también encontrado en otros estudios (Schmidt et al., 2005; Lu et al., 2007). Esto podría considerarse normal ya que el Fe tiene una baja variabilidad en el medio ambiente, es por eso que se utiliza como elemento normalizador (Okedeyi et al., 2014).

Para las selección de los mejores modelos por metal, se utilizó el resultado del índice de mejora (IR en inglés). En el caso de *C. equisetifolia*, se obtuvo mejores IR con SVM en 6 de los 7 MPs; Fe, Cu, Pb, Ni, V y Zn, únicamente el Cr presentó un R^2 ajustado ligeramente más bajo (-3%) a los obtenidos con los modelos de MLR. Para el *C. lusitanica* y el polvo de carretera SVM mostró mejores resultados IR para todos los MPs. Dejando claro que los mejores modelos se lograron con el abordaje de SVM, simple (S) o múltiple (M) dependiendo del MP.

Se identificó que *C. equisetifolia* presentó los valores R^2 ajustado más altos para todos los MPs tanto para los datos de entrenamiento como para los de prueba, por lo cual se consideraría el mejor monitor entre los estudiados. Además, se obtuvieron resultados similares en los que SVM mostró un coeficiente de correlación de entrenamiento (R) más alto, y un MAE y RMSE más bajos, que MLR, en la medición de MPs en PM colectados en filtros de microfibra de cuarzo (Whatman, Maidstone, Reino Unido), lo que demuestra la similitud de los biomonitores con el uso

de filtros utilizados en el monitoreo ambiental tradicional (Leng et al., 2017). Considerando que el grado de retención y encapsulación de las partículas en las plantas dependen de varios factores tales como las características de la hoja, la composición química de la cutícula y la estructura de la cutícula se requerirían realizar estudios fitoquímicos más detallados en las plantas como para explicar con certeza la superioridad de la *C. equisetifolia* sobre los otros monitores estudiados.

En cuanto a la validación de los modelos con los datos de prueba, los valores R^2 ajustado mostraron valores más altos para los modelos SVM y para la *C. equisetifolia*. Los valores de RMSE y MAE fueron similares o más bajos que los obtenidos con los datos de entrenamiento, tanto para los biomonitores como para el polvo de carretera. Demostrando que si se utilizan los modelos con datos nuevos los valores serían correctamente estimados, dando validez a los modelos obtenidos con los datos de entrenamiento.

Con respecto al segundo método de validación de los modelos predictivos, se muestrearon los mismos biomonitores y polvo de carretera en cuatro nuevos sitios. Luego se determinó su contenido de MPs por métodos químicos, y estos se compararon con los valores estimados por los modelos predictivos mediante los parámetros de RMSE y MAE. *C. equisetifolia* obtuvo valores de error (MAE y RMSE) similares o inferiores para todos los MPs. En el caso de *C. lusitánica* los valores de error fueron menores o similares para 5/7 de los MPs (Fe, Cu, Cr, Ni, V), solo el Pb y Zn presentaron errores superiores a los obtenidos con los datos de entrenamiento. En cuanto al polvo de carretera los valores de RMSE y MAE, fueron inferiores para todos los MPs estudiados. Estos resultados demuestran que los modelos generados, en especial los de SVM, son modelos válidos para predicción de contenido de MPs por medio de las propiedades magnéticas en biomonitores.

En el tercer método de validación se evaluó propiamente los valores estimados de MPs, utilizándolos para identificar la carga de contaminación por MPs, mediante el cálculo PLI. Para este se definicieron valores límites de contaminación para los biomonitores estudiados y el polvo de carretera a partir de los cuales se consideraría la existencia de algún tipo de contaminación por MPs.

El análisis de correlación mostró correlaciones significativas entre todos los MPs, χlf y los valores de PLI para C. *equisetifolia. Para* la *C. lusitanica* la correlación fue significativa para el Fe, Pb, Cr, V, Zn, χlf y los valores de PLI. Resultados comparables fueron obtenidos por un estudio realizado en Isfahan, Irán, en un árbol (*Platanus orientalis* L., Platanaceae) en el que se demostró una correlación significativa entre la χlf, el contenido de MPs (Cu, Fe, Mn, Ni, Pb, and Zn) y el PLI (Norouzi et al., 2016). Con respecto al polvo de la carretera los estimados de PLI obtenidos con los modelos resultaron significativamente correlacionado con; Fe, Cu, Cr, Ni, V y Zn.

Propiamente los resultados obtenidos por este método de validación construyendo una matriz de confusión, utilizando los valores de PLI según las clases identificadas por los análisis químicos, 4 clases para *C. equisetifolia,* 5 clases para *C. lusitánica* y 6 clases para polvo de carretera, comparándolos con los valores de PLI estimados obtenidos por los modelos, se obtuvieron resultados de porcentaje de exactitud generales de 63%, 75% y 50% para la *C. equisetifolia, C. lusitánica* y el polvo de carretera respectivamente. Sin embargo si se consideran únicamente las 3 clases referidas en la literatura para PLI (un valor de 0 indica una buena calidad, un valor de 1 indica la presencia de niveles base de contaminantes y un valor superior a 1 indica un deterioro progresivo de la calidad del lugar) los porcentajes de exactitud que se obtienen mejoran considerablemente para todos los monitores (exactitud de 69%, 81% y 81% respectivamente), denotando la viabilidad de los modelos creados para a identificar la presencia de contaminación por MPs (Ihl et al., 2015; Olusegun et al., 2021).

Haciendo una comparación en costos de recursos y tiempo invertidos en este trabajo para los análisis químicos y los magnéticos se identificó que los costos económicos eran para cada MP de aproximadamente de 30 USD por análisis químico frente a 0.5 USD por propiedad magnética determinada. En cuanto al tiempo invertido en el análisis de un MP se requirieron alrededor de 2h por el método químico (digestión, calibración de equipo y lectura en AA) para cada metal, mientras que una propiedad magnética obtuvo en 2 min (calibración y lectura en Medidor de susceptibilidad magnética). Esto demuestra la posibilidad de utilización de las propiedades magnéticas como método de cribado de menor costo económico y de tiempo, para la identificación de posible contaminación por MP.

Los aportes derivados de este trabajo fueron varios: Se encontró evidencia de la relación entre propiedades magnéticas y la concentración de metales pesados en material partículado para Costa Rica, lo que permitirá su eventual uso para estudios ambientales en el país. Se demuestra el uso de propiedades magnéticas como un indicador indirecto para evaluar la amenaza por concentración de metales pesadas, con lo que se podría evaluar el riesgo en un sitio vulnerable en Costa Rica. Se demuestra por primera vez que, el algoritmo de soporte de vectores automático incrementa la precisión de estimación de la concentración de metales pesados por propiedades magnéticas para material particulado depositado en bioindicadores. Además, se obtuvieron resultados de una nueva especie que puede emplearse como biomonitor de metales pesados y que no se había reportado en estudios similares en ciudades de zonas tropicales, *Casuarina equisetifolia.*

6. Conclusiones

Se obtuvo una correlación significativa positiva entre la *χlf* de las hojas de *C. equisetifolia* y *C. lucitanica* y el contenido de los todos MPs estudiados. Para el polvo de urbano la correlación significativa con la *χlf* se identificó únicamente con el Fe.

Los resultados mostraron tanto en la etapa de entrenamiento como en la de prueba, que las concentraciones de Fe, Cu, Cr, V y Zn fueron bien estimadas por los modelos de predicción SVM, con valores R^2 ajustados > 0.7 y las concentraciones de Pb y Ni fueron estimados con menor precisión, con valores R^2 ajustados < 0.7.

Los resultados del monitor *C. equisetifolia* fueron los más acertados para determinar la concentración de MPs a partir de sus propiedades magnéticas, con los mejores valores de R^2 ajustado y RMSE y MAE más bajos, siendo por ello superior al *C. lucitanica* y al polvo de carretera, para el monitoreo de la contaminación del aire por MPs.

Se obtuvo un modelo de monitoreo de la contaminación atmosférica en zonas de flujo vehicular basado en un algoritmo de SVM, y que emplea las propiedades magnéticas de biomonitores y polvo de carretera para estimar la concentración de metales pesados.

El recurso material y de tiempo invertido resultó ser considerablemente más bajo para los análisis magnéticos que para los químicos, lo cual confirma esta alternativa como más barata, rápida y eficiente para obtener valores estimados de varios MPs con buena precisión.

7. Recomendaciones

Se considera muy oportuno para el país la implementación de este tipo de monitoreo, utilizando biomonitores y sus propiedades magnéticas, como las trabajadas en esta tesis, como sustitutos de los filtros tradicionales, ya que los mismos son más rentables, generan menor intrusión e impacto ambiental en el seguimiento de la contaminación del aire. Considerar que en la

aplicación de esta metodología de monitoreo se debe tomar en cuenta la selección adecuada del biomonitor, así como realizar los muestreos en época de no lluvia.

Se sugiere la utilización de las propiedades magnéticas de los diferentes muestras ambientales para la identificación de metales pesados, como método *screening*, eficaz y económico.

Ampliar la existente red de monitoreo a distintas áreas geográficas del país y mantener la información actualizada y disponible a la población.

La realización de estudios fitoquímicos que ayuden a entender la diferencia en afinidad de las plantas a la adsorción y absorción de material particulado.

El reconocimiento y utilización de los servicios ambientales de los árboles, no solo como barreras naturales de los contaminantes sino también para la purificación del aire en las zonas urbanas, mediante la absorción, adsorción, metabolización, acumulación y retención de contaminantes.

8. Referencias

Aguilar, B., Bautista, F., Goguitchaichvili, A., & Morton, O. (2011). Magnetic monitoring of top soils of Merida (Southern Mexico). *Studia Geophysica et Geodaetica*, *55*(2), 377–388. https://doi.org/10.1007/s11200-011-0021-6

Aguilar, B., Cejudo, R., Martínez, J., Bautista, F., Goguitchaichvili, A., Carvallo, C., & Morales, J. (2012). Ficus benjamina leaves as indicator of atmospheric pollution: A reconaissance study. *Studia Geophysica et Geodaetica*, *56*(3), 879–887. https://doi.org/10.1007/s11200-011-0265-1

Bautista, F., & Gogichaishvili, A. (2018). *Sistema de monitoreo de la contaminación por metales pesados en polvos urbanos de la Ciudad de México*.

Bisht, L., Gupta, V., Singh, A., Gautam, A. S., & Gautam, S. (2022). Heavy metal concentration and its distribution analysis in urban road dust: A case study from most populated city of Indian state of Uttarakhand. *Spatial and Spatio-Temporal Epidemiology*, *40*(October 2021), 100470. https://doi.org/10.1016/j.sste.2021.100470

Briseño-Castillo, J., Herrera-Murillo, J., Solórzano-Arias, D., Beita-Guerrero, V. H., & Rojas-Marin, J. F. (2015). *VI Informe de Calidad del Aire Área Metropolitana de Costa Rica*. MINAE.

Bussotti, F., Pollastrini, M., Killi, D., Ferrini, F., & Fini, A. (2014). Ecophysiology of urban trees in a perspective of climate change. *Agrochimica*, *58*(3), 247–268. https://doi.org/10.12871/0021857201431

Cai, C., Xiong, B., Zhang, Y., Li, X., & Nunes, L. M. (2015). Critical Comparison of Soil Pollution Indices for Assessing Contamination with Toxic Metals. *Water, Air, and Soil Pollution*, *226*(10). https://doi.org/10.1007/s11270-015-2620-2

Cejudo, R., Bautista, F., Quintana, P., Delgado, M. del C., Aguilar, D., Goguitchaichvili, A., & Morales, J. J. (2015). Correlación entre elementos potencialmente tóxicos y propiedades magnéticas en suelos de la Ciudad de México para la identificación de sitios contaminados: definición de umbrales magnéticos. *Revista Mexicana de Ciencias Geológicas*, *32*(1).

Chaparro, M. A. E., Chaparro, M. A. E., Castañeda-Miranda, A. G., Marié, D. C., Gargiulo, J. D., Lavornia, J. M., Natal, M., & Böhnel, H. N. (2020). Fine air pollution particles trapped by

street tree barks: In situ magnetic biomonitoring. *Environmental Pollution*, *266*, 115229. https://doi.org/10.1016/j.envpol.2020.115229

Dai, Q., Zhou, M., Li, H., Qian, X., Yang, M., & Li, F. (2020). Biomagnetic monitoring combined with support vector machine: a new opportunity for predicting particle-bound-heavy metals. *Scientific Reports*, *10*(1), 1–11. https://doi.org/10.1038/s41598-020-65677-8

Davila, A. F., Rey, D., Mohamed, K., Rubio, B., & Guerra, A. P. (2006). Mapping the sources of urban dust in a coastal environment by measuring magnetic parameters of Platanus hispanica leaves. *Environmental Science and Technology*, *40*(12), 3922–3928. https://doi.org/10.1021/es0525049

Davis, S. C., & Robert, G. B. (2021). *Transportation Energy Data Book* (39th ed.). Oak Ridge National Laboratory. https://tedb.ornl.gov/wp-content/uploads/2021/02/TEDB_Ed_39.pdf

de Paula, P. H. M., Mateus, V. L., Araripe, D. R., Duyck, C. B., Saint'Pierre, T. D., & Gioda, A. (2015). Biomonitoring of metals for air pollution assessment using a hemiepiphyte herb (Struthanthus flexicaulis). *Chemosphere*, *138*, 429–437. https://doi.org/10.1016/j.chemosphere.2015.06.060

Dearing, J. A. (1999). Using the Bartington MS2 System. *Environmental Magnetic Susceptibility*, 52.

Evans, M. E., & Heller, F. (2003). *Environmental Magnetism: Principles and Applications of Enviromagnetics*. Acadeic Press.

Gillooly, S. E., Michanowicz, D. R., Jackson, M., Cambal, L. K., Shmool, J. L. C., Tunno, B. J., Tripathy, S., Bain, D. J., & Clougherty, J. E. (2019). Evaluating deciduous tree leaves as biomonitors for ambient particulate matter pollution in Pittsburgh, PA, USA. *Environmental Monitoring and Assessment*, *191*(12). https://doi.org/10.1007/s10661-019-7857-6

Goodarzi, M., Jensen, R., & Vander Heyden, Y. (2012). QSRR modeling for diverse drugs using different feature selection methods coupled with linear and nonlinear regressions. *Journal of Chromatography B: Analytical Technologies in the Biomedical and Life Sciences*, *910*, 84–94. https://doi.org/10.1016/j.jchromb.2012.01.012

Hofman, J., Maher, B. A., Muxworthy, A. R., Wuyts, K., Castanheiro, A., & Samson, R. (2017). Biomagnetic Monitoring of Atmospheric Pollution: A Review of Magnetic Signatures from

Biological Sensors. *Environmental Science and Technology*, *51*(12), 6648–6664. https://doi.org/10.1021/acs.est.7b00832

Hofman, J., & Samson, R. (2014). Biomagnetic monitoring as a validation tool for local air quality models: A case study for an urban street canyon. *Environment International*, *70*(2014), 50–61. https://doi.org/10.1016/j.envint.2014.05.007

Ihl, T., Bautista, F., Cejudo Ruíz, F. R., Delgado, M. del C., Quintana Owen, P., Aguilar, D., & Goguitchaichvili, A. (2015). Concentración de elementos tóxicos en suelos del área metropolitana de la Ciudad de México: análisis espacial utilizando kriging ordinario y kriging indicador. *Revista Internacional de Contaminación Ambiental*, *31*(1), 47–62. http://www.scielo.org.mx/scielo.php?script=sci_arttext&pid=S0188-49992015000100004&lng=es&nrm=iso&tlng=en

Kardel, F., Wuyts, K., De Wael, K., & Samson, R. (2018). Biomonitoring of atmospheric particulate pollution via chemical composition and magnetic properties of roadside tree leaves. *Environmental Science and Pollution Research*, *25*(26), 25994–26004. https://doi.org/10.1007/s11356-018-2592-z

Kawasaki, K., Horikawa, K., & Sakai, H. (2017). Magnetic biomonitoring of roadside pollution in the restricted. *Environmental Science and Pollution Research*, 10313–10325. https://doi.org/10.1007/s11356-017-8702-5

Khamesi, A., Khademi, H., & Zeraatpisheh, M. (2020). Biomagnetic monitoring of atmospheric heavy metal pollution using pine needles: the case study of Isfahan, Iran. *Environmental Science and Pollution Research*, *27*(25), 31555–31566. https://doi.org/10.1007/s11356-020-09247-5

Leng, Xiang'zi, Wang, J., Ji, H., Wang, Q., Li, H., Qian, X., Li, F., & Yang, M. (2017). Prediction of size-fractionated airborne particle-bound metals using MLR, BP-ANN and SVM analyses. *Chemosphere*, *180*, 513–522. https://doi.org/10.1016/j.chemosphere.2017.04.015

Leng, Xiang, Qian, X., Yang, M., Wang, C., Li, H., & Wang, J. (2018). Leaf magnetic properties as a method for predicting heavy metal concentrations in PM2.5 using support vector machine: A case study in Nanjing, China. *Environmental Pollution*, *242*, 922–930. https://doi.org/10.1016/j.envpol.2018.07.007

Leng, Xiangzi, Wang, C., Li, H., Qian, X., Wang, J., & Sun, Y. (2017). Response of magnetic properties to metal deposition on urban green in Nanjing, China. *Environmental Science and Pollution Research*, *24*(32), 25315–25328. https://doi.org/10.1007/s11356-017-0133-9

Li, H., Dai, Q., Yang, M., Li, F., Liu, X., Zhou, M., & Qian, X. (2020). Heavy metals in submicronic particulate matter (PM1) from a Chinese metropolitan city predicted by machine learning models. *Chemosphere*, *261*(March). https://doi.org/10.1016/j.chemosphere.2020.127571

Li, H., Qian, X., Wei, H., Zhang, R., Yang, Y., Liu, Z., Hu, W., Gao, H., & Wang, Y. (2014). Magnetic properties as proxies for the evaluation of heavy metal contamination in urban street dusts of Nanjing, Southeast China. *Geophysical Journal International*, *199*(3), 1354–1366. https://doi.org/10.1093/gji/ggu253

Li, H., Wang, J., Wang, Q., Tian, C., Qian, X., & Leng, X. (2017). Magnetic Properties as a Proxy for Predicting Fine-Particle-Bound Heavy Metals in a Support Vector Machine Approach. *Environmental Science and Technology*, *51*(12), 6927–6935. https://doi.org/10.1021/acs.est.7b00729

Losacco, C., & Perillo, A. (2018). Particulate matter air pollution and respiratory impact on humans and animals. In *Environmental Science and Pollution Research* (Vol. 25, Issue 34, pp. 33901–33910). Springer Verlag. https://doi.org/10.1007/s11356-018-3344-9

Lu, S. G., Bai, S. Q., & Xue, Q. F. (2007). Magnetic properties as indicators of heavy metals pollution in urban topsoils: A case study from the city of Luoyang, China. *Geophysical Journal International*, *171*(2), 568–580. https://doi.org/10.1111/j.1365-246X.2007.03545.x

Maher, B., & Thompson, R. (1999). *Quaternary Climates, environments and Magnetism* (Vol. 4, Issue 1). Cambridge University Press.

Maurya, P., & Kumari, R. (2021). Toxic metals distribution, seasonal variations and environmental risk assessment in surficial sediment and mangrove plants (A. marina), Gulf of Kachchh (India). *Journal of Hazardous Materials*, *413*(January), 125345. https://doi.org/10.1016/j.jhazmat.2021.125345

Naciones Unidas. (n.d.). *Objetivos de Desarrollo Sostenible*. https://www.un.org/sustainabledevelopment/es/

Nation State Program. (2020). *Capítulo 4 : Aspectos sobre la composición de las emisiones en la*

flota vehicular que afectan la salud y el ambiente [Informe Estado de la Nación 2020]. 151–174.

Norouzi, S., Khademi, H., Cano, A. F., & Acosta, J. A. (2016). Biomagnetic monitoring of heavy metals contamination in deposited atmospheric dust, a case study from Isfahan, Iran. *Journal of Environmental Management*, *173*, 55–64. https://doi.org/10.1016/j.jenvman.2016.02.035

Okedeyi, O. O., Dube, S., Awofolu, O. R., & Nindi, M. M. (2014). Assessing the enrichment of heavy metals in surface soil and plant (Digitaria eriantha) around coal-fired power plants in South Africa. *Environmental Science and Pollution Research*, *21*(6), 4686–4696. https://doi.org/10.1007/s11356-013-2432-0

Oliva, S. R., & Espinosa, A. J. F. (2007). Monitoring of heavy metals in topsoils, atmospheric particles and plant leaves to identify possible contamination sources. *Microchemical Journal*, *86*(1), 131–139. https://doi.org/10.1016/j.microc.2007.01.003

Olusegun, O. A., Osuntogun, B., & Eluwole, T. A. (2021). Assessment of heavy metals concentration in soils and plants from electronic waste dumpsites in Lagos metropolis. *Environmental Monitoring and Assessment*, *193*(9), 1–19. https://doi.org/10.1007/s10661-021-09307-4

Organización Mundial de la Salud. (2018). *Calidad del aire y salud*. https://www.who.int/es/news-room/fact-sheets/detail/ambient-(outdoor)-air-quality-and-health

Polezer, G., Tadano, Y. S., Siqueira, H. V., Godoi, A. F. L., Yamamoto, C. I., de André, P. A., Pauliquevis, T., Andrade, M. de F., Oliveira, A., Saldiva, P. H. N., Taylor, P. E., & Godoi, R. H. M. (2018). Assessing the impact of PM2.5 on respiratory disease using artificial neural networks. *Environmental Pollution*, *235*, 394–403. https://doi.org/10.1016/j.envpol.2017.12.111

Poveda, L., Publicaciones, P. De, & Rica, C. (2020). Calidad ambiental en Costa Rica : Análisis y perspectivas desde la UNA. *Ambientico*, *274*(3), 11–15. http://www.galeriaambientalista.una.ac.cr/pdfs/ambientico/274.pdf#page=34

Programa Estado de la Nación. (2022). Capítulo 4: Armonía con la naturaleza. *Informe Estado de La Nación*, 135–182.

Rai, P. K., & Panda, L. L. S. (2015). Roadside plants as bio indicators of air pollution in an

industrial region, Rourkela, India. *International Journal of Advancements in Research & Technology*, *4*(1), 14–36.

RECOPE. (2016). *Gasolina sin plomo desde hace dos décadas*. RECOPE En Transformación. https://www.recope.go.cr/gasolina-sin-plomo-desde-hace-dos-decadas/

Salazar-Rojas, T., Cejudo-Ruiz, F. R., & Calvo-Brenes, G. (2023). Assessing magnetic properties of biomonitors and road dust as a screening method for air pollution monitoring. *Chemosphere*, *310*(September 2022). https://doi.org/10.1016/j.chemosphere.2022.136795

Schmidt, A., Yarnold, R., Hill, M., & Ashmore, M. (2005). Magnetic susceptibility as proxy for heavy metal pollution: A site study. *Journal of Geochemical Exploration*, *85*(3), 109–117. https://doi.org/10.1016/j.gexplo.2004.12.001

Sharma, P., Yadav, P., Ghosh, C., & Singh, B. (2020). Heavy metal capture from the suspended particulate matter by Morus alba and evidence of foliar uptake and translocation of PM associated zinc using radiotracer (65Zn). *Chemosphere*, *254*, 126863. https://doi.org/10.1016/j.chemosphere.2020.126863

Solano, J., Villalobos, R., & Instituto Meteorológico Nacional de Costa Rica (IMN). (2020). Regionalización de Costa Rica. *Regiones y Subregiones Climáticas de Costa Rica*, *mapa 1*, 1–32. https://doi.org/10.15517/psm.v18i2.45179

U.S. EPA. (2022). *IRIS. United States, Environmental Protection Agency, Integrated Risk Information System.* https://www.epa.gov/iris

Wang, G., Chen, J., Zhang, W., Ren, F., Chen, Y., Fang, A., & Ma, L. (2019). Magnetic properties of street dust in Shanghai, China and its relationship to anthropogenic activities. *Environmental Pollution*, *255*, 113214. https://doi.org/10.1016/j.envpol.2019.113214

Wehle, H. (2017). ML – AI- COGNITIVE. *Conference: Data Scientist Innovation Day*, *July*.

Wilson, J. G., Kingham, S., Pearce, J., & Sturman, A. P. (2005). A review of intraurban variations in particulate air pollution: implications for epidemiological research. *Atmospheric Environment*, *39*, 6444e6462.

Winkler, A., Contardo, T., Vannini, A., Sorbo, S., Basile, A., & Loppi, S. (2020). Magnetic emissions from brake wear are the major source of airborne particulate matter

bioaccumulated by lichens exposed in Milan (Italy). *Applied Sciences (Switzerland)*, *10*(6). https://doi.org/10.3390/app10062073

Winkler, A., Moreno, E., Sagnotti, L., Dinarès-Turell, J., & Cascella, A. (2003). Biomonitoring of traffic air pollution in Rome using magnetic properties of tree leaves. *Atmospheric Environment*, *37*(21), 2967–2977. https://doi.org/10.1016/S1352-2310(03)00244-9

World Air Quality Index Team. (2020). *The World Air Quality Project*. World-Wide Air Quality Monitoring Data Coverage. https://aqicn.org/contact/

World Air Quality Index Team. (2022). *Contaminación del aire de San Jose US Embassy*. Datos Históricos de La Calidad Del Aire.

World Health Organization, W. (2021). *Ambient (outdoor) air pollution*. https://www.who.int/news-room/fact-sheets/detail/ambient-(outdoor)-air-quality-and-health

Yap, J., Ng, Y., Yeo, K. K., Sahlén, A., Lam, C. S. P., Lee, V., & Ma, S. (2019). Particulate air pollution on cardiovascular mortality in the tropics: Impact on the elderly. *Environmental Health: A Global Access Science Source*, *18*(34), 1–9. https://doi.org/10.1186/s12940-019-0476-4

Zhao, C. Y., Zhang, H. X., Zhang, X. Y., Liu, M. C., Hu, Z. D., & Fan, B. T. (2006). Application of support vector machine (SVM) for prediction toxic activity of different data sets. *Toxicology*, *217*(2–3), 105–119. https://doi.org/10.1016/j.tox.2005.08.019

ANEXO 1. Material suplementario artículo: Assessing Magnetic Properties of Biomonitors and Road Dust as a Screening Method for Air Pollution Monitoring

Table S1. Sampling dates and average meteorological conditions measured at the closest weather stations to each sampling site[1](Salazar-Rojas et al., 2023).

Site	Sampling dates	Rain (mm)		Temperature (°C)						Humidity (%)		Wind (km/h)		Wind Direction[2]	
				High		Low		Medium							
		February	March	February	March	February	March	February	March	February	March	February	March	February	March
1	03/20/2020 03/26/2021	19.1	16.1	23.5	24.5	13.1	13.3	18.3	18.9	82.1	81.7	N/A	N/A	N/A	N/A
2	03/01/2020 02/15/2021	10.7	13.0	30.3	31.1	18.8	19.0	24.5	25.0	57.3	58.3	11.7	10.4	3	3
3	03/01/2020 02/15/2021	20.9	38.8	25.4	26.4	14.8	15.0	20.1	20.7	72.4	71.0	N/A	N/A	N/A	N/A
3’	03/01/2020 02/15/2021	10.9	6.9	26.9	27.5	18.1	18.4	22.5	23.0	64.3	63.5	21.9	21.6	3	3
4	03/05/2020 02/26/2021	8.6	9.5	21.8	22.7	12.2	12.6	17.0	17.7	81.9	82.0	19.1	17.6	4	4
5	03/05/2020 02/26/2021	9.0	10.9	20.7	21.6	11.8	12.2	16.2	16.9	89.7	89.4	9.4	9.2	4	4
6	03/01/2020 02/15/2021	9.5	12.8	28.9	29.7	18.4	18.7	23.7	24.2	60.0	60.0	22.3	20.5	3	3
6’	03/01/2020 02/15/2021	8.9	9.5	28.6	29.5	18.8	19.2	23.7	24.4	60.8	60.3	26.2	25.1	3	4
7	03/05/2020 02/26/2021	10.1	10.1	23.6	24.5	16.4	16.7	20.0	20.6	72.9	72.1	13.9	13.9	2	2
8	03/01/2020 02/15/2021	10.9	6.9	26.9	27.5	18.1	18.4	22.5	23.0	64.3	63.5	21.9	21.6	3	3

1. Source: Department of Meteorological Orientation. National Meteorological Institute, Costa Rica, 2022.

2. Wind Direction: 1 North, 2 Northeast , 3 East, 4 Southeast, 5 South, 6 Southwest, 7 West, 8 Northeast, 9 Variable.

N/A: Not Available